



저작자표시-비영리-변경금지 2.0 대한민국

이용자는 아래의 조건을 따르는 경우에 한하여 자유롭게

- 이 저작물을 복제, 배포, 전송, 전시, 공연 및 방송할 수 있습니다.

다음과 같은 조건을 따라야 합니다:



저작자표시. 귀하는 원저작자를 표시하여야 합니다.



비영리. 귀하는 이 저작물을 영리 목적으로 이용할 수 없습니다.



변경금지. 귀하는 이 저작물을 개작, 변형 또는 가공할 수 없습니다.

- 귀하는, 이 저작물의 재이용이나 배포의 경우, 이 저작물에 적용된 이용허락조건을 명확하게 나타내어야 합니다.
- 저작권자로부터 별도의 허가를 받으면 이러한 조건들은 적용되지 않습니다.

저작권법에 따른 이용자의 권리는 위의 내용에 의하여 영향을 받지 않습니다.

이것은 [이용허락규약\(Legal Code\)](#)을 이해하기 쉽게 요약한 것입니다.

[Disclaimer](#)

A THESIS

FOR THE DEGREE OF MASTER OF SCIENCE

**Molecular and Functional Characterization of
Two serpins
Protease nexin-1 and Heparin cofactor II
from Rock bream (*Oplegnathus fasciatus*)**

Navaneethaiyer Umasuthan

Department of Marine Life Sciences

GRADUATE SCHOOL

JEJU NATIONAL UNIVERSITY

2011. 08

**Molecular and Functional Characterization of
Two serpins**

**Protease nexin-1 and Heparin cofactor II
from Rock bream (*Oplegnathus fasciatus*)**

**Navaneethaiyer Umasuthan
(Supervised by Professor Jehee Lee)**

A thesis submitted in partial fulfillment of the requirement for the degree of

Master of Science

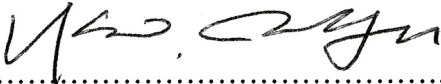
2011. 08

This thesis has been examined and approved by


.....

Thesis Director,

Gi-Young Kim, Professor of Marine Life Sciences


.....

In-Kyo Yeo, Professor of Marine Life Sciences

.....
Jehee Lee, Professor of Marine Life Sciences

08. 2011
Date

Department of Marine Life Sciences
GRADUATE SCHOOL
JEJU NATIONAL UNIVERSITY
REPUBLIC OF KOREA

CONTENTS

요약문	IV
Summary	IX
List of Figures	XII
List of Tables	XIV
Introduction	01
Chapter I. Heparin cofactor II (RbHCII) from rock bream (<i>Oplegnathus fasciatus</i>): Molecular characterization, cloning and expression analysis	
1. Abstract	07
2. Materials and methods	
2.1. Rock bream cDNA library construction and isolation of RbHCII cDNA	09
2.2. Sequence characterization and phylogenetic analysis of RbHCII	09
2.3. Homology modeling	10
2.4. Experimental animals	10
2.5. RbHCII mRNA expression analysis	10
2.5.1. Fish tissues for the specific distribution analysis	10
2.5.2. Expression pattern of RbHCII after stimulated by LPS, bacterium and virus	11
2.5.3. Total RNA isolation and first strand cDNA synthesis	12
2.5.4. qRT-PCR-based RbHCII mRNA expression analysis	12
2.6. Cloning of RbHCII coding sequence	13
2.7. Overexpression and purification of recombinant RbHCII (rRbHCII)	15
2.8. Biochemical properties of rRbHCII	16
2.9. Statistical analysis	17

3. Results

3.1. Molecular characterization of RbHCII primary structure	18
3.2. Pair-wise and multiple alignment analysis of RbHCII	20
3.3. Analysis of phylogenetic position of the RbHCII	26
3.4. Molecular modeling of tertiary structure of the RbHCII	31
3.5. Tissue distribution analysis of RbHCII mRNA	34
3.6. Transcriptional modulation of RbHCII expression during immune stimulation	36
3.7. Expression and purification of recombinant RbHCII	39
3.8. Biochemical characterization of recombinant RbHCII	41

4. Discussion

44

Chapter II. Rock bream (*Oplegnathus fasciatus*) serpin, protease nexin-1: Transcriptional analysis and characterization of its antiprotease and anticoagulant activities

1. Abstract

52

2. Materials and methods

2.1. Experimental animals, tissue collection and RNA isolation	54
2.2. Multi-tissue cDNA synthesis and normalization	54
2.3. Rock bream genome sequence database and identification of rock bream PN-1	54
2.4. Molecular characterization of RbPN-1	55
2.5. Cloning of RbPN-1 open reading frame (ORF)	55
2.6. Overexpression and purification of recombinant RbPN-1 (rRbPN-1)	58
2.7. Antiprotease activity assays	58
2.8. Anticoagulation assay	59

2.9. Immune and injury challenge experiments	60
2.10. RNA extraction and cDNA synthesis	60
2.11. RbPN-1 transcriptional analysis by qRT-PCR	61
3. Results	
3.1. Molecular characterization of RbPN-1	62
3.1.1. Sequence characterization of the full length RbPN-1	62
3.1.2. Pair-wise and multiple alignment analysis of RbPN-1 vs. PN-1 orthologues	65
3.1.3. Molecular modeling	73
3.1.4. Phylogenetic study	75
3.2. Overexpression and purification of recombinant RbPN-1 (rRbPN-1)	78
3.3. <i>In vitro</i> antiprotease activity assays	80
3.4. <i>In vitro</i> anticoagulation assay	82
3.5. Analysis of tissue specific expression profile of RbPN-1	84
3.6. Transcriptional responses of RbPN-1	86
3.6.1. Against LPS, bacterium and RBIV stimulation	86
3.6.2. Against muscle injury	90
4. Discussion	
4.1. Molecular structural characterization	92
4.2. Functional characterization of recombinant RbPN-1	95
4.3. Expression analysis	96
References	100
Acknowledgment	110

한글 요약문

Serine protease inhibitors (Serpins)은 흔히 발견되는 serine 단백질분해효소(Serine Proteases, SPs)와 함께, 항상성 균형과 응고 및 섬유소용해폭포작용, 면역 및 염증조절과 세포사멸 등 다양한 생리학적 반응 등에 관여한다. 이번 연구에서 확인한 돌돔 (Rock bream, Rb)의 heparin cofactor II (HCII)와 protease nexin-1 (PN-1)은 중요한 serpin 유전자들이다. 이 두 유전자는 각각 clades D와 E로 분류되며 각각의 활성은 heparin과 같은 glycosaminoglycans (GAGs)에 의해 조절된다. HCII와 PN-1에 의해 억제되는 대표적인 serine 단백질분해효소로는 thrombin이 있으며, 응고 및 면역 조절 등 다방면의 생물적인 측면에서 중요한 역할을 한다.

이 논문은 돌돔 cDNA library에서 분리한 HCII와 PN-1 유전자 동정뿐만 아니라 여러 자극에 대한 *in vitro*와 실제 injury와 같은 스트레스를 주었을 때 생체 내 유전자 발현 정도를 알아보는 연구이다.

RbHCII와 RbPN-1의 전체서열(full-length sequence)은 ClustalW pairwise 를 이용하여 이미 알려진 유사 serpin 유전자서열들과 비교 및 분석하였고 다른 유전자들과의 연관관계를 알아보려고 계통수 분석을 하였다. RbHCII과 RbPN-1의 coding sequence는 발현벡터인

pMAL-c2X를 이용하여 클로닝한 후 재조합 단백질을 얻어내었다. *In vitro* assay 를 통해 재조합 단백질인 recombinant (r)RbHCII와 rRbPN-1의 생물학적 특성을 확인하였다. 면역자극제를 주사한 돌돔에서 조직을 추출한 후 Quantitative real-time PCR 를 통해 RbHCII와 RbPN-1의 발현양상을 조직별로 확인하였다. 또한 돌돔 근육에 상처를 낸 후 시간별로 serpin 유전자 발현양상을 관찰하였다.

RbHCII와 RbPN-1의 전체염기서열은 각각 1950 bp와 1951 bp이며, RbHCII의 Open Reading Frame (ORF)는 1512 bp로 504개의 아미노산을 암호화하고 있고 RbPN-1의 ORF는 1191 bp로 397개의 아미노산을 암호화하고 있다. RbHCII와 RbPN-1의 단백질 서열은 신호서열을 포함하고 있으며 분자량은 각각 58 kDa과 44 kDa으로 분석되며 serpin 단백질들의 특징인 serpin 도메인과 signature 서열이 확인된다. 돌돔의 두 serpin 서열은 stickleback (*Gasterosteus aculeatus*)에서 동정된 HCII과 PN-1 유전자와 가장 높은 상동성(Identity)과 유사성(similarity)을 보인다. Multiple alignment 분석을 통해 RbHCII와 RbPN-1은 단백질 서열 중 C-말단 부분이 N-말단 부분보다 더 보존되어 있음을 알 수 있고 다른 종에서 확인된 serpin과 비교하였을 때 다양한 단백질 기능을 담당하는 reactive centre loop와 serpin signature, heparin binding site, hinge region 등이 보존적이다. 계통수 분석 결과 RbHCII는 넙치의 HCII와 가장 연관관계가 가깝다는 것을 알 수 있고 RbPN-1은 green spotted puffer 및 Japanese pufferfish 와

가깝다. 인간의 HCII (PDB; 1jmoA)와 PAI-1 (chain A, PDB; 1dvmA)을 토대로 단백질의 3차원 구조를 작성해 보니 돌돔 serpin 단백질의 folding 구조는 전형적인 serpin family 와 유사한 형태의 구조를 가지고 있다.

RbHCII와 RbPN-1 유전자는 pMAL-c2x 벡터에 삽입하였고, 유전자가 삽입된 벡터는 각각 Rosetta-gami와 BL21(DE3)에 형질전환시킨 후 IPTG를 이용하여 단백질 발현을 유도하였다. 재조합 단백질의 활성은 크로마토그래피를 통해 정제한 후 확인하였다. rRbHCII는 chymotrypsin (43.5%)과 thrombin (54%) 과 같은 serin protease 활성을 억제하며, rRbPN-1은 48%의 trypsin과 89%의 thrombin 의 활성을 억제하는 것으로 나타나며 이러한 억제 활성은 단백질의 양에 비례하였다. 흥미롭게도 heparin은 rRbHCII와 rRbPN-1 이 두 단백질의 thrombin 억제활성을 증가시켜주었다. 또한 APTT assay를 통해 rRbPN-1의 항응고 활성을 확인해본 결과, 응고시간을 102.1 s/14 µg 만큼 지연시켰다.

RbHCII와 RbPN-1 유전자의 조직별 발현 정도는 각각 돌돔의 간과 심장에서 가장 높았다. 다른 연구와 비교해보면 포유류에서 HCII는 간에서, PN-1의 경우는 뇌에서 그 발현이 높았다. *In vivo* 실험에서는 RbHCII와 RbPN-1이 돌돔 조직에서 항상 발현되는 것을 알 수 있었고, 이는 다양한 생체기능을 가지고 있음을 예상할 수 있다. 이 논문은 경골어류의 HCII과 PN-1과 같은 serpin의 조직별 특징적인 발현양상을 살펴보는 첫 번째 연구결과라 할 수 있다.

돌돔에 면역자극을 주었을 때 조직마다 RbHCII는 down-regulation 되었고 RbPN-1는 up-regulation 되는 것을 확인하였다. LPS 자극 시 혈구세포와 간세포에서 RbHCII는 down-regulation되었으나 RbPN-1는 간세포와 아가미에서 up-regulation 되었다. 또한 *Edwardsiella tarda*를 돌돔에 감염시켰을 때 돌돔의 간과 혈구세포에서 RbHCII은 down-regulation 되었다. 반면에 RbPN-1의 경우 *E. tarda* 감염 초기에만 혈구세포에서 up-regulation 되었고 아가미에서는 감염 후 강하게 발현되었다. 돌돔 이리도 바이러스(RBIV)를 돌돔에 감염시켰을 경우 RbHCII 발현은 혈구와 간세포에서 down-regulation 되었다. RbPN-1의 경우 RBIV를 접종하였을 때 혈구세포에서 유전자 발현량이 아주 많았으며, 아가미에서는 감염 후기에서만 발현량 증가를 확인할 수 있었다. 이처럼 조직별로 다른 양상을 보여주는 것은 병원체가 침입하였을 때 중요한 면역 매개자로서 serine proteases들은 활성을 나타내기 시작하며 serpin은 전사적 조절을 통해 serine protease와의 평형을 조절하는 중요한 역할을 한다고 볼 수 있다.

돌돔이 상처를 입었을 경우 (injury 실험) RbHCII과 RbPN-1의 발현양상은 매우 흥미로웠다. 상처가 난 돌돔의 간세포에서 두 유전자의 발현은 모두 감소하였다. 이는 돌돔에 상처가 날 당시에 단백질분해효소들을 조절하는 serpin의 기능이 늦춰져야 하기 때문이라 생각된다. 이 연구에서 보여주는 전사적 발현분석결과는 SPs와 Serpins 사이의 균형 조절이 매우 중요하다는 것을 뒷받침한다.

이 연구에서는 어류의 serpin system에 대해서 살펴보고 특별히 seprin의 면역학적 기능에 대해서 분석하였다. 이를 통해 serpin의 특성과 발현양상을 이해할 수 있었으며 앞으로 분자수준에서 다양한 serpin 유전자에 대한 연구가 더욱 필요하다고 생각된다.

SUMMARY

The serine protease inhibitors (serpins) are ubiquitously distributed protein family, a functional pair of serine proteases (SPs) that establish a balanced homeostasis and involved in various physiological aspects including coagulation and fibrinolytic cascades, immune and inflammatory modulation and apoptosis etc. Heparin cofactor II (HCII) and protease nexin-1 (PN-1) are two important serpin genes focused on this study. They have been categorized under clades D and E, respectively. Both HCII and PN-1 activity is modulated by glycosaminoglycans (GAGs) such as heparin. Thrombin is a common serine protease inhibited by both HCII and PN-1 that plays critical roles in multiple biological aspects including coagulation and immune modulation.

In this study, both HCII and PN-1 genes were isolated from a multi tissue normalized cDNA library of Rock bream (Rb) and characterized. The full-length RbHCII and RbPN-1 sequences were compared with other known serpin sequences using ClustalW pairwise and multiple analysis modes. Phylogenetic analysis was performed in order to establish the relationship between known orthologues. The coding regions of RbHCII and RbPN-1 were individually cloned into an expression vector, pMAL-c2X, in order to express the recombinant proteins. The purified recombinant proteins, rRbHCII and rRbPN-1 were used to evaluate the biological functions in *in vitro* assays. Quantitative real-time PCR was employed to determine the tissue-specific transcription of RbHCII and RbPN-1 as well as to investigate their transcriptional regulatory pattern upon challenged with different immune stimulants. In addition, an injury experiment was designed to evaluate the roles of these serpins upon muscle injury.

The full-length sequences of RbHCII (1950 bp) and RbPN-1 (1951 bp) possessed coding regions with the sizes of 1512 bp and 1191 bp encoding polypeptides of 504 and 397 amino acids, respectively. Putative polypeptides of RbHCII and RbPN-1 contained signal peptides and had molecular masses of 58 kDa and 44 kDa, respectively. Both of them demonstrated the serpin family

characteristics of having a serpin domain and a specific serpin signature. The corresponding orthologues of HCII and PN-1 from stickleback (*Gasterosteus aculeatus*) demonstrated high degree of identity and similarity with that of rock bream. Multiple alignment analysis showed that C-terminal part of RbHCII and RbPN-1 is more conserved than that of N-terminal part. Various functionally vital regions of these proteins including reactive centre loop, serpin signature, heparin binding site and hinge region were found to be strongly conserved with respect to the corresponding members from other species. In a phylogenetic point of view, RbHCII was closely related to HCII of Japanese flounder. RbPN-1 was phylogenetically positioned with PN-1s of green spotted puffer fish and Japanese pufferfish. Human HCII (PDB; 1jmoA) and human PAI-1 (chain A, PDB; 1dvmA) were chosen as templates and 3D structures of RbHCII and RbPN-1 were built on them to visualize the folding pattern of the tertiary protein structures. Both models resembled the typical serpin folding.

RbHCII and RbPN-1 genes were cloned into pMAL-c2X, transformed into Rosetta-gami and BL21 (DE3) cells, respectively and induced with IPTG to overexpress the proteins. The recombinant proteins were purified in MBP-fused form using an affinity chromatography and used in activity assays. rRbHCII exhibited its inhibitory activity against chymotrypsin (43.5%) and thrombin (54%), where as rRbPN-1 demonstrated its protease inhibitory potential against trypsin (48%) and thrombin (89%). In all the assays, serpin activity was dose-dependent. Interestingly, heparin potentiated the thrombin inhibitory activity of both rRbHCII and rRbPN-1. In addition, the anticoagulation potential of rRbPN-1 was revealed by an APTT assay on which clotting time was prolonged by 102.1 s/ 14 µg.

RbHCII and RbPN-1 demonstrated tissue specific expression profiles where the higher levels of mRNA were detected in liver and heart, respectively. In mammals, HCII is highly transcribed in liver and however PN-1 is predominantly found in brain. Constitutive expression of RbHCII and

RbPN-1 in an array of tissues suggests a broader range of tasks being played by these serpins *in vivo*. This is the first report revealing the differential tissue specific expression of HCII and PN-1 from a teleostic fish.

Immune stimulation investigations demonstrated that generally RbHCII was down-regulated and RbPN-1 was up-regulated in different tissues after being challenged. The LPS injection down-regulated the hematic and hepatic cell expression of RbHCII while up-regulating the hematic and gill expression of RbPN-1. *Edwesiella tarda* down-regulated the liver and blood cell expression of RbHCII. Whereas the RbPN-1 manifested an up-regulation only at mid-phase of *E. tarda* post-challenge in blood cells and a strong induction at all time points in gill tissue. Rock bream iridovirus (RBIV) down-regulated the expression of RbHCII at both hematic and hepatic cells. On the other hand RBIV induced strong RbPN-1, in hematic cells throughout the experiment and in gills only at late-phase of the experiment, respectively. Each induction generated a distinct profiling of gene expression in different tissues. During pathogen invasion, various serine proteases are coming into play and thrombin is a vital immune mediator among them. The transcriptional control of serpins in different fashion at various tissues ensures that the critical serpin: serine protease equilibrium is properly balanced.

The cause of injury in the expression profile of RbHCII and RbPN-1 was interestingly identical. Both serpins were hypoexpressed in hematic cells of injured animals, suggesting that there is a requirement to loosen their role of controlling proteases in post injury events. All of our transcriptional analysis emphasizes the importance of the tight regulation of counter balance between SPs and Serpins.

Collectively, this study could be considered as a significant contribution to the serpin biology of fish especially with immunological perspectives. To extend our understanding on this aspect, more serpin genes are required to be mined and investigated at molecular level.

List of Figures

- Fig. 1.** Schematic diagram representing the formation of a serpin-protease complex.
- Fig. 2.** The full-length nucleotide and deduced amino acid sequences of rock bream heparin cofactor II.
- Fig. 3.** ClustalW multiple sequence alignment of the deduced amino acid sequence of RbHCII with known homologous heparin cofactor II amino acid sequences.
- Fig. 4.** Un-rooted phylogenetic tree showing the relationship between rock bream heparin cofactor II amino acid sequence and other known HCII, as well as other serpin clades of A - I.
- Fig. 5.** Phylogenetic analysis of RbHCII with selected vertebrate HCII members.
- Fig. 6.** Predicted 3D structure of RbHCII and its important functional components.
- Fig. 7.** Tissue-expression analysis of RbHCII mRNA determined by quantitative real-time PCR.
- Fig. 8.** RbHCII mRNA expression in rock bream tissues in response to challenges by different stimulants.
- Fig. 9.** SDS-PAGE of overexpressed recombinant RbHCII in Rosetta-gamiTM (DE3) cells and purified recombinant fusion protein.
- Fig. 10.** Inhibition of thrombin by RbHCII and effect of heparin on RbHCII activity.
- Fig. 11.** Inhibition of chymotrypsin by RbHCII.
- Fig. 12.** The complete nucleotide and deduced amino acid sequences of rock bream PN-1 cDNA.
- Fig. 13.** ClustalW multiple alignment of the deduced primary sequence of rock bream PN-1 with known vertebrate homologous PN-1 sequences.
- Fig. 14.** Structural model of mature RbPN-1.
- Fig. 15.** Phylogenetic analysis of protease nexin-1 orthologues and PAI-1 members.
- Fig. 16.** SDS-PAGE analysis of overexpressed and purified mature recombinant RbPN-1 fusion protein.

Fig. 17. *In vitro* antiprotease activity assays against trypsin, thrombin and the potentiating effect of heparin.

Fig. 18. *In vitro* anticoagulant activity assays for recombinant RbPN-1.

Fig. 19. Tissue-expression analysis of RbPN-1 mRNA determined by quantitative real-time PCR.

Fig. 20. RbPN-1 mRNA expression in hematic cells in response to challenge by LPS and iridovirus.

Fig. 21. RbPN-1 mRNA expression in gills in response to challenge by LPS and *E. tarda*.

Fig. 21. Impact of muscle injury on mRNA expression of protease nexin-1 and heparin cofactor II in rock bream hematic cells.

List of Tables

- Table 1.** Description of primers used in RbHCII cloning and its transcriptional analysis.
- Table 2.** Homology analysis of the rock bream heparin cofactor II to other vertebrate homologues and serpin clade A member, Alpha 1-Antitrypsin (A1AT) from corresponding vertebrate species.
- Table 3.** Conservation of reactive site loop, serpin signature and boundary of serpin domain in vertebrate HCIIIs.
- Table 4.** Description of primers used in RbPN-1 cloning and its transcriptional analysis.
- Table 5.** Homology index of the rock bream protease nexin-1 to other vertebrate serpin, clade E, member 2 (PN-1) homologues and serpin clade E, member 1 (PAI-1) homologues from corresponding vertebrate species.
- Table 6.** Sequence similarity - identity matrix showing the percent identity/similarity between PN-1 orthologues.
- Table 7.** Conservation and characteristics of functional regions of RbPN-1 and its orthologues.

INTRODUCTION

Serine Protease Inhibitors (Serpins)

Serine proteases (SPs) are a family of functionally related enzymes involved in a variety of important biological processes including digestion, blood clotting (Di Cera and Cantwell, 2001), immune activation (Mark et al., 1988; Sim and Laich, 2000) and cell differentiation (Chasan and Anderson, 1989). The critical regulation of proteolytic activity of SPs is essential to maintain a balanced homeostasis. These molecular events are controlled at different regulatory levels and inhibition is one of such key mechanism and this is achieved by a functional pair of SPs known as serine protease inhibitors (Serpins).

The endogenous serpins are ubiquitous ancient homologous proteins found universally in all domains of life including viruses (Clynen et al., 2005; Irving et al., 2000; Rawlings et al., 2004; Roberts and Hejgaard, 2008) that form the largest superfamily of serine protease inhibitors (Irving et al., 2000). Even though most serpins are protease (largely serine protease) inhibitors, there are serpins like ovalbumin, maspin and angiotensinogen possessing no inhibitory functions. The inhibitory serpins play a diverse role mainly controlling both intracellular and extracellular proteolytic pathways, which are very critical for blood clotting, homeostasis, coagulation, complement activation, fibrinolytic cascade (Rau et al., 2007), inflammatory responses, apoptosis, angiogenesis and tumor suppression and immune defense (Mangan et al., 2008; Mark et al., 1988).

The structure-function relationship of serpins is well elucidated. Serpins have been described as 'molecular mouse traps', in accordance with their mode of action. They sacrifice themselves in order to entrap the targeted protease into an irreversible enzyme-inhibitor complex which is then targeted for degradation. Specifically, the serpins exist in the metastable state with a 'bait' exposed that is targeted to its cognate protease; this molecular 'bait' is known as the reactive centre loop (RCL), a motif of serpin found in the C-terminus and composed of approximately 20 amino acids

which determines specificity of serpin/substrate protease interaction. It contains a scissile bond designated as P₁-P₁' between two amino acid residues, which is the attacking hinge point of target protease to cleave it (Fig. 1). Following bond cleavage, the interaction between serpin and target enzyme may proceed via two types of paths.

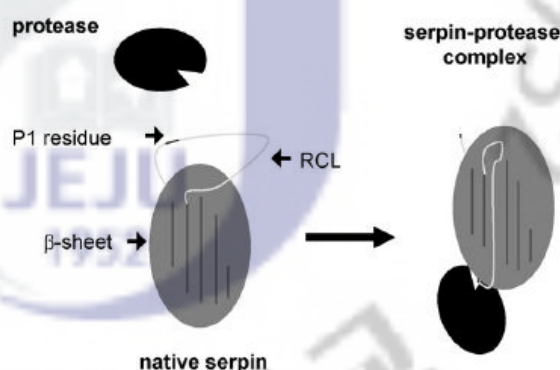


Fig. 1. Formation of a serpin-protease complex (Heutinck et al., 2010). A schematic view of the general mechanism by which serpins inactivate serine proteases is shown. Target proteases bind and cleave the reactive centre loop (RCL) of the serpin. Cleavage of the RCL results in a conformational change, the so called stressed-to-relaxed (S ↔ R) transition. The RCL becomes incorporated into the serpin body rendering the protease covalently bound to the serpin and thereby inactive (Huntington et al., 2000).

Along the first path, RCL cleavage occurs and the serpin undergoes a conformational change from the 'stressed' to 'relaxed' (S to R) state in which the RCL becomes inserted into the β -sheet A. The 'trapped' cognate protease is irreversibly and covalently confined in the form of an acyl enzyme intermediate (Huntington et al., 2000) which is hyperstable. The inhibitory serpins act in a suicide substrate fashion, as they irreversibly deactivate the proteases by forming 1:1 serpin-protease covalent complex. The serpin-enzyme complex (SEC) is then recognized by a specific receptor system, known as the low density lipoprotein receptor-related protein (LRP), which

endocytoses and catabolizes the SEC by cellular-mediated degradation. Plasma clearance is carried out when serpins are in the form of SECs, and not when they are in the native intact form and/or the RCL cleaved form (Mast et al., 1991). Along the second path, cleaved and conformationally altered serpin is rendered inactive where it is associated with other biological functions such as antiangiogenic activity and chemotactic activity (Gettins, 2000). In some cases, allosteric cofactors alter the rate of these enzymatic reactions. Silverman et al. (Silverman et al., 2001) classified the superfamily into 16 clades (A-P), and 10 diverged 'orphans' based on phylogenetics suggested by Irving et al. (Irving et al., 2000). The vertebrate serpins have been categorized into 6 groups by Ragg et al. on a genomic organization perspective (Ragg et al., 2001). Our understanding of serpin biology continues to expand as new family members are added to the MEROPS database (<http://merops.sanger.ac.uk/>) which currently lists more than 1980 serpins under the family I4 (Rawlings et al., 2004). Serpin proteins commonly known as heparin cofactor II and protease nexin-1 are the two important genes from rock bream focused on this study.

Rock bream (*Oplegnathus fasciatus*) is an important marine fish with high economic value and it is cultured in South East Asia, yet there are few reports on the biology of this important fish and currently threatened by significant pathogen attack.

Heparin cofactor II

Heparin cofactor (HCII) is a single chain glycoproteinous serpin that belongs to clade D or group 2. It resembles anti-thrombin III (ATIII) both functionally and structurally to a certain extent. It shares a position with some of the other serpins in a subclass of 'glycosaminoglycan (GAG)-binding serpins' as their inhibitory mechanism depends on GAGs such as heparin. However, HCII is unique in the way it requires stimulation by dermatan sulfate (DS) (Tollefsen et al., 1983). Thrombin is the only SP involved in the clotting cascade that is regulated by HCII (Parker and

Tollefsen, 1985), and there is evidence for chymotrypsin inhibition (Church et al., 1985) by HCII. In fact, GAG cofactors accelerate the HCII-mediated thrombin inhibition. Thrombin is engaged in numerous physiological roles including coagulation, and therefore HCII potentially controls all thrombin-involved biochemical processes (He et al., 2002). Even though the biochemical properties of HCII have been well investigated, detailed physiological roles of HCII still require investigation. There are two types of characteristic domains in HCII, which are essential for its regulatory function. One type is a pair of N-terminally located acidic domains with negative charges. The other is a GAG-binding site that is composed of a cluster of basic and positively charged residues, located in the central region. In the absence of the GAG, these domains are bound together. In the presence of GAG, it displaces the acidic domains and allows them to interact with thrombin and act as template for HCII and thrombin to bring them to an optimal proximity, and thereby increases the rate of inhibition (Ragg et al., 1990; Tollefsen, 1994).

The HCII gene has been identified from numerous vertebrates and deposited in the NCBI database and the plasma purification of HCII has been successfully achieved in a few species. Furthermore, there are few literature reports regarding the corresponding work on the gene characterization, molecular cloning and expression including human (Blinder et al., 1988), rabbit (Sheffield et al., 1994), frog and chicken (Colwell and Tollefsen, 1998).

In the present study, heparin cofactor II cDNA from the rock bream was cloned, sequenced and characterized at the molecular level. Phylogenetic analysis was conducted to determine the evolutionary relationships. The tissue-specific expression profile was determined by analyzing HCII mRNA in eleven rock bream tissues using quantitative real time PCR (qRT-PCR). In addition, rock bream HCII was overexpressed, purified using a pMAL-c2X protein fusion system, and then the biochemical properties of the recombinant rock bream HCII were characterized.

Protease nexin-1

Protease nexin-1 (PN-1)/serpin E2, the glia-derived nexin (GDN), is a glycoprotein secreted by various *in vitro* cultured fibroblasts (Baker et al., 1980), platelets (Gronke et al., 1989), glial cells, neurons and various other nonvascular cells (Eaton and Baker, 1983). PN-1 was found to be able to effectively inhibit several common proteases, including thrombin, trypsin, urokinase-type plasminogen activator (uPA) (Stone et al., 1987), plasmin, tissue plasminogen activator (tPA), factor XIa (FXIa) and prostasin. PN-1 levels in plasma reach the lower limits of detectability and are associated with cell surface and extracellular matrix (ECM) (Farrell et al., 1988) where binding to glycosaminoglycans (GAGs) or ECM co-factors occurs. GAGs modulate the specificity and activity of PN-1, while heparin markedly potentiates the thrombin inhibitory action (Baker et al., 1980; Wallace et al., 1989) and facilitates PN-1's reputation as the most effective thrombin inhibitor in ECM. PN-1 is able to form SDS-stable acyl-intermediate complexes with cognate proteases (Baker et al., 1980), subsequently binding to the cell which secreted it and rapidly being internalized via LRP (Knauer et al., 1997b) and degraded (Low et al., 1981). Thus, PN-1 provides an effective mechanism to control the activity of certain proteases and remove them from the ECM.

Although the primary site of PN-1 expression and action is localized in the brain (Gloor et al., 1986; Simpson et al., 1994) and around the blood vessels (Choi et al., 1990), expression has also been found in other tissues (Mansuy et al., 1993). PN-1 is known to play important roles in neuronal growth, development and differentiation. It also plays a protective role against extravasated proteases (Choi et al., 1990), inhibits and clears proteases from the ECM, promotes neurite outgrowth and modulates ECM degradation (Bergman et al., 1986). Not surprisingly, the expression level of PN-1 has been found to be tightly and dynamically regulated under various patho-physiological (Choi et al., 1990; Mansilla et al., 2008; Wu et al., 2008), inflammatory (Nitsch et al., 1993) and injury (Mbebi et al., 1999; Meier et al., 1989) conditions and at different

developmental stages (Gloor et al., 1986; Mansuy et al., 1993; Zhang et al., 2007). Thus, it is likely that equilibrium between PN-1 and its various cognate proteases under these conditions is carefully controlled to ensure the *in vivo* steady state and homeostatic processes of an organism.

PN-1 sequences from various organisms exist in the public databases, but only a few have been investigated to date. PN-1 orthologues from *Xenopus* (Onuma et al., 2006), chicken (Rodriguez-Niedenfuhr et al., 2003), rat (Arcone et al., 2009; Gloor et al., 1986; Sommer et al., 1987) and human (McGrogan et al., 1988) have been cloned and characterized and some have been evaluated in *in vitro* expression assays. However, the PN-1 gene and its encoded protein from lower vertebrates have not been the subject of such studies and to our knowledge, there is yet no information in the literature on gene characterization and/or mRNA/protein expression of any teleost PN-1.

In the present study, we used the rock bream Genome Sequencer FLX (GS-FLX™) database to identify a Rb PN-1 gene that was then isolated, cloned and characterized. In addition, we overexpressed the RbPN-1 in *E. coli* BL21 (DE3) cells and purified using a pMAL-c2X fusion protein purification system in order to evaluate the functional properties of recombinant PN-1. The antiprotease and anticoagulant capacities of the recombinant protein were individually assayed. Quantitative real-time PCR (qRT-PCR) was employed to perform transcriptional analysis in different rock bream tissues. Furthermore, *in vivo* investigations were carried out to determine the role of PN-1 in post-injury mechanisms and immune defense of rock bream, as well as to elucidate its gene expression responses to muscle injury and immune challenges with LPS, *Edwardsiella tarda* bacterium and rock bream iridovirus (RBIV).

Chapter I

Heparin cofactor II (RbHCII) from rock bream (*Oplegnathus fasciatus*):

Molecular characterization, cloning and expression analysis

1. ABSTRACT

Heparin cofactor (HCII) is a serine protease inhibitor (SPI), and plays important physiological roles in various biological events including hemostasis. The gene encoding the HCII was isolated from GS-FLX™ genomic data of rock bream (*Oplegnathus fasciatus*), designated as RbHCII. The RbHCII (1950 bp) consists of a 1512 bp open reading frame (ORF) encoding 504 amino acids, with a signal peptide of 19 amino acid residues. The predicted molecular mass and the estimated isoelectric point of RbHCII were 58 kDa and 5.9, respectively. The deduced amino acid sequence of RbHCII displayed a characteristic serpin domain and a serpin signature motif (FTVDQPFLFLI). RbHCII demonstrated homology with vertebrate HCIIs and the greatest degree of similarity (90.1%) was observed with *Gasterosteus aculeatus* HCII. Various functional domains including the reactive center loop (RCL), glycosaminoglycan (GAG) and thrombin binding sites and acidic repeats of human and RbHCII were found to be orthologs through the molecular modeling studies. Phylogenetic analysis revealed that RbHCII belongs to the clade D serpins, and is closely related to the clade A members. Constitutive expression of RbHCII mRNA was detected at different levels in various tissues in a tissue-specific manner. Interestingly, RbHCII transcription was significantly downregulated ($p < 0.05$) in liver after challenge with LPS, *Edwardsiella tarda* and rock bream iridovirus (RBIV). However, after the immune challenges, RbHCII showed a significant downregulation in blood tissue only at the late-phase of investigation. The recombinant RbHCII (rRbHCII) was overexpressed in Rosetta-gami (DE3) cells and purified using the pMAL™

system. The rRbHCII inhibited thrombin and chymotrypsin in a dose-dependent manner. Remarkably, heparin was found to be an enhancer of RbHCII's thrombin-inhibitory activity. Correlating the heparin-dependent thrombin-inhibition activity of RbHCII with its temporal downregulation against immune stimulants, it could be suggested that it is not only involved in the blood coagulation cascade, but RbHCII also plays an incognito role in immune modulation.

2. MATERIAL AND METHODS

2.1. Rock bream cDNA library construction and isolation of RbHCII cDNA

We have constructed a rock bream cDNA sequence database by the genome sequence FLX™ genome sequencing technique (Droege and Hill, 2008). Briefly, total RNA was isolated using Tri Reagent™ (Sigma, USA) from several tissue pools including gills, blood, liver, spleen, pituitary gland, head kidney and kidney of three healthy rock bream fish. Then, the mRNA was purified using an mRNA isolation kit (FastTrack® 2.0, Invitrogen, USA). The first strand cDNA synthesis and normalization were carried out with the Creator™ SMART™ cDNA library construction kit (Clontech, USA) and Trimmer-Direct cDNA normalization kit (Evorgen, Russia). Thereafter, the GS-FLX™ sequencing of rock bream cDNA was performed according to the manufacturer's instructions (Roche Applied Science, USA). From the rock bream cDNA sequence library, a single putative EST gene was identified during homology screening using the BLAST program available on NCBI (<http://blast.ncbi.nlm.nih.gov/Blast>) and was designated as RbHCII.

2.2. Sequence characterization and phylogenetic analysis of RbHCII

The RbHCII full-length sequence was analyzed by BLAST. Similarities were compared with other known HCII and serpin sequences available in the NCBI and ENSEMBL databases. To obtain the open reading frame (ORF) amino acid sequence of RbHCII, DNAssist (version 2.2) was used. Characteristic domains or motifs were identified using the PROSITE profile database (Bairoch et al., 1997) and SMART proteomic database (Letunic et al., 2009). Identity, similarity and gap percentages were calculated using EMBOSS pair-wise alignment algorithms. Prediction of signal peptide was accomplished using the SignalP worldwide web server (Bendtsen et al., 2004). Disulfide bond prediction was carried out by the DISULFIND program (<http://disulfind.dsi.unifi.it>). Prediction of tyrosine sulfation sites was performed using the SulfoSite (Chang et al., 2009).

Multiple sequence alignments and phylogenetic analyses were performed on the amino acid sequence of RbHCII versus known HCII, using ClustalW (2.0) (Thompson et al., 1994). The amino acid sequences were aligned using the ClustalW program and the phylogenetic tree was reconstructed using the neighbor-joining (NJ) method by the molecular evolutionary genetic analysis (MEGA 4.1) software package (Kumar et al., 2004) with bootstrapping values taken from 1000 replicates.

2.3. Homology modeling

To generate the structure models, the amino acid sequence of the mature RbHCII was submitted to Swiss-Model (<http://swissmodel.expasy.org/>), and analyzed using the Project (optimize) mode (Arnold et al., 2006). The 2.2 Å resolution crystal structure of human heparin cofactor II (PDB, 1jmoA) was selected from the PDB database (<http://www.pdb.org/pdb/home/home.do>) and used as a template. The three-dimensional (3D) images were generated by Swiss-Pdb viewer version 4.0.1.

2.4. Experimental animals

Healthy rock bream fish (average body weight of 50 g) were obtained from the Jeju Special Self-Governing Province Ocean and Fisheries Research Institute (Jeju, Republic of Korea). They were maintained in 40 L tanks with aerated and sand filtered seawater at a temperature of 24 ± 1 °C and salinity of 34 ± 1 ‰. All fish were acclimatized to laboratory conditions for 1 week prior to the experiment before being injected with immune stimulators/ injured.

2.5. RbHCII mRNA expression analysis

2.5.1. Fish tissues for the specific distribution analysis

To examine the tissue-specific expression profile of RbHCII, healthy individuals were selected. Fish were carefully dissected on ice and tissues from gills, liver, heart, spleen, intestine, head kidney, kidney, skin, muscle and brain were collected and pooled from 3 fish for RNA extraction. Using a sterilized syringe, the blood (1-2 mL per fish) was collected from the rock bream caudal fin and immediately centrifuged at 3000 x g for 10 min at 4°C. The supernatant was removed and cells were harvested for RNA extraction. All tissue samples were snap-frozen in liquid nitrogen immediately after they were collected from fish, and stored at -80°C until the total RNA was isolated.

2.5.2 Expression pattern of RbHCII after stimulated by LPS, bacteria and virus

To determine the immune responses of RbHCII, pathogenic bacteria *E. tarda*, rock bream iridovirus (RBIV) and LPS were used as immunostimulants in time course experiments. For bacterial challenge, the fish were intraperitoneally-injected with *E. tarda* (5×10^6 CFU/mL) suspended in 1× phosphate buffered saline (PBS; 100 µL/animal). RBIV was prepared from kidney of RBIV-infected rock bream. Kidney was homogenized in approximately 10 volumes of 1× PBS (1 mL PBS/ 100 mg tissue). The homogenate was centrifuged at 3000 × g for 10 min, and the supernatant was filtered with a 0.45 µm syringe filter and stored at -80 °C until future use. For RBIV challenge experiment, the supernatant was injected into fish intramuscularly at a dosage of 100 µL per 50 g fish. For LPS-induced transcriptional analysis, the fish were injected with 100 µL LPS in PBS suspension (1.25 µg/ µL, 055:B5 from *E. coli*, Sigma-Aldrich, USA).

At time points of 3, 6, 12, 24 and 48 h post-injection/ infection (p.i.), tissues (liver, gills and blood) were taken from *E. tarda*, RBIV-challenged, and LPS-injected rock bream to determine the transcriptional profiles of RbHCII. Untreated and PBS-injected animals were kept separately as

the control groups. All samples were obtained and analyzed in triplicate and the results are expressed as relative-fold change as mean \pm standard deviation.

2.5.3. Total RNA isolation and first strand cDNA synthesis

The total RNA was extracted from pooled tissues of 3 animals of untreated control, *E. tarda*-RBIV-, and LPS-induced individuals using Tri Reagent™ (Sigma, USA) according to the manufacturer's protocol. Originally purified RNA was diluted to 1 $\mu\text{g}/\mu\text{L}$ concentration prior to cDNA synthesis. 2.5 μg RNA was used to synthesize cDNA from each tissue using a SuperScript III first strand synthesis system for RT-PCR (Invitrogen, USA). Briefly, RNA was incubated with 1 μL of 50 μM oligo(dT)₂₀ and 1 μL of 10 mM dNTP for 5 min at 65 °C. After incubation, 2 μL of 10 \times cDNA synthesis buffer, 2 μL of dithiothreitol (DTT, 0.1 M), 4 μL of 25 mM MgCl₂, 1 μL of RNaseOUT™ (40 U/ μL) and 1 μL of SuperScript III reverse transcriptase (200 U/ μL) were added and incubated for 1 h at 50 °C. The reaction was terminated by raising the temperature to 85 °C for 5 min. Finally, 1 μL of RNase H was added to each synthesized cDNA and incubated for 20 min at 37 °C. The resulting cDNA was diluted 10-fold before being stored at -20 °C for further experiments.

2.5.4. Quantitative real-time-PCR (qRT-PCR)-based RbHCII mRNA expression analysis

The RT-PCR was carried out to analyze the mRNA expression of RbHCII, in a 20 μL reaction volume containing 4 μL of cDNA from each tissue, 10 μL of 2 \times TaKaRa Ex Taq™ SYBR premix, 0.5 μL of each gene-specific primer (20 pmol/ μL) and 5 μl dH₂O. The qRT-PCR cycle profile was: 1 cycle of 95 °C for 10 s, followed by 35 cycles of 95 °C for 5 s, 58 °C for 10 s and 72 °C for 20 s, and finally, 1 cycle of 95 °C for 15 s, 60 °C for 30 s and 95 °C for 15 s. The same qRT-PCR cycle profile was used for the internal reference gene, β -actin. The primers used in this study

are presented in Table 1. β -actin primers were designed based on the EST of the 1879 bp sequence (Accession No. FJ975145) from rock bream. The baseline was set automatically using the Thermal Cycler Dice™ Real Time System Software (version 2). The relative expression was determined by means of the $2^{-\Delta\Delta CT}$ method (Livak and Schmittgen, 2001). All data represent means \pm standard deviation.

2.6. Cloning of RbHCII coding sequence

The open reading frame (ORF) of RbHCII was amplified, using cloning oligos (RbHCII-1F, RbHCII-1R) with corresponding restriction enzyme sites of *EcoRI* and *HindIII* at the N-terminus and the C-terminus for RbHCII, respectively, listed in Table 1. The PCR was performed in a TaKaRa thermal cycler in a total volume of 50 μ L with 5 U of Ex Taq polymerase (TaKaRa, Japan), 5 μ L of 10 \times Ex Taq buffer, 8 μ L of 2.5 mM dNTP, 50 ng of template and 20 pmol of each primer. The reaction was carried out with an initial incubation at 94 $^{\circ}$ C for 2 min, 30 cycles (94 $^{\circ}$ C, 30 s; 55 $^{\circ}$ C, 30 s; 72 $^{\circ}$ C, 60 s), followed by a final extension at 72 $^{\circ}$ C for 5 min. The PCR product was analyzed on a 1% agarose gel and ethidium bromide staining. Subsequently, the amplified product was excised from a parallel gel and purified using the Accuprep™ gel purification kit (Bioneer Co., Korea). The PCR product and maltose binding protein (MBP)-fused expression vector pMAL-c2X (New England Biolabs Inc, USA) were digested with respective restriction enzymes and the vector was dephosphorylated with calf intestine phosphatase (NEB, USA), in accordance with the vendor's protocol. Thereafter, the vector and PCR product were purified by a 1% agarose gel using the Accuprep™ gel purification kit (Bioneer Co., Korea). Ligation was carried out at 16 $^{\circ}$ C, overnight with 100 ng of pMAL-c2X vector, 70 ng of PCR product, 1 μ L of 10 \times ligation buffer and 0.5 μ L of 1 \times T4 DNA ligase (TaKaRa, Japan). The ligated product, pMAL-c2X/RbHCII, was transformed into XL1 blue cells, followed by Rosetta-gami™ (DE3) (Novagen, Germany) competent cells for protein expression.

Table 1. Description of primers used in RbHCII cloning and its transcriptional analysis.

Name	Target	Primer Sequence (5'→3')
RbHCII-1F	ORF amplification (<i>EcoRI</i>)	(GA) ₃ <u>gaattc</u> ATGTGGGTCATCACCGTCATCTCT
RbHCII-1R	ORF amplification (<i>HindIII</i>)	(GA) ₃ <u>aagctt</u> TTAGCTCTGTGAAGGATTGACCACCC
RbHCII-2F	RT-PCR amplification	TTGGCTACACACTACGCTCTGTGA
RbHCII-2R	RT-PCR amplification	TCAGCCCTTTGGTCAGCTTTAGGA
Rb-β-actin-F	RT-PCR Internal reference	TCATCACCATCGGCAATGAGAGGT
Rb-β-actin-R	RT-PCR Internal reference	TGATGCTGTTGTAGGTGGTCTCGT

2.7. Overexpression and purification of recombinant RbHCII (rRbHCII)

The recombinant protein was overexpressed in Rosetta-gami (DE3) cells in the presence of isopropyl- β -thiogalactopyranoside (IPTG). Briefly, 10 mL volume of Rosetta-gami (DE3) starter culture was inoculated in 100 mL Luria broth with kanamycin, tetracycline, ampicillin, chloramphenicol (at final concentrations of 15, 12.5, 100, 34 μ g/ mL, respectively) and 10 mM glucose (2% final concentration). The culture was incubated at 37 °C with shaking at 200 rpm until the cell count reached 0.8 at OD₆₀₀. Then culture was shifted to 15 °C for 15 min and induced by IPTG at 0.2 mM final concentration for 5 h. The induced cells were cooled on ice for 30 min, and harvested by centrifugation at 3500 rpm for 30 min at 4 °C. The cells were resuspended with 5 mL column buffer (Tris-HCl, pH 7.4, 200 mM NaCl) and frozen at -20 °C overnight. The recombinant RbHCII (rRbHCII) was purified in the form of fusion protein with MBP by pMALTM protein fusion and purification system (NEB, USA). Briefly, the thawed resuspended Rosetta-gami (DE3) cells were placed in an ice-water bath and sonicated 6-8 times in short pulses for 15 s. Then the sonicated cell suspension was centrifuged at 15000 rpm for 30 min at 4 °C and the resulting supernatant considered as crude rRbHCII extract. In the final purification step, amylose resin was poured into a 1 \times 5 cm size column. The crude extract was loaded onto the column and washed with 12 \times volume of the column buffer. Finally, the rRbHCII fusion protein was eluted by applying a total of 1.5 mL elution buffer (column buffer + 10 mM maltose) in 0.5 mL aliquots. To determine the protein induction, solubility level, state of purity and molecular weight, the rRbHCII samples were collected from different purification steps and then subsequently analyzed on 12% SDS-PAGE with protein size markers (TaKaRa, Japan). The gel was stained with 0.05% Coomassie blue R-250, followed by a standard de-staining procedure. All of the activity tests performed in this study were conducted using this purified rRbHCII fused with MBP. The concentration of the

purified protein was determined via the Bradford method, using bovine serum albumin (BSA) as the standard (Bradford, 1976).

2.8. Biochemical properties of rRbHCII

To characterize the inhibitory activity of rRbHCII, trypsin, thrombin and chymotrypsin were employed and the hydrolysis of synthetic chromogenic substrates was monitored. The trypsin inhibitory activity assay was carried out by measuring residual activity of trypsin in the reaction mixture. The standard reaction mixture (1 mL) contained 50 mM Tris-Cl, pH 8.0 with 0.2 mg/mL trypsin (final concentration) from porcine pancreas (Sigma) and either rRbHCII (100 nM – 1 μ M final concentration) or buffer as a control. The reaction was initiated by the addition of 500 μ L 0.1% w/v azocasein (Sigma) in the same buffer and incubated for 50 min at 37 °C. The reaction was stopped by adding 500 μ L 15% trichloroacetic acid and then kept on ice for 15 min. The precipitate was separated by centrifugation, and OD₄₄₀ of the colored compound obtained was measured spectrophotometrically (Bio-Rad, USA). The inhibitory activity of rRbHCII on the digestion of N-benzoyl-L-tyrosine ethyl ester (BTEE) (Sigma) by chymotrypsin was measured using a reaction mixture (200 μ L) containing 80 mM Tris-HCl, pH 7.8 with 50 mM CaCl₂, 0.2 nM bovine α -chymotrypsin type II (Sigma) and rRbHCII (5 - 320 nM final concentration) or buffer as a control. The reaction mixture was pre-incubated for 5 min at 25 °C. The reaction was initiated by the addition of 0.5 mM final concentration of BTEE, and OD₂₅₃ was measured at a 30 s interval for 10 min. The inhibitory activity of rRbHCII towards thrombin (bovine plasma, Sigma) was assayed with and without heparin separately. The inhibition tests were carried out in a buffer of 100 mmol/L Tris-HCl, pH 8.0, with a total volume of 200 μ L. 0.25 μ M thrombin was separately pre-incubated with increasing concentration of inhibitor (1/4-, 1/2-, 1-, 2-, 4-, 8-, 16-fold to the enzyme) in the buffer for 5 min at 30 °C. Then, the remaining activity was tested by addition of

chromogenic substrate solution of Phe-Val-Arg-p-nitroanilide hydrochloride (Sigma). To determine the effect of heparin, it was added at final concentration of 10 U/mL, and separately assayed. The reaction mixture was incubated at 30 °C for 15 min and the absorbance of p-nitroaniline formed was determined at OD₄₀₅. The blanks were prepared similarly to the samples, just without enzyme or substrate solution. In addition, all assays were conducted with the MBP to determine the effect of fusion protein on the activity of rRbHCII. All determinations were performed with three replicates, and mean values were used for the calculation. The percentage of inhibition (%I) was calculated using the formula: $\%I = [(A_o - A_i) / A_o] \times 100$, where A_i and A_o are the absorbance with and without rRbHCII, respectively.

2.9. Statistical analysis

For comparison of relative RbHCII mRNA expression and inhibition properties, statistical analysis was performed using one-way ANOVA and mean comparisons were performed by Duncan's Multiple Range Test using SPSS 11.5 at the 5% significance level.

3. RESULTS

3.1. Molecular characterization of RbHCII primary structure

The RbHCII cDNA was identified by the screening of rock bream cDNA database sequences using the BlastX program. The identified sequence showed similarity to known HCII family members, therefore it was designated as rock bream heparin cofactor II (RbHCII). The nucleotide and deduced amino acid sequences of the HCII from rock bream are shown in Fig. 2. The RbHCII nucleotide sequence has been deposited in GenBank under accession number HM582203. The full-length RbHCII consisted of 1950-bp with a 1512-bp coding sequence which encodes a putative polypeptide of 504 amino acids. Sequence analysis indicated the presence of a 70-bp 5' untranslated region (UTR) and 365-bp 3' UTR region, which contains an RNA instability motif (¹⁷⁸³ATTTA¹⁷⁸⁷), with a typical polyadenylation signal (¹⁹³³AATAAA¹⁹³⁸). RbHCII has putative molecular mass of 58 kDa with a 5.9 isoelectric point (*pI*). Importantly, RbHCII is highly conserved in a serpin domain spanning the residues from 140 to 501. The PROSITE program (<http://kr.expasy.org/prosite>) revealed a motif of serpins signature (⁴⁷⁴FTVDQPFLFI⁴⁸⁴) in the C-terminal end of deduced amino acid sequence. The N-terminal region of the RbHCII was found to have a signal peptide which was determined by the SignalP 1.1 server with a cleavage site at ¹⁹A-²⁰G. Five N-glycosylation sites (¹⁵¹NQSD¹⁵⁴, ¹⁹³NASH¹⁹⁶, ²⁰⁰NTTV²⁰³, ³⁵⁷NISM³⁶⁰, ³⁹²NRTR³⁹⁵) were identified in the RbHCII amino acid sequence by the NetNGlyc 1.0 server and were shown in primary structure. Even though the protein contains 3 Cys residues, there was no indication of any disulfide cross linkage by the DISULFIND program. With a prediction sensitivity of 90%, SulfoSite detected 3 potential Tyr residues for sulfation, where 2 (Tyr⁷² and Tyr⁸⁶) were found within the N-terminal acidic tails. Interestingly, RbHCII possesses a relatively high number of Leu residues (50) representing 9.9% of the total amino acid sequence.

TTCTTTGCTC TTAGTCTACAAACA GAAGCCACACAGCAC TTCCTGCCAGCAC AGTAAAGCCTTCAGG -70

*ATGTGGGTTCATCAC GTCATCTCTGTGGCC TGTCTGTGGTCA GTTCCATCCAGGCTGGG ATCAAAGACCTGAGC 75
M W V I T V I S V A C L L V S P S Q A G I K D L S 25

TCTCACTTCGCTGAC CCTAACCCAGACCCC AGAGGCTTTGAAGG GATGAAGTGGATATA GGGCCATCCCTTG 150
 S H F A D P K P D P R G F E G D E V D I G A I P L 50

GAGTTCACAAAGAA AACACTGTCTACTAAT GACCTTGTTTTIGAT GGCTTTGAGGATGAA GATTATATTGATTT 225
 E F H K E N T V T N D L V F D G F E D E D Y I D F 75

GATAAGATCCTAGT GCGGGCAGTGACGAC TACATTGAAGGGAT GAGATAGATGAGATT GCCACACGAGCTCCA 300
 D K I L A A G S D D Y I E G D E I D E I A T P A P 100

GACATTGACATCTT GCCGAACCCCTCCGAC CCAAGATTCGCGGT GCCAGACTCCTGGGG CTGTTCCACGGTCGG 375
 D I D I F A E P S D P K I R R A R L L R L F H G V 125

TCTCGCCTCCAACGC CTCAACATTGTTAAT GCCCATTTGGTTTT AACCTCTATCGAAGT CTTCGTAACGATGC 450
 S R L Q R L N I V N A H F G F N L Y R S L R N D V 150

AACCAGAGTGACAAC ATCCTGCTAGCACCT GCTGGGATCCTCCATC GCTATGGGGATGATG TCTTTAGGGGCAGGA 525
N Q S D N I L L A P A G I S I A M G M M S L G A V 175

CCTGGAACCCAGAT CAGATCTACAAAGCT CTGGGATTCGCTGAG TTTGTCAATGCTAGC CATCACTATGACAAC 600
 P G T H D Q I Y K A L G F A E F V N A S H H Y D N 200

ACAACAGTGACAAG CTCTTCAGAAAGCTG ACACACAGGCTCTC AGGAGAACTTTGGC TACACACTACGCTCT 675
T T V H K L F R K L T H R L F R R N F G Y T L R S T 225

GTGAACGATGCTAC GTAAGAAGGAAGTC TCAGTGAAGACGCT TTTGAGCAGAGACA AAGCTTATATTTT 750
 V N D V Y V K K E V S V K D A F R A E T K A Y Y F 250

GCAGAGCCGAGTCA GTGGACTTCAGGAC CCTGCCTTCTCGAC AAGGCCAACCGTCGC ATCCTAAAGCTGACC 825
 A E P Q S V D F R D P A F L D K A N R R I L K L T 275

AAAGGCTGATCAGG GAACCGCTCAGAGT GTGGACCAAAATG GTGCTGATGCTGCTA AACTACCTGACTTC 900
 K G L I R E P L K S V D P N M V L M L L N Y L Y F 300

AAAGTACATGGGAA CAGAAATTCGCCAAA GAAATGACTCACTAT CGCAACTCAGAGTT AACGAAAAACAAT 975
 K G T W E Q K F P K E M T H Y R N F R V N E K T N 325

TACGCTGCCAATG ATGACCAACAAGGGG AACTATCTGGCTGCA GCAGACCAAGCACTA GAGTGTGACATCTTA 1050
 V R V P M M T N K G N Y L A A A D H E L E C D I L 350

CAGTCCCATACACA GGAAACATCAGCATG CTCATTGCCCTGCCT AGGAAGATCACTGGC ATGAGGACCTTGAG 1125
 Q L P Y T G N I S M L I A L P R K I T G M R T L E 375

CAGGAGATCTCTCC ACTGTGTGAACAAG TGGCTCAAAAACATG ACAACAGGACTCGA GAGGTGGTGGCTGCT 1200
 Q E I S P T V V N K W L K N M T N R T R E V V L P 400

CGTTTAACTGGAG CAGAGCTATGACTTG ATTGAAAATTGAAG GAGATGGGCTCACT GACTTGTTCAGAG 1275
 R F K L E Q S Y D L I E N L K E M G L T D L F Q E 425

AGTGGAGATTCTCT GGAATGACCTCGAA AAGTTGTTCATGAC TGGCTGAGCACCAG GGAACCATCACTGTG 1350
 S G D F S G M T S E K V V M N W L K H Q G T I T V 450

AATGAAGAGGGGACA GAGGCTGCTGCTG ACCCAGGTGGGCTTC ATGCCCTCTCCTCT CAGATCCGCTCACT 1425
 N E E G T E A A A L T Q V G F M P L S S Q I R **F T** 475

GTGGACCAGCTTTC CTCTCCTCATCTAC GAGCACCACAGAC TGCCTTGTGTTTCATG GGCCGGTGGTCAAT 1500
V D Q P F L F L I Y E H R T D C L V F M G R V V N 500

CCTTCACAGAGCTAAACTTGACAAAAAGC CTTTCAACAGCTA AACTATCCCTACAA ATCCCATGTTGGTT 1575
 P S Q S 504

AGACCTCCGACTAA AACATCCGGTGCTTC GAATAGCTGGAGTGT TGTTTTTAATAGTC AGTTACTTCTGTTAG 1650

TACAATATGTACATG TGACATCAAGTAATG AGTCTTTATGTGTAT GTAGTCTCTACTGA **ACTTAA**ACTTCTC 1725

CTTCTCAGTGTGT GAGTCTGTCGAGTG ACTCAATGTAAGCTT GTTATCTGCTGTGA ATGTTTTATCTTATT 1800

CAATGAGGCTAGTG ACAATGTGCCACAA AAAATGACATTATAT AACTGTCAATTACCT **ATAATAA**ATAATAT 1875

ATAAC 1880

Fig. 1: The full-length nucleotide and deduced amino acid sequences of rock bream heparin cofactor II. The start (ATG) and stop (TAA) codon sequences are bold underlined with an asterisk (*). Predicted signal peptide is bold and underlined. The putative serpin signature motif (⁴⁷⁴FTVDQPFLFLI⁴⁸⁴) is boxed shaded. The potential putative N-glycosylation sites are shaded in italics. The RNA instability motif (ATTTA) and the polyadenylation signal sequence (AATAAA) are bold underlined in italics.

3.2. Pair-wise and multiple alignment analysis of RbHCII

Pair-wise alignment of RbHCII with different vertebrate members was performed by the ClustalW program maintaining an open gap penalty and gap extension penalty levels at 10.0 and 0.5, respectively. We also investigated the sequence identity, similarity and gap percentages of RbHCII with sequences of vertebrate orthologs and serpin clade A member, Alpha 1-Antitrypsin (A1AT) from corresponding vertebrates, available in GenBank, ENSEMBL, and MEROPS databases (Table 2). Notably, RbHCII showed significant high homology to all sequences considered, with percentages (%) above 52.2 and 69.6 of identity and similarity, respectively, and showed gaps (%) below 7.8. The greatest degree of identity (90.1%) was observed with the stickleback, *Gasterosteus aculeatus* HCII. Interestingly, teleost HCII showed distinct characteristic features of a comparatively lengthy polypeptide with a range of 502 – 507 amino acid and high degree of similarity to RbHCII ranging from 72 to 94.5 (%). Furthermore, our results on the variation of RbHCII identity in comparison to A1AT members indicated that identity varies within only from 19 to 29.9 (%). However, RbHCII shares more homology with mammalian serpin A members (A1AT) than the corresponding members from different teleosts.

Additionally, RbHCII amino acid sequence was aligned with vertebrate representative HCII sequences in ClustalW multiple analysis (Fig. 3). Results indicated that 2 partially conserved acidic repeats located at the N-terminus and the corresponding residues of rock bream were ⁶⁸EDEDYID⁷⁴ and ⁸¹AGSDDYIEGD⁹⁰ (Fig. 6E). Comparatively, the C-terminal region showed a higher degree of conservation than the N-terminal region, especially in the C-terminally expanding region (~120-520 amino acid), which was identified as a characteristic serpin domain by the SMART program. Table 3 shows the remarkable strong conservation of the reactive site loop and serpin signature of the vertebrates analyzed. Exclusively, the scissile bond and the 6th residue of the signature (Pro) are highly conserved among all species of interest. Furthermore, all HCII amino

acid sequences displayed a signal peptide of 19 residues, except the sequence from rat which possesses 24 residues, and among 3 Cys found in RbHCII, 2 were completely conserved among all HCIIIs analyzed.



Table 2: Percentage identity, similarity and gaps of the rock bream heparin cofactor II to other vertebrate homologues and serpin clade A member, Alpha 1-Antitrypsin (A1AT) from corresponding vertebrate species.

Gene	HCII	A1AT								
Species	Accession No	aa	I (%)	S (%)	G (%)	Accession No	aa	I (%)	S (%)	G (%)
Stickleback	ENSGACP00000005614 ^a	503	90.1	94.5	0.6	ENSGACP00000010699 ^a	408	22.7	37.6	26.0
Fugu	ENSTRUP000000033122 ^a	502	88.1	94.0	0.4	ENSTRUP00000014672 ^a	400	21.8	39.6	25.5
Puffer fish	MER123872 ^b	504	87.3	93.7	0	ENSTNIP00000020507 ^a	353	19.0	34.0	35.2
Medaka	ENSORLP00000002789 ^a	505	86.6	93.9	0.6	ENSORLP00000020052 ^a	408	21.3	38.7	25.9
Zebrafish	AAN71003	507	75.3	87.6	1.8	AAI24742	429	29.9	45.3	17.8
Frog	NP_001080817	484	55.1	72.1	4.7	NP_001080271	432	28.7	45.7	17.2
Lizard	ENSACAP00000002155 ^a	476	54.1	69.6	7.8	ENSACAP00000003935 ^a	437	25.3	44.9	15.5
Turkey	ENSMGAP00000000330 ^a	489	56.7	73.3	3.8	ENSMGAP00000013918 ^a	439	28.5	46.9	14.4
Zebra finch	ENSTGUP00000009056 ^a	471	55.8	71.7	6.5	ENSTGUP00000018172 ^a	381	23.9	39.8	28.2
Rat	NP_077358	479	53.6	72.4	5	AAH78824	411	23.8	39.0	29.9
Bat	ENSPVAP00000011102 ^a	492	52.7	71.0	6.2	ENSPVAP00000013508 ^a	413	24.7	43.8	20.5
Human	AAA52641	499	52.2	71.7	5.2	AAV38262	418	26.6	44.8	19.6

Pair-wise identity percentage was calculated using EMBOSS alignment (<http://www.ebi.ac.uk>) maintaining open gap penalty and gap extension penalty levels at 10.0 and 0.5, respectively. aa: amino acids; I: identity; S: similarity; G: gaps.

^a: ENSEMBL database accession number

^b: MEROPS database identifier

Table 3: Conservation of reactive site loop, serpin signature and boundary of serpin domain in vertebrate HCIIIs.

Species	Reactive site loop & Serpin signature [¶]	Serpin domain [§]	Accession No	aa	
	▼ "Signature"				
Rb	454 GTEAAALTQVGFMP LSSQIR-FTVDQ PFLFLI	484	140 - 501	HM582203	504
Jf	455 GTEAAALTQVGFMP LSSQIR-FTVDHPFLFLI	485	141 - 502	ACC86113	505
Pf	454 GTEAAALTQVGFMP LSSQIR-FTVDHPFLFLI	484	140 - 501	MER123872 ^b	504
Zf	457 GTEAAAMTHI GFMP LSTQTR-FIVDRPFLFLI	487	143 - 504	AAN71003	507
Fr	434 GTEAAAVTVVGFMP LSTQAR-FVADR PFLFLI	464	121 - 481	NP_001080817	484
Ch	438 GTEAGAITNVGFMP LSTQIR-FIVDRPFLFLI	468	124 - 485	MER018706 ^b	488
Rt	429 GTQAAAVTVVGFMP LSTQVR-FTVDRPFLFLV	459	115 - 476	NP_077358	479
Ms	428 GTQAAAVTVVGFMP LSTQVR-FTVDRPFLFLV	458	114 - 475	AAA18452	478
Ra	430 GTQAAAVTVVGFMP LSTQVR-FTVDRPFLFLV	460	116 - 477	AAB32401	480
Op	432 GTQAAAVTVVGFMP LSSQVR-FIVDRPFLFLI	462	118 - 479	MER069155 ^b	482
Pg	445 GTQAAAVTVVGFMP LSTQAR-FSVD R PFLFLI	475	131 - 492	XP_001929601	495
Bv	447 GTQAAAVTAVGFMP LSTQVR-FSVD R PFLFLI	477	132 - 493	NP_001098516	496
Mk	477 GTQATAVTVVGFMP LSTQVR-FTVDRPFLFLI	507	163 - 524	XP_001086351	527
Cz	477 GTQATTVTVVGFMP LSTQVR-FTVDRPFLFLI	507	163 - 524	XP_001167937	527
Hu	449 GTQATTVTVVGFMP LSTQVR-FTVDRPFLFLI	479	135 - 496	AAA52641	499

: * : : * : **: * * - * . * : *****:

[¶]by SMART program; [§]by PROSITE program; ^bMEROPS identifier; amino acid: amino acids; “*” Identical; “:” conserved; “.” Semi-conserved. ▼ denotes the scissile bond; “signature” is shown separated by a dash from reactive site loop. Rb, rock bream; Jf, japanese flounder; Pf, puffer fish; Zf, zebrafish; Fr, frog; Ch, chicken; Rt, rat; Ms, mouse; Ra, rabbit; Op, opossum; Pg, pig; Bv, bovine; Mk, monkey; Cz, chimpanzee; Hu, human.

Signal peptide	
Rock bream	<i>MWVITVISVACLLVSPSQAGIKDLSSHADFADPKP-----DPRGFEGD--EVDIGAIPLE</i> 51
Flounder	<i>MWVITVISAAACLLVSPSLAGVKDLSSHFTLQ-----DPRGFEPDG-AVNIEAIPLE</i> 52
Puffer fish	<i>MWVISLVCVAWLMAASPSEAETKHPSSPLSDPKP-----DPRGFEGT--EMDIEALPLE</i> 51
Zebrafish	<i>MWLVVPVIVVACLNSPALAGVKDLSSHFTLEKEKTV---DARGLSPGGENTDMESIPLD</i> 57
Frog	<i>-MKLLHLATIFLLIHATLGGVKDLQEH-----FEDTSTGIN-PRGSQTQAVE</i> 45
Chicken	<i>MKFLFPLLALAVIITSTFCGIKDFSDHFES-----LKDAHTHENGTYNMPDLPLE</i> 50
Rat	<i>MKHPAYTLLLSLIMS-MCAGSKG-----LAEQLTKEN--LTVSLLPPN</i> 40
Human	<i>MKHSNLALLIFLIITSAWGGSKGPLDQLEKGGETAQSADPQWEQLNKN--LSMPLPAD</i> 58
	:: * ::
	←A.D→ ←A.D→
Rock bream	<i>FHKENTVTNDLVDFGFEDEYIDFDKILAAGSDDYIEGDEIDEIATPAPDIDIFAEPDSDP</i> 111
Flounder	<i>FHKENTVTNDLVDFGFEDEYIDFDKILAAGSDDYIEGDEIDDIATPAPDIDIFAEPDSDP</i> 112
Puffer fish	<i>FHKENTVTKETIFDGFDEYIDFDKILAAGSDDYSDGDNDIETATPAPDIDIFAEPDSDP</i> 111
Zebrafish	<i>FHKENTVTNDLP-EGQDDEYVDFDKILGE--DDYSEGHIDESTPAPDLDFYEPSDP</i> 114
Frog	<i>NLLDDTVTNDLSTEGEDEEDYVDFDKIFGE--DEDYIDIID--AAPEIKN-----S</i> 92
Chicken	<i>FHRENTIITNDLIPEEEEEDYLDLDKILGE--DD-YSDIID--AAPHIV-----S</i> 95
Rat	<i>FHKENTVTNDWIPEGEEDDYLDLEKLLSE--DDYIYVVD--AVSPTD-----S</i> 86
Human	<i>FHKENTVTNDWIPEGEEDDYLDLEKIFSE--DDYIDIVDLSVVSPTD-----S</i> 106
	:::*:*:: : :::**:*::*:. * :* :*
Rock bream	<i>KIRRARLLRLFHGRSRLQRLNIVNAHFGFNLYRSLRNDVNQSDNILLAPAGISIAMGMMS</i> 171
Flounder	<i>KIRRARLLRLFHGRTRLQRLNIVNAHFGFNLYRSLRNDVNQSDYILLAPAGISIAMGMMS</i> 172
Puffer fish	<i>KIRRARLLRLFHGQSRLQRLNIVNAHFGFNLYRSLRNTVNVQSDNILLAPAGISIAMGMMS</i> 171
Zebrafish	<i>KIRRARLLRLFHGQTRLQRLINVVNARFGRLYRKLNRNLNQTNDNILLAPVGISIAMGMMG</i> 174
Frog	<i>ETQQGNIFELEHGKTRVQRLNIIANFGFNLYRAIKNNTDASENILLAPVGISTAMATIS</i> 152
Chicken	<i>EIQQGNILELEQKGKTRIQRLNIIANFGFNLYRSVADKANSSDNILMAPVGISTAMAMIS</i> 155
Rat	<i>ESSAGNILQLEQKSRIRQRLNIIANFGFNLYRVLKDQATSSDNIFIAPVGISTAMGMIS</i> 146
Human	<i>DVSAGNILQLEHGSRIQRLNIIANFGFNLYRVLKQVNTFDNIFIAIPVGISTAMGMIS</i> 166
**:*::**:*::**:*::**:*::**:*::*::*::**:*::**:. . . . : *::**:*::** * . . .
	←'GAG' binding site→
Rock bream	<i>LGAGPGTHDQIYKALGFAEFVNASHHNDNTTVHKLFRKLTHRLFRNFGYTLRSVNDVYV</i> 231
Flounder	<i>LRAGPGTHHPYQALGFAELVNASHHNNTTVHKLFRKVTHRLFRNFGYTLRSVNDVYM</i> 232
Puffer fish	<i>LGAGAETQDQIYKMGFSEFVNASHHNDNTTVHKLFRKLTHRLFRNFGYTLRAVNDVYI</i> 231
Zebra fish	<i>LGVGPNTEQQLFQTVGFAEFVNASNHNNDNTTVHKLFRKLTHRLFRNFGYTLRSVNDLYV</i> 234
Frog	<i>LGTKGQTEQVLLTGFKDFLNASKVEILT LN HNVFRKLTHRLFRNFGYTLRSVNDIYV</i> 212
Chicken	<i>LGKLGQTQEQVLSVLGFEDFINASAKVELMTVHNLFKLTHRLFRNFGYTLRSVNDLYI</i> 215
Rat	<i>LGLRGETEHEVHVSVLHFKDFVNASKVEVTTIHNLFKLTHRLFRNFGYTLQSVNDLYI</i> 206
Human	<i>LGLKGETHEQVHSILHFKDFVNASKVEITT IHNLFKLTHRLFRNFGYTLRSVNDLYI</i> 226
	* * . : : * ::*** * : ***:***:*****.*::**:*::**
Rock bream	<i>KKEVSVKDAFRAETKAYFYFAEPQSVDFRDPAFLDKANRRILKLTKGLIREPLKSVDPNMV</i> 291
Flounder	<i>KKDIQIKDTRFAETKAYFYFAEPQSVDFRDPAFLDKANRRIQKLTKGLIREPLKSVDPNMV</i> 292
Puffer fish	<i>KKDVAVKDAFRAETKAYFYFAEPQSVNFRDPAFLDKANSRILKLTKGLIRQPLKSIDPNMV</i> 291
Zebrafish	<i>KRNVIQDSFRADAKTYFYFAEPQSVDFAADPAFLVKANQRIQKIYTKGLIKEPLKSVDPNMA</i> 294
Frog	<i>KRDFLIREFPKNNLKNYFYFAEAQTVDFGYKDFLTKANRIQQLTKGLIEEALTNVDPALL</i> 272
Chicken	<i>RKDFSILNDFRNNMKTYFYFADAQPAFSDPNFITKTNERILKLTKGLIKEALVNVNPTTL</i> 275
Rat	<i>QKQFPPIREDFKAAMREFYFAEAQEAQSDPAFISKANSHILKLTKGLIKEALENTDSATQ</i> 266
Human	<i>QKQFPILLDFKTKVREYFYFAEAQIADFSADPAFISKTNNHIMKLTKGLIKDALENIDPATQ</i> 286
	:::. : * : :***:* :.* * :* :* :* :* :*****:.* :* :*
Rock bream	<i>LMLLNLYLYFKGTWEQKFPKEMTHYRNFRVNEKTNVRVPMMNKGNLAAADHELECDILO</i> 351
Flounder	<i>LMLLNLYLYFKGTWEQKFPKERTHYRNFRVNEKTNVRVPMMNKGNLAAADHELECDILO</i> 352
Puffer fish	<i>LMLLNLYLYFKGTWEQKFPKESTHYRNFRVNEKTQVRVPMMINRGNLAAADHDLDCDILQ</i> 351
Zebrafish	<i>VMLLNLYLYFKGTWEQKFPKELTHHRQFRVNEKKQVRVLMMNQKGSYLAADHELNCDILO</i> 354
Frog	<i>MLLVNCLYLYFKGTWENKFPVEYTMNMNFRLNEKELVKVPMMKTKGNFLAADPELDCAVLQ</i> 332
Chicken	<i>MMILNCLYLYFKGTWENKFPVEMTTKRSFRLNEKQTKVPMMQTKGNFLAANDPELDCGVIQ</i> 335
Rat	<i>MMILNCLYLYFKGAWMNKFPVEMTHNHFRLNEREVVKVSMMQTKGNFLAANDPELDCDILQ</i> 326
Human	<i>MMILNCLYLYFKGSWVNKFPVEMTHNHFRLNEREVVKVSMMQTKGNFLAANDPELDCDILQ</i> 346
	:::* :***:* :*** * * .**:*:: :* ** .*:..* * :*:* :*

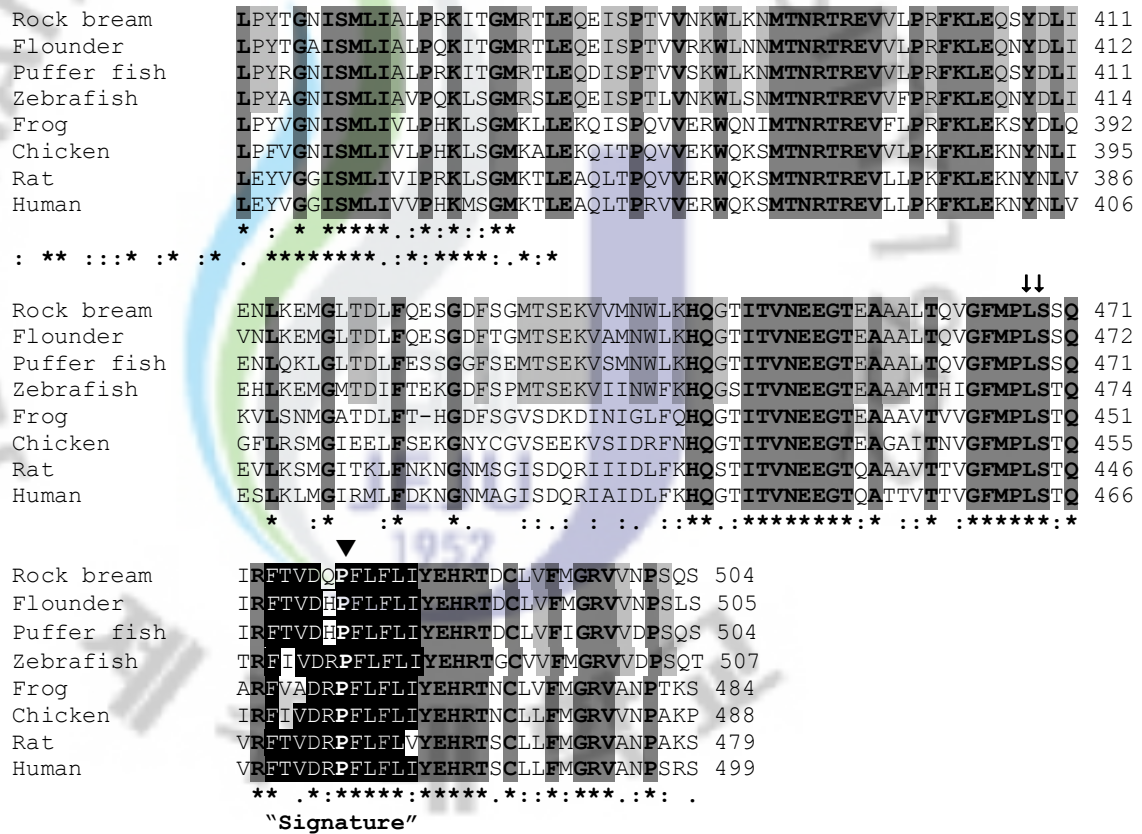


Fig. 3: ClustalW multiple sequence alignment of the deduced amino acid sequence of RbHCII with known homologous heparin cofactor II amino acid sequences. Residues shaded with dark grey and boldface represent the completely conserved (100%) amino acid, indicated by (*) and residues strongly conserved and weakly conserved are indicated by colons (:), or dots (.), respectively. Only the light grey shade represents identical residues among rock bream and other teleost HCII sequences. The numbers at right indicate the amino acid position of HCII in the corresponding species and the dashes indicate the gaps introduced to maximize the alignment. N-terminal signal peptides are shown in italics and two N-terminal acidic domains are named as A.D. The conserved serpin signature motifs are highlighted in black, and highly conserved Pro residue within the signature is shown in bold and marked as ▼. The P1 – P1' reactive site scissile bond is shown by downward arrows (↓) for Leu and Ser. The accession numbers are given in Table 3.

3.3. Analysis of phylogenetic position of the RbHCII

We were interested to determine the phylogenetic position of RbHCII among various serpins. Representatives (60) from several clades of serpins were analyzed to construct an unrooted phylogenetic tree by the NJ method using 2 sequences from fruitfly and sea squirt as out-groups (Fig. 4). Our results showed that all investigated serpin members were divided mainly into 9 clades A-I, which have been denoted following each species name. All HCII distictively clustered to form clade D, which had a closer relationship with clade A. To further understand the ancestral relationship of rock bream HCII with other HCII, a traditional tree was generated (Fig. 5). Results indicated that vertebrate HCII members showed two main clusters of teleostic HCII, and all other vertebrate HCII, among which, the amphibianic HCII deviated to form a sub-cluster. Aves and reptilian HCII were sub-clustered and mammalian HCII formed several branches. Rock bream reserved a position with Japanese flounder within the teleost cluster, with moderate bootstrap support.



Fig. 4: Un-rooted phylogenetic tree showing the relationship between rock bream heparin cofactor II (serpin clade D) amino acid sequence and other known HCIIIs, as well as other serpin clades of A - I. The clade identifiers are shown next to each species. The tree is based on an

alignment corresponding to full-length amino acid sequences by the NJ method using ClustalW and MEGA (4.1). It was bootstrapped 1000 times. The scale bar represents a genetic distance 0.1 as the frequency of substitutions in pair-wise comparison of two sequences. The sequences of serpin 28D (NP_609172) from fruitfly (*Drosophila melanogaster*) and neuroserpin-like protein (XP_002129317) from sea squirt (*Ciona intestinalis*) were used as out-groups. Accession numbers of the sequences used to construct the tree are as follows: from clade A (Alpha 1-Antitrypsin or α 1-antitrypsin (A1AT)): zebrafish *Danio rerio* (AAI24742); grass carp *Ctenopharyngodon idella* (ACC95535); rainbow trout *Oncorhynchus mykiss* (NP_001117869); frog *Xenopus laevis* (NP_001080271); rat *Rattus norvegicus* (AAH78824); horse *Equus caballus* (BAG69583); human *Homo sapiens* (AAV38262); from clade B (ovalbumin1 (OVA1)): zebrafish *Danio rerio* (AAQ97848); fugu *Takifugu rubripes* (ENSTRUP00000016778)^a; frog *Xenopus (Silurana) tropicalis* (AAH88021); human *Homo sapiens* (AAP35574); zebra finch *Taeniopygia guttata* (ENSTGUP00000002180)^a; dolphin *Tursiops truncatus* (ENSTTRP00000003632)^a; from clade C (Antithrombin (AT)): salmon *Salmo salar* (CAB64714); zebrafish *Danio rerio* (CAK05346); lizard *Anolis carolinensis* (ENSACAP00000015125)^a; frog *Xenopus laevis* (NP_001080079); rat *Rattus norvegicus* (NP_001012027); human *Homo sapiens* (CAI19423); elephant *Loxodonta africana* (ENSLAFP00000003638)^a; from clade D (heparin cofactor II (HCII)): rock bream *Oplegnathus fasciatus* (HM582203); puffer fish *Tetraodon nigroviridis* (MER123872)^b; zebrafish *Danio rerio* (AAN71003); frog *Xenopus (Silurana) tropicalis* (AAH89647); rat *Rattus norvegicus* (NP_077358); human *Homo sapiens* (AAA52641); lizard *Anolis carolinensis* (ENSACAP00000002155)^a; chicken *Gallus gallus* (MER018706)^b; turkey *Meleagris gallopavo* (ENSMGAP00000000330)^a; from clade E (nexin (NX1)): zebrafish *Danio rerio* (NP_001108031); frog *Xenopus laevis* (NP_001090520); lizard *Anolis carolinensis* (ENSACAP00000001243)^a; human *Homo sapiens* (AAH10860); megabat *Pteropus vampyrus* (ENSPVAP00000009035)^a;

bovine *Bos Taurus* (AAI03452); from clade F (alpha-2 antiplasmin, pigment epithelium derived factor (PEDF)): zebrafish *Danio rerio* (NP_001004539); frog *Xenopus laevis* (NP_001085983); lizard *Anolis carolinensis* (ENSACAP00000014427)^a; platypus *Ornithorhynchus anatinus* (XP_001507178); sheep *Ovis aries* (NP_001132919); human *Homo sapiens* (EAW90577); from clade G (C1 inhibitor (C1)): rat *Rattus norvegicus* (AAH61860); pig *Sus scrofa* (NP_001116666); human *Homo sapiens* (AAH11171); opossum *Monodelphis domestica* (XP_001376402); turkey *Meleagris gallopavo* (ENSMGAP00000009949)^a; from clade H (heat shock protein 47): zebrafish *Danio rerio* (XP_682911); rainbow trout *Oncorhynchus mykiss* (BAD90029); frog *Xenopus laevis* (NP_001121311); dog *Canis lupus familiaris* (XP_542305); human *Homo sapiens* (AAH36298); lizard *Anolis carolinensis* (ENSACAP00000002176)^a; from clade I (neuroserpin1): zebrafish *Danio rerio* (XP_685811); salmon *Salmo salar* (NP_001133889); frog *Xenopus laevis* (NP_001086240); chicken *Gallus gallus* (ENSGALP00000015400)^a; mouse *Mus musculus* (AAH06776); human *Homo sapiens* (EAW78573).

^a ENSEMBL database accession number

^b MEROPS database accession number

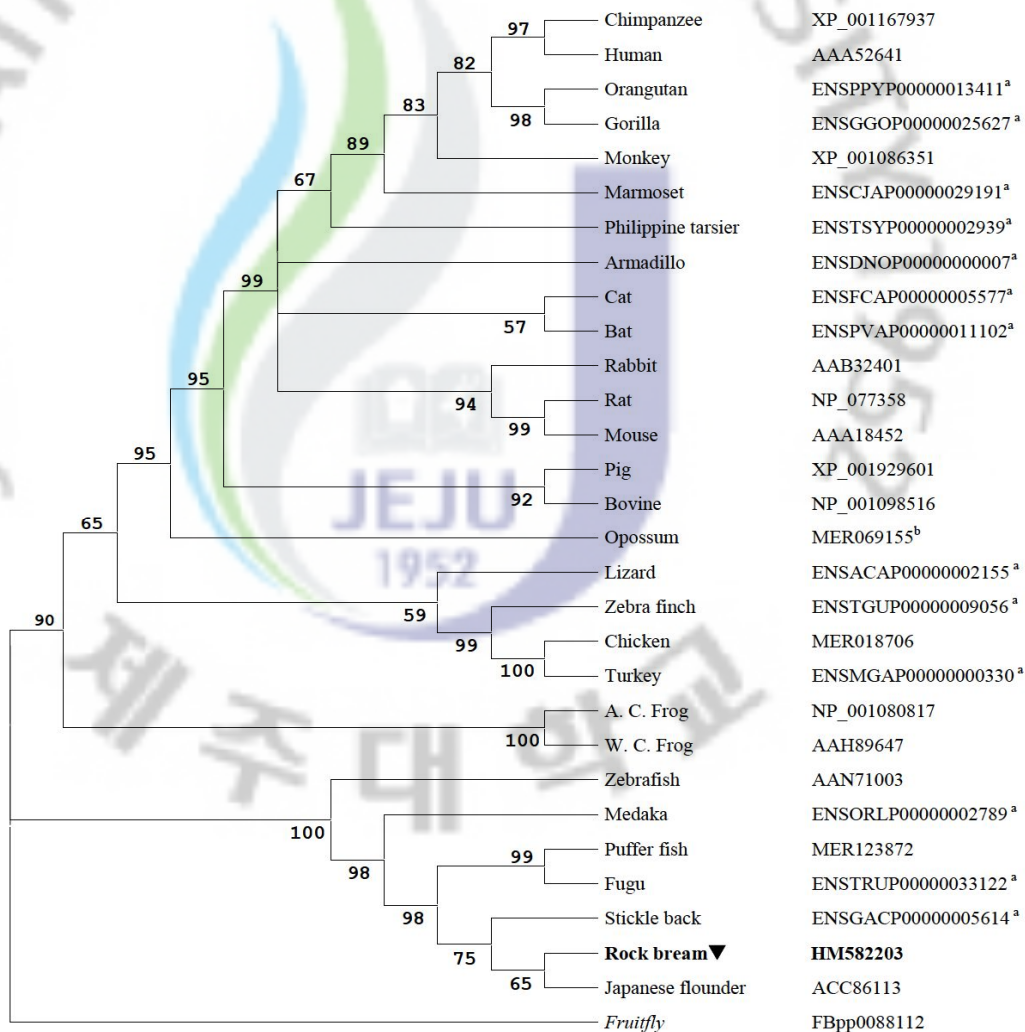


Fig. 5. Phylogenetic analysis of RbHCII with selected vertebrate HCII members. The tree is constructed by the NJ method, based on an alignment corresponding to full-length amino acid sequences, using ClustalW (2.0) and MEGA (4.1). The sequence of Serine protease inhibitor 43Aa from fruitfly (*Drosophila melanogaster*) was used as out-group. The numbers at the branches denote the bootstrap majority consensus values on 1000 replicates. The accession numbers are shown next to each species.

^a ENSEMBL database accession number

^b MEROPS database identifier

3.4. Molecular modeling of tertiary structure of the RbHCII

To further understand the structure-function relationships and comparisons, we generated the 3D structure of RbHCII using the Swiss-Model prediction algorithm, based on the template (PDB code: 1jmoA) of human HCII. The homology between RbHCII and template was 57.4 % on the direct sequence level of amino acids, suggesting a high reliability of the predicted structure. In addition, the Ramachandran plot statistics revealed that 96% and 84% of the residues of RbHCII were in the tolerable and most favored regions, respectively. The overall structure of RbHCII was composed of eight α -helices and three β -sheet domains, two of them with five parallel sheets (Fig. 6, A). RCL was partially incorporated into a five-stranded β -sheet A. Furthermore, the components and majority of the residues essential for the inhibitory activity of RbHCII were conserved between rock bream and human HCIIs (Fig. 6, B-E), however the amino acid positions were slightly different.

Baglin et al. (2002) established the crystal structures of native and thrombin-complexed human HCII and postulated its allosteric mechanism (Baglin et al., 2002). Investigations revealed that ¹⁷³Lys, ¹⁸⁴Arg ¹⁸⁵Lys, ¹⁸⁹Arg, ¹⁹²Arg and ¹⁹³Arg residues in helix D, the GAG-binding site of human mature HCII, play a critical role in cofactor binding (Bourin and Lindahl, 1993; Colwell et al., 1999). Surprisingly, except the ¹⁷³Lys→¹⁷⁸His, all of the other residues were conserved in helix D (Fig. 6C) of RbHCII. Another GAG-binding region of HCII is helix A and the residues that take part in this activity are ¹⁰¹Lys, ¹⁰³Arg and ¹⁰⁶Arg (Baglin et al., 2002; Hayakawa et al., 2002). In RbHCII, only ¹⁰¹Lys was substituted by a basic residue, ¹⁰⁶Arg (Fig. 6B). A hydrophobic pocket formed by ²⁸⁸Met, ³⁰⁸Gln and ²⁹⁰His buries a Trp residue of thrombin. Without affecting its hydrophobicity, the substitution of Gln→Thr occurred in RbHCII. An Asn residue of thrombin establishes hydrogen bonds with atoms of residues, ²⁸⁷Glu, ²⁸⁹Thr and ²⁸⁶Val in human HCII. In RbHCII, ²⁹¹Lys replaces the ²⁸⁶Val (Fig. 6D) and other residues remain conserved. The N-terminal

hirudin domain is rich in negatively-charged residues (Fig. 6E), and upon formation of Michaelis complex with thrombin, it interacts with the anion binding exosite 1 of thrombin.



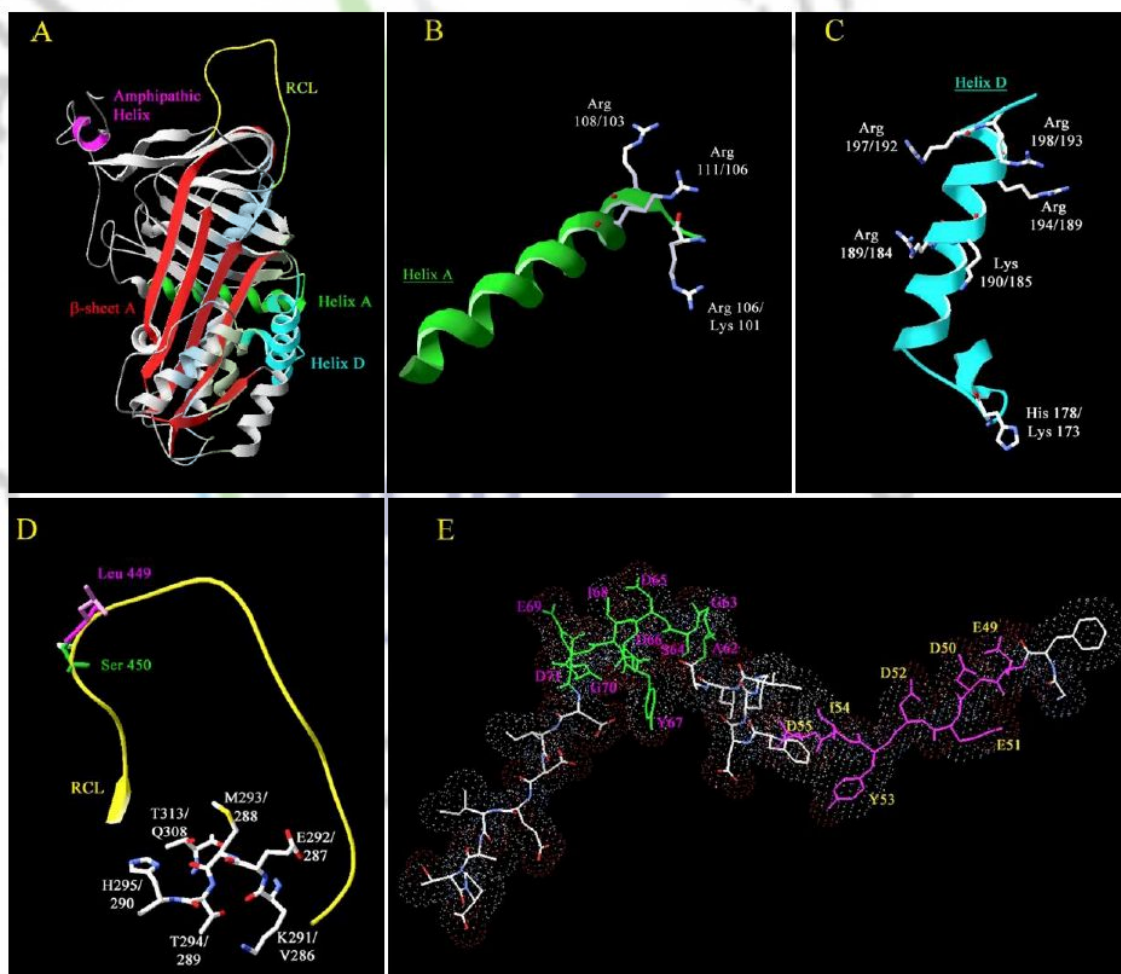


Fig. 6: Predicted 3D structure of RbHCII and its important functional components. (A) The native structure of mature RbHCII constructed by Swiss-Model; reactive center loop, RCL (yellow) is partially incorporated into β -sheet A (red); heparin/ dermatan sulfate binding sites, helix D (cyan) and helix A (green); an amphipathic helix (magenta) in between two acidic repeats. (B) Helix A; and, (C) helix D and their active residues. (D) RCL, scissile bond (L-S) and residues that interact with thrombin. (E) The uninterrupted density and two acidic (hirudin) domains of the N-terminus. (B), (C), (D) show the view overlays between rock bream and human HCII and conserved residues.

3.5. Tissue distribution analysis of RbHCII mRNA

To determine the tissue-specific expression profile of RbHCII mRNA, qRT-PCR was performed using gene-specific primers designed for the ORF of RbHCII. The relative expression of each tissue was calculated using rock bream β -actin as a reference gene, where β -actin expression remained relatively constant in all tissues. The results were further compared with muscle expression levels to determine the relative tissue-specific expression profile (Fig. 7). RbHCII mRNA was detected in all tissues in a tissue-specific fashion, highlighting its significant physiological role in multiple tissues. Further analysis indicated a significantly ($p < 0.05$) higher constitutive expression level in the liver (12800 \times), followed by skin (275 \times), gill (39 \times) and blood (28 \times). In contrast, RbHCII was poorly expressed in intestine (11 \times), spleen (10 \times), kidney (8 \times), head kidney (4 \times) and muscle (1 \times). The tissues of heart (22 \times) and brain (18 \times) displayed a moderate abundance of RbHCII transcripts.

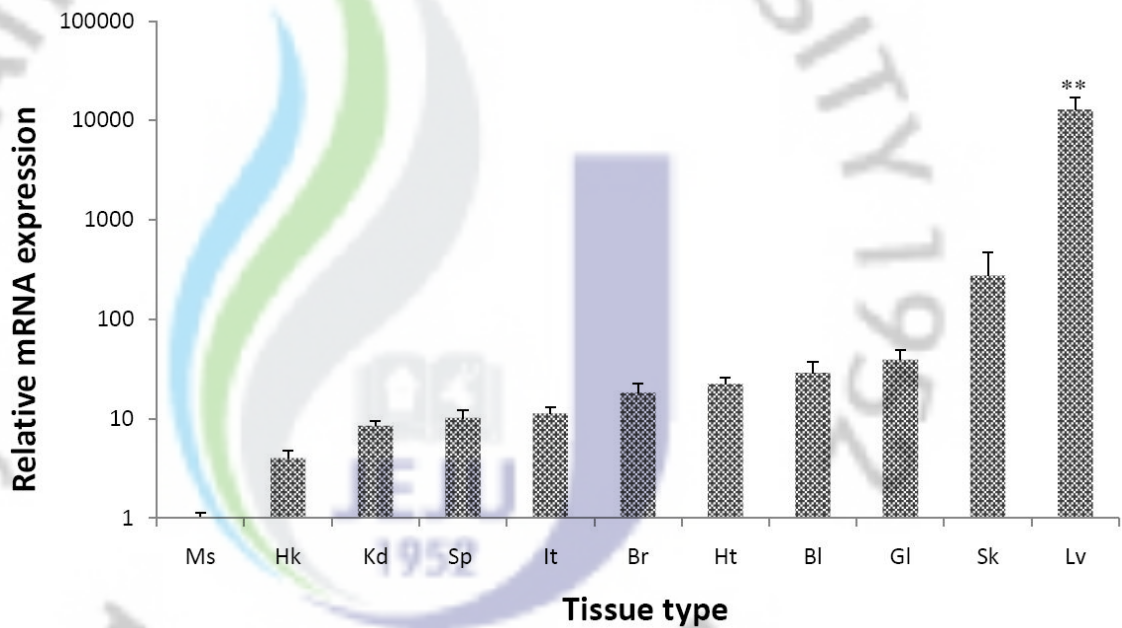


Fig. 7. Tissue-expression analysis of RbHCII mRNA determined by quantitative real-time PCR. The relative RbHCII mRNA expression of each tissue was calculated by the $2^{-\Delta\Delta CT}$ method using rock bream β -actin as a reference gene. Then, the relative mRNA level was compared with muscle expression to determine the tissue-specific expression. Ms-muscle; Hk-head kidney; Kd-kidney; Sp-spleen; It-intestine; Br-brain; Ht-heart; Bl-blood; Gl-gill; Sk-skin; Lv-liver. The bars represent the standard deviation (n=3). Statistical analysis was performed by one-way analysis of variance (ANOVA) followed by Duncan's Multiple Range test using the SPSS 11.5 program. Differences were considered statistically significant (**) at $p < 0.05$.

3.6. Transcriptional modulation of RbHCII expression during immune stimulation

Next, RbHCII mRNA expression levels in the liver and blood following an *in vivo* immune challenge were determined. The relative transcriptional levels of the RbHCII were calculated using rock bream β -actin expression as a reference, and the results were further compared to respective PBS-injected control expression levels to determine the fold induction. No significant difference was observed in un-induced control and PBS-injected controls at 3 and 48 h p.i. Therefore, the 3 h p.i. PBS sample was used to determine the transcriptional regulation by different stimulants in this study.

Interestingly, the RbHCII transcript level was downregulated in liver tissue after all challenges during the period of the experiment, 3 h - 48 h p.i. (Fig. 8A). During the LPS induction, RbHCII expression was significantly ($p < 0.05$) downregulated after 3 h and subsequently reached its lowest relative expression (27%) at 6 h compared to the control. Although, it was slightly upregulated after 12 h and 24 h p.i., the expression levels of those time points were significantly lower ($p < 0.05$) than that observed for the control. As a late-phase response for LPS, RbHCII mRNA level had again decreased significantly at 48 h p.i. RbHCII transcript level varied in a slightly different pattern for the *E. tarda* injection from the LPS induction in liver. Initially, it was downregulated until 12 h p.i. with mild alteration, however the level of expression was significantly ($p < 0.05$) lower than the control at all time points. Subsequently, the transcript level was further significantly ($p < 0.05$) downregulated at 24 h and 48 h p.i. Moreover, the lowest relative expression (26%) was observed at 24 h p.i. compared to control. In liver of RBIV-injected individuals, transcription level was significantly ($p < 0.05$) downregulated gradually up to 24 h p.i, except for a slightly increased expression level observed at 12 h compared to 6 h p.i. The lowest level (61%) of RbHCII expression was observed at 24 h after RBIV infection. A mild increase in expression level occurred at 48 h p.i. compared to 24 h p.i.

The expression pattern of RbHCII transcripts in rock bream blood after different challenges is shown in Fig. 8B. In fish stimulated with LPS, there were no significant changes observed in the transcription level at 3 h and 6 h p.i. However, mRNA of RbHCII was significantly ($p < 0.05$) upregulated at 12 h with 137% expression. Then levels decreased at 24 h and 48 h p.i. At 48 h p.i. RbHCII transcription level reached its lowest level (80%), which was significantly lower than the level observed at 12 h p.i. The *E. tarda*-infected individuals showed a result similar to LPS induction up to 6 h p.i. However, a clear late-phase response was observed for *E. tarda* infection from 12 h - 48 h p.i., where transcription level was significantly ($p < 0.05$) downregulated at all time points. The lowest relative expression (33%) was observed at 48 h p.i. compared to the control. As a response to RBIV, RbHCII was significantly ($p < 0.05$), but transiently downregulated at 3 h p.i., then gradually reached basal level and remained at that level. Thereafter, the RbHCII transcriptional level was significantly ($p < 0.05$) downregulated to its lowest level at 48 h with 65% expression. All these findings indicated that RbHCII expressed in liver and blood tissues of rock bream, *Oplegnathus fasciatus*, differentially responded to the LPS, *E. tarda* and RBIV immune challenges undertaken in this study. It is noteworthy that each induction profile of RbHCII in rock bream tissues investigated was specific to a particular immune challenge.

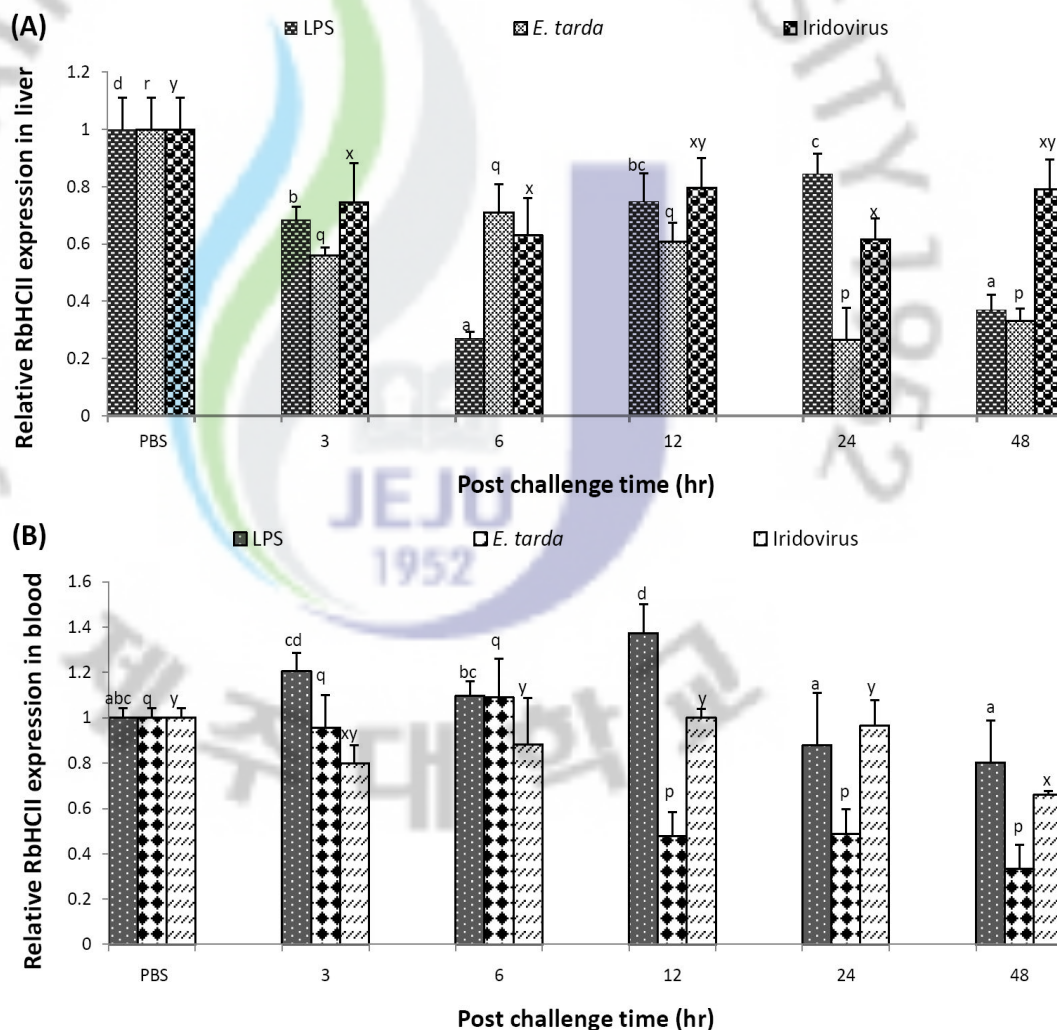


Fig. 8. RbHCII mRNA expression in rock bream tissues in response to challenges by different stimulants. As determined by SYBR green real time RT-PCR in (A) liver tissue and (B) blood after challenges. The relative RbHCII mRNA expression was calculated by the $2^{-\Delta\Delta CT}$ method using rock bream β -actin as a reference gene and relative to PBS control. The vertical bars represent the mean SD (n= 3). Statistical analysis was performed by one-way analysis of variance (ANOVA) followed by Duncan's Multiple Range test using the SPSS 11.5 program. Data in the same exposure time with different letters (for LPS challenge: a-d; *E. tarda* challenge: p-r; RBIV: x-y) are significantly different (P < 0.05) among the times compared.

3.7. Expression and purification of recombinant RbHCII

The recombinant RbHCII was overexpressed in Rosetta-gamiTM (DE3) cells by IPTG-driven induction and purified as a MBP fusion protein. Aliquots of different fractions during the purification steps were analyzed by SDS-PAGE (Fig. 9). It was clear that RbHCII was induced (lane I) compared to un-induced cells (lane U). Lane P shows the purified recombinant RbHCII fusion protein. The molecular mass of this fusion protein rRbHCII was approximately 100.5 kDa, as determined by SDS-PAGE. Since the molecular mass of MBP is 42.5 kDa, predicted and determined molecular mass values of RbHCII appeared to be the same (58.5 kDa).

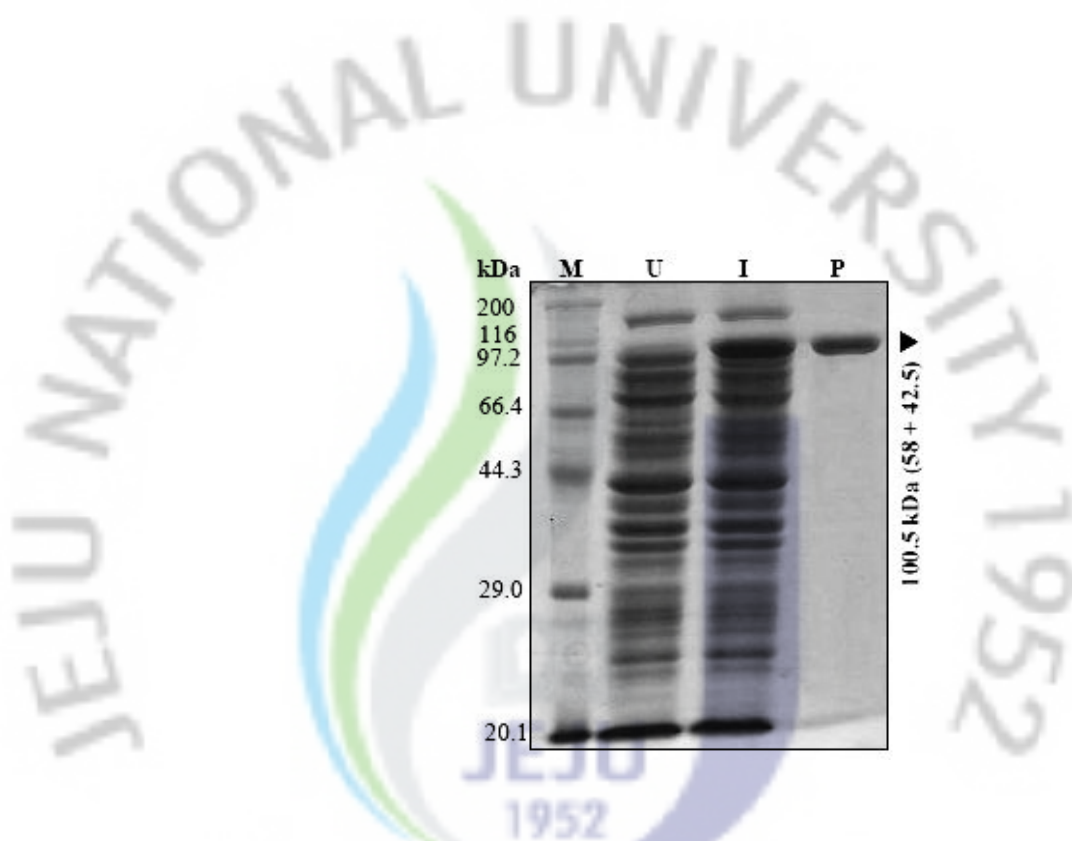


Fig. 9. SDS-PAGE of overexpressed recombinant RbHCII in Rosetta-gamiTM (DE3) cells and purified recombinant fusion protein. Lane M: protein marker (Takara, Japan); lane U: before IPTG-driven induction; lane I: after IPTG induction at 15 °C for 5 h; lane P: purified recombinant protein in MBP-fused form using the pMALTM protein fusion and purification system.

3.8. Biochemical characterization of recombinant RbHCII

The inhibitory effect of rRbHCII on the hydrolysis of synthetic chromogenic substrates by serine proteases (trypsin, chymotrypsin and thrombin) was investigated. Among these proteases tested, rRbHCII was able to inhibit chymotrypsin and thrombin activity under the assay conditions in a dose-dependent manner (Fig. 10, 11 (A), (B)).

The sigmoidal curve (Fig. 10, 11A) indicates the best fit for the %-inhibition data and rRbHCII (320 nM)-inhibited chymotrypsin activity by 43.5% on average. Investigation of the time course inhibitory effect of rRbHCII on chymotrypsin activity (Fig. 11B) revealed the progression of inhibition with time-frame. At high concentrations, the required time for a certain level of inhibition was low. However there was a slight increase in relative enzymatic activity by 2 min. Furthermore, no inhibitory activity was obtained for trypsin on azocasein hydrolysis, even up to 320 nM concentration of rRbHCII. However, RbHCII displayed inhibitory activity against thrombin (Fig. 10). The maximum inhibitory activity of RbHCII towards thrombin in the presence (86%) and absence (54%) of heparin were significantly ($p < 0.05$) different within the tested range of its concentration. The data also suggested that there was no significant ($p < 0.05$) inhibitory activity from MBP compared to the inhibitory activity of rRbHCII at corresponding concentrations towards chymotrypsin and thrombin.

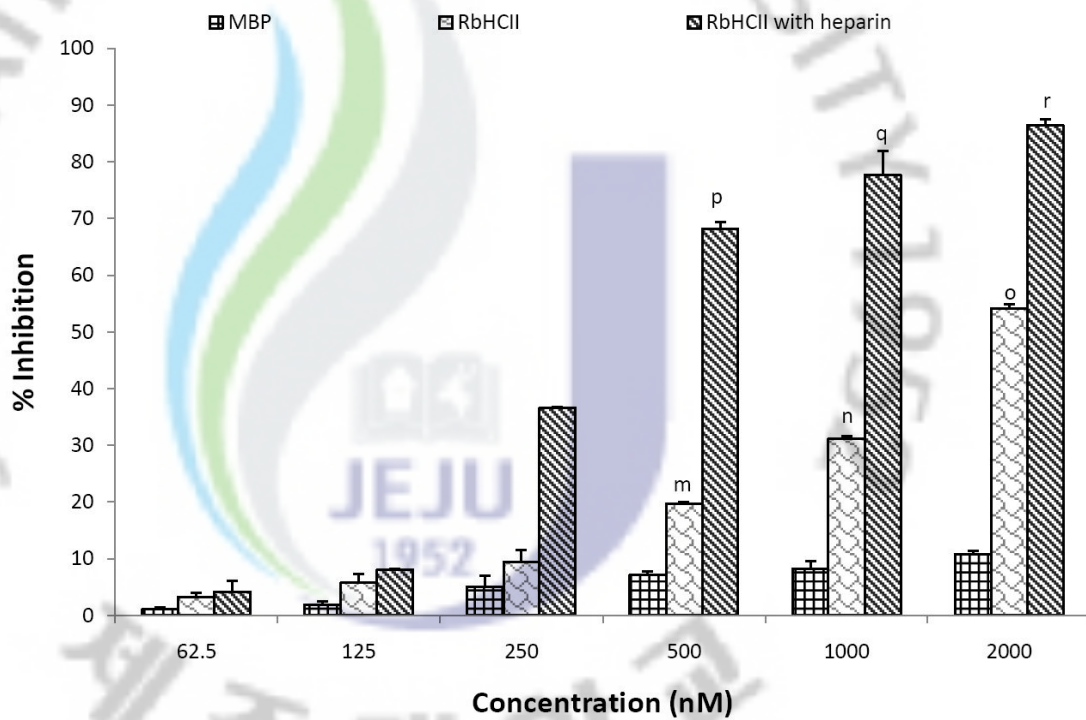


Fig. 10. Inhibition of thrombin by RbHCII and effect of heparin on RbHCII activity. Columns represent the %-inhibition of MBP, RbHCII and RbHCII in the presence of heparin, respectively, at different concentrations. The vertical bar represents the mean SD (n=3). Data with different letters are significantly different ($P < 0.05$) among different groups.

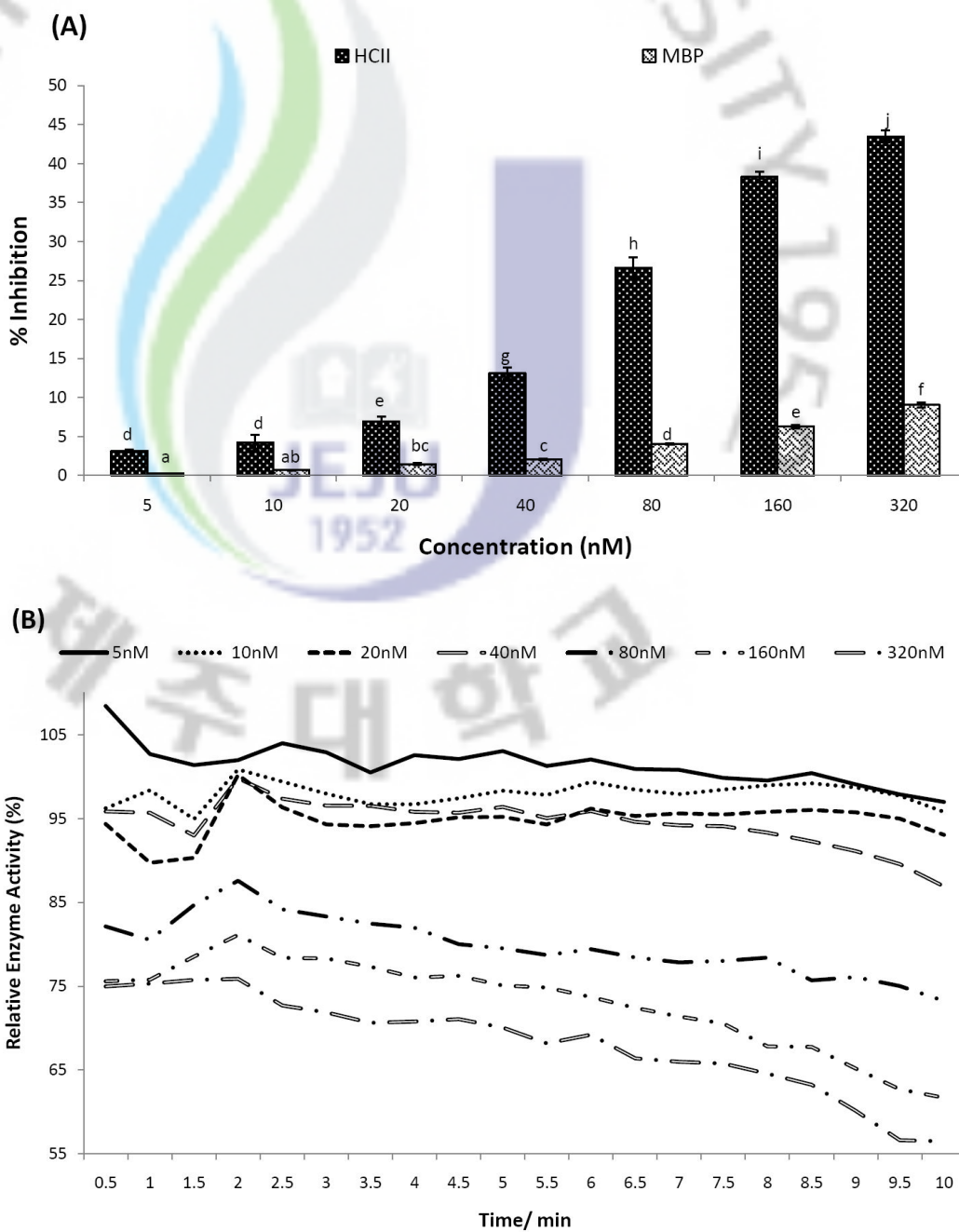


Fig. 11. Inhibition of chymotrypsin by RbHCII. (A) Inhibitory curve. Gray and black columns represent the RbHCII and MBP, respectively, at different concentrations. The vertical bar represents the mean SD (n = 3). Data with different letters are significantly different (P < 0.05) among different groups. (B) Relative enzyme activity and its dose-dependence.

4. DISCUSSION

Hemostasis, a phenomenon that ultimately causes the bleeding process to stop, is an important feature for the response to vascular injury and the pathophysiology of vertebrates. The molecules and pathways involved with hemostasis in human being have been extensively studied, as they are involved in the dysregulatory diseases such as thrombosis. The biochemical pathways of hemostasis are comprised of various proteins including SPs and serpins. Unfortunately, compared with mammals, the molecular information regarding the genes involved in coagulation and anti-coagulation is relatively scarce from lower order vertebrates such as the teleost fishes, as only a few genetic elements have been identified.

Various studies demonstrated the presence of several elements of coagulation proteins (kallikrein, prothrombin, factor VII, IX, and X), anti-coagulation elements (protein C, ATIII and HCII) (Jagadeeswaran and Sheehan, 1999; Sheehan et al., 2001), as well as other serpins from the plasma of different teleosts. In addition, the recently established *Fugu rubripes* and *Tetradon nigroviridis* fish genome databases contain most hemostatic and serpin genes. Although such genes have been identified in different fish species, including serpins such as ATIII from *Atlantic halibut* (Park et al., 2005), A1AT, ATIII, C1 inhibitor from Japanese flounder, only a few of them have been characterized, for instance, factor VII, IX, X, prothrombin, ATIII and HCII from zebrafish (Hanumanthaiah et al., 2002), a SPI from carp (Huang et al., 1995) and ATIII from salmon (Andersen et al., 2000). In this study, we report a novel heparin cofactor II gene from rock bream, *Oplegnathus fasciatus*. RbHCII gene was cloned and characterized at molecular level. The tissue-specific distribution of RbHCII transcript was determined. The transcriptional response of the RbHCII to various immune stimulants was investigated. Furthermore, the recombinant protein was expressed and purified to examine its biological activity.

Striking similarities between rock bream and other mammalian primary protein sequence,

domain architecture and postulated 3D tertiary structure suggest that this cDNA is orthologous to mammalian HCII. Heparin cofactor II shares several characteristic features of serpins including medium molecular weight (40-60 kDa), a C-terminally located serpin domain, RCL-interacting sequence and its suicide inhibitory mechanism of physiologically important proteases, based on conformational change. In agreement with the common features of serpins, RbHCII displays 58 kDa molecular weight, a serpin domain (140-501 residues), and RCL (~454-474 residues). Unsurprisingly, RbHCII possessed a serpin signature within its serpin domain, but had a characteristic substitution of ⁴⁷⁸Gln residue for Arg in mammals. It was reported that human HCII possesses 3 N-glycosylation sites and contains 10% of carbohydrate by weight (Pratt et al., 1989). It can be postulated that the carbohydrate content of RbHCII might be higher than that of human as it contains 5 N-glycosylation sites. It was reported that the antithrombin III (ATIII), a functional homologue of HCII, contains an essential disulfide bond for heparin-dependent thrombin inhibition (Church et al., 1987). However, similar to human HCII, no disulfide bond was predicted in RbHCII even though both HCIIs contain 3 Cys residues. Two of the three Tyr-sulfation sites found in RbHCII occurred in two tandem repeats, rich in acidic residues which were also observed in human HCII. It has been described that a feature of many of the serpins is that they regulate the factors in the coagulation system and they themselves are under the control of GAGs. HCII was shown to bind with physiological GAGs including heparin, DS and few polyanions. In fact, the binding of GAGs to HCII takes place through a basic stretch in the D-helix, which in turn modulates the HCII-thrombin interaction (Pike et al., 2005). Various Lys and Arg residues on or near the helix D are found to be important in GAG binding (Bourin and Lindahl, 1993; Colwell et al., 1999). RbHCII was observed to contain a substituted His to ¹⁷³Lys and all other residues were conserved (Fig. 6C). The degree of conservation among acidic domains and the GAG binding site of teleost HCIIs vary from that of mammalian HCIIs, suggesting that interaction of teleost HCII to its

cognate thrombin and mediation of GAG may be slightly different from mammalian counter parts. Table 3 illustrates the three main conserved features of HCII of vertebrates: (1) RCL; (2) serpin signature; and, (3) scissile bond. As Leu is present in the P₁ position of the reactive bond, HCII gains a synonym of 'leuserpin-2' (Pratt et al., 1989) and it contributes to the relatively slow rate of thrombin inhibition, if GAG is absent (Tollefsen, 2007). ATIII was found to inhibit an array of coagulation factors, whereas HCII shows a narrow spectrum, and specifically inhibits thrombin. This is because the P₁-P₁' bonds are Arg-Ser and Leu-Ser, respectively, and most coagulation elements require P₁-Arg as a catalytic residue. To further validate the sequence homology of RbHCII with other members, we performed the pair-wise and multiple alignments. Previously published studies have shown that HCII from zebrafish (Hanumanthaiah et al., 2002) and fugu share 53% of identity to human HCII. We observed this to be 52.2% for RbHCII. Furthermore, Table 2 clearly shows the high degree of sequence similarity among teleosts with an average of 93.7%, and in general, teleost HCII is longer than any other vertebrate HCII. As our phylogenetic analysis indicated that the clade A serpin is the closest sub-family to clade D, HCII, we were tempted to determine the homology between HCII and A1AT which are members of these two sub-families. Though the overall similarity between the RbHCII and A1AT from various species was low (Table 2), notably RbHCII showed more similarity with other non-teleost A1AT compared to teleost A1AT, ranging from 39% to 47%. In addition, a multiple alignment study of HCII from 8 different vertebrate species clearly displayed the closer homology and distinctive similarity of teleost HCII from other HCII and further supports HCII's conservation throughout evolution. It also revealed the patterns of conservation in functional domains including acidic repeats, GAG binding site and RCL. A signal peptide is common for HCII, interestingly; all HCII including the partial sequence from bighead carp (*Aristichthys nobilis*; EMBL ACO51109) had a signal peptide of 19 residues, except the rat HCII which possesses a lengthy (24 residues) signal peptide. If HCII

is considered regional-wise, the C-terminal zone was more conserved than the N-terminal zone, which could be due to the presence of a catalytic functional domain at carboxy terminal. However, it was observed N-terminal selective cleavage of HCII, with no disturbance to its inhibitory activity by various enzymes (Pratt et al., 1989) and N-terminally derived bio-active peptides proposed to have leukocyte-recruiting duty at the sites of thrombosis and inflammation (Church et al., 1991). We were interested in finding the position of RbHCII among serpin clades of A-I by phylogenetic analysis. The un-rooted tree generated with various serpins was in an agreement with the traditional classification put forward by Silverman et al. (2001). A traditional tree was constructed to further determine the relationship of RbHCII with the other members of HCII, and revealed that RbHCII is within the teleost branch and it is closely related to flounder HCII. The relationship order displayed in the phylogenetic tree was generally in agreement with the evolutionary order. The sequence homology, domain distribution, phylogenetics and other common features suggest that RbHCII belongs to the teleost serpin, clade D. Our results are consistent with the emerging facts those proposed the fish as a model for mammalian hemostasis, based on the homology analysis of hemostatic genes (Hanumanthaiah et al., 2002). Moreover, our tertiary structural (3D) model comparison results showed that GAGs binding sites (helices A and D), thrombin binding sites, and RCL of RbHCII are conserved and matched with human HCII for their 3D-folding pattern, suggesting functional similarity to human HCII.

Several studies have indicated that in human, a substantial amount of HCII mRNA is transcribed in liver. As blotting techniques showed low detectability, Kamp et al. (Kamp et al., 2001) analyzed various human tissues with RT-PCR and reported the expression of HCII in liver, placenta, lung, heart, kidney and brain. Hoffman et al. reported the localization of HCII in injured human skin and proposed a model for skin-residing HCII and its role (Hoffman et al., 2003). In addition, their results indicated the expression of HCII mRNA in human leukocytes and

macrophages. For the first time, our study reveals the tissue distribution pattern of HCII from a teleost, rock bream. RbHCII mRNA was found to be constitutively expressed in all tissues examined, but at different levels. The predominant expression was, as similar to human, in the liver. RbHCII was also detected in skin, gills and blood at considerable levels. Detection in skin might be due to the contamination of either blood or vascular tissues and therefore was not taken for further analysis in immune stimulation experiments. The presence of HCII mRNA in gills suggests its role in thrombin regulation to mediate the blood fluidity and flow, which requires further biochemical investigation. Even though liver contributes a large extent of circulatory HCII, our results indicate that certain tissues can locally produce low levels of HCII in rock bream.

The control of proteases by serpins and their relative balance in quantities localized the effects of proteases and regulate their functions by means of tissue and time. In the coagulation cascade, ATIII is the primary intravascular inhibitor of thrombin whereas thrombin activity is mainly controlled by HCII, extravascularly. This fact was further strengthened by the biochemical properties of these serpins and their cofactor distribution. For instance, ATIII has a broader spectrum of targets and stimulated by heparin, it is mainly found intravascularly. On the other hand, HCII displays limited specificity, but prompted by mainly an extravascular GAG, DS. The final aim of modulating the action of thrombin was found to be pivotal, as thrombin is a key player in multiple biological events. Other than its procoagulant activity, it has various cytokine-like roles. Thrombin was found to interact directly and/or indirectly with fibroblast (Dawes et al., 1993), polymorphonucleocytes (PMNs) (Cohen et al., 1991), monocytes/ macrophage (Bar-Shavit et al., 1983a) and smooth muscle cells as a chemotactic and mitogenic agent. It can activate the neutrophils and platelets to promote the release of various mediators including pro-inflammatory factors, chemotactic agents, cytokines and growth factors that have an impact on the inflammation, wound healing and revascularization. Thrombin transduces the signal through protease-activated

receptors (PARs) found in these cell types. By taking all these in to account, a recent review, Shrivastava et al. discussed the ways in which coagulation proteases and inhibitors associate with the inflammation, innate systems and the adaptive immunity (Shrivastava et al., 2007). In addition, the ability to produce thrombin was found in some immune cells including monocytes and macrophage. Therefore it is clear that understanding of the interface between the coagulation and immunity is advancing. As HCII controls thrombin activity, it is appropriate to assume that HCII may have relationship with immunity. To resolve this hypothesis, we conducted the transcriptional response analysis of RbHCII with different immune stimulants.

E. tarda is a gram-negative bacterium, an increasing threat to Korean fish aquaculture. LPS is an outer membrane compound of gram-negative bacteria whose immune inducibility was intensively studied. In liver tissue, LPS and *E. tarda* induced a clear downregulation pattern of RbHCII with minute variation. Both of them suppress the expression of RbHCII at early and late phases of investigation, but the level of suppression was relaxed at the mid-phase. Numerous studies have documented the activation of the coagulation system following LPS administration in animal models. This concept is bolstered by the action of anticoagulant in pathogenesis of liver damage by abolishing the hepatotoxicity (Hewett and Roth, 1995). Thrombin is found to be a critical mediator of changes in hepatocytes following the LPS administration. Yee proposed a model and suggested that PMNs and coagulation systems, especially thrombin, cooperate to induce the responses to LPS administration (Yee et al., 2003). These responses include the accumulation of PMNs and various inflammatory mediators that have the potential to alter hepatocellular homeostasis (Michie et al., 1988). Thus, it is obvious that in an LPS-induced coagulation system, the interplay between thrombin and inflammatory factors is critical (Copple et al., 2003). Our challenge experiment data bridge the SPI, HCII level with the immune response. To generate an innate inflammatory response for LPS administration, it is essential to maintain active thrombin at

a considerable level, which indeed requires the inhibitor expression at lower levels. Cathepsin G activates factor X, which converts the prothrombin to thrombin. As HCII also inhibits the cathepsin G, it might be another reason to maintain a lower HCII transcript level at post-LPS challenge. Moreover, the experiment of Vasseur et al., who analyzed the p8 gene by mutagenesis and LPS sensitivity of liver, revealed that HCII was downregulated during LPS challenge in normal and mutant mouse (Vasseur et al., 2003). Furthermore, the iridovirus (RBIV), a serious catastrophic disease agent of rock bream was also employed in the challenge experiments. In contrast to other challenges, RBIV seems to be a poor stimulant for RbHCII transcription in liver. However, RBIV also suppressed the RbHCII level below the control level at all time points investigated. Our results suggest that all three stimulants caused a time-dependent downregulation of RbHCII transcription in liver.

In contrast to liver tissue, blood displayed a different set of response patterns for the challenges. It is noteworthy that in comparison to liver, blood RbHCII expression was suppressed to a low level. *E. tarda* induced a strong late-phase suppression, where as LPS and RBIV caused a mild suppression of the RbHCII transcription. When gill tissue was investigated with these stimulants, completely different results were obtained (data not shown). Only RBIV suppressed the RbHCII expression at all time points investigated. Even though LPS and *E. tarda* did suppress the mRNA level of RbHCII in gills, at 6 h p.i., there was a prominent upregulation in both challenges. However, a more detailed study of RbHCII gene expression with response to various microbial challenges is required to fully understand the mechanisms behind its transcriptional regulation and its multiple physiological roles. The constitutive and ubiquitous expression of RbHCII in liver as well as in other tissues with transcriptional (down) regulation against challenges would suggest that it has an important function of regulating the host defense against pathogens.

We successfully expressed the recombinant RbHCII using pMALTM c2X and Rosetta-gamiTM (DE3) expression systems, and purified it in the form of MBP fusion protein. We investigated the primary biochemical function of RbHCII by inhibitory assays against proteases. rRbHCII (320 nM and 2 μ M) inhibited chymotrypsin activity by 43.5% on average, and thrombin activity by 54% and 86% on average, in the absence and presence of heparin, respectively. In the lowest concentration of RbHCII, there was no significant difference ($p < 0.05$) between inhibition of thrombin regardless of the presence or absence of heparin. In the presence of heparin, thrombin activity was significantly increased at all points, and this result supports the idea that for the effective inhibition of thrombin, RbHCII requires heparin.

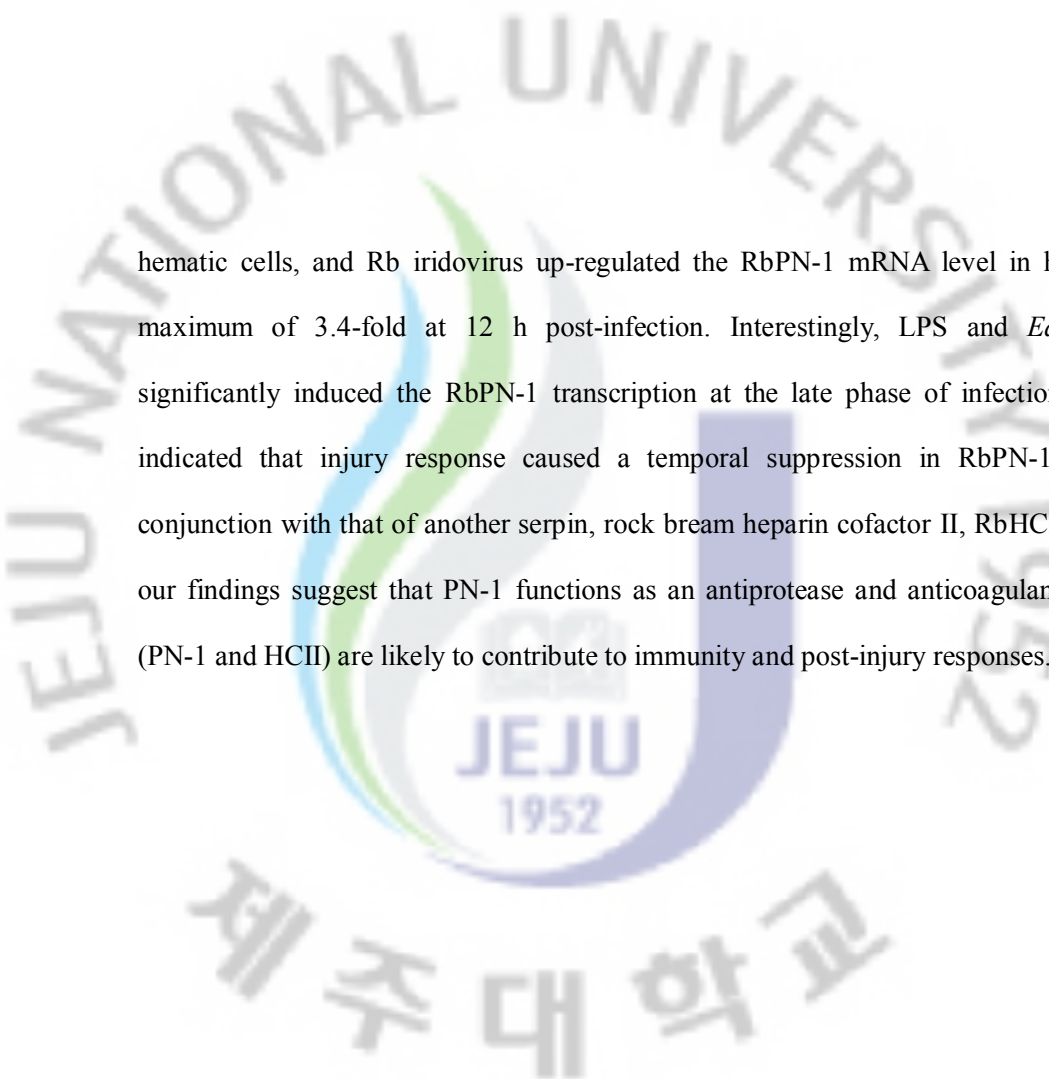
In conclusion, a new heparin cofactor II (RbHCII) from rock bream (*Oplegnathus fasciatus*) was identified and characterized at both primary and tertiary levels. With molecular characterization, phylogenetic analysis showed its similarity to other serpins, especially the clade D, HCII members. Constitutive RbHCII mRNA expression was observed in a tissue-specific manner, suggesting its physiological importance. Furthermore, RbHCII expression was downregulated upon being challenged with different immune stimulants, indicating its inhibitory role against immune- and coagulation-related proteins. Moreover, functional study of the recombinant protein suggested that RbHCII was active against thrombin and chymotrypsin where its thrombin inhibitory function was dependent on heparin. According to our knowledge, this is the first report on rock bream HCII cloning, characterization and expression analysis, and this study could be further expanded to delve into the molecular insight of understanding the biochemistry and physiological roles of teleostic heparin cofactor II.

Chapter II

Rock bream (*Oplegnathus fasciatus*) serpin, protease nexin-1: Transcriptional analysis and characterization of its antiprotease and anticoagulant activities

1. ABSTRACT

Protease nexin-1 (PN-1) is a serine protease inhibitor (Serpine) protein with functional roles in growth, development, patho-physiology and injury. Here, we report our work to clone, analyze the expression profile and characterize the properties of the PN-1 gene in rock bream (Rb), *Oplegnathus fasciatus*. RbPN-1 encodes a peptide of 397 amino acids with a predicted molecular mass of 44 kDa and a 23 amino acid signal peptide. RbPN-1 protein was found to harbor a characteristic serpin domain comprised of a serpin signature and having sequence homology to vertebrate PN-1s. The greatest identity (85%) was observed with PN-1 from the three-spined stickleback fish, *Gasterosteus aculeatus*. The functional domains, including a heparin binding site and reactive centre loop were conserved between RbPN-1 and other fish PN-1s; in particular, they were found to correspond to components of the human plasminogen activator inhibitor 1, PAI-1. Phylogenetic analysis indicated that RbPN-1 was closer to homologues of green spotted pufferfish and Japanese pufferfish. Recombinant RbPN-1 demonstrated antiprotease activity against trypsin (48%) and thrombin (89%) in a dose-dependent manner, and its antithrombotic activity was potentiated by heparin. The anticoagulant function prolonged clotting time by 3.7-fold, as compared to the control in an activated partial thromboplastin time assay. Quantitative real-time PCR results indicated that RbPN-1 is transcribed in many endogenous tissues at different levels. Lipopolysaccharide (LPS) stimulated a prolonged transcriptional response in

The image contains a large, semi-transparent watermark of the Jeju National University logo. The logo is circular, featuring a stylized flame or leaf design in blue, green, and purple. The text "JEJU NATIONAL UNIVERSITY" is written in a semi-circle at the top, and "제주대학교" is written in a semi-circle at the bottom. In the center of the logo, the text "JEJU 1952" is visible.

hematic cells, and Rb iridovirus up-regulated the RbPN-1 mRNA level in hematic cells to a maximum of 3.4-fold at 12 h post-infection. Interestingly, LPS and *Edwardsiella tarda* significantly induced the RbPN-1 transcription at the late phase of infection. *In vivo* studies indicated that injury response caused a temporal suppression in RbPN-1 transcription, in conjunction with that of another serpin, rock bream heparin cofactor II, RbHCII. Taken together, our findings suggest that PN-1 functions as an antiprotease and anticoagulant and that serpins (PN-1 and HCII) are likely to contribute to immunity and post-injury responses.

2. MATERIALS AND METHODS

2.1. Experimental animals, tissue collection and RNA isolation

Animal rearing was performed as described in the Part I, Section 2.4. Blood samples (1-2 mL/fish) were collected from the caudal fin of healthy, unchallenged fish and immediately centrifuged at $3000 \times g$ ($4\text{ }^{\circ}\text{C}$) for 10 min to harvest the hematic cells. Three fish were dissected and ten tissues (part I, section 2.5.1) were collected. All tissue samples were snap frozen in liquid nitrogen and stored at $-80\text{ }^{\circ}\text{C}$. Total RNA was isolated from tissues using the Tri ReagentTM (Sigma, USA). The mRNA was purified using an mRNA isolation kit (FastTrack[®] 2.0; Invitrogen, USA). The concentration and purity of RNA were determined using a UV-spectrophotometer (BioRad, USA) at 260 and 280 nm.

2.2. Multi-tissue cDNA synthesis and normalization

Individual purified RNA samples were diluted to $1\text{ }\mu\text{g}/\mu\text{L}$ and pooled for multi-tissue cDNA synthesis. Using $1.5\text{ }\mu\text{g}$ of mRNA, the first-strand cDNA synthesis was carried out with the CreatorTM SMARTTM cDNA library construction kit (Clontech, USA); amplification was then carried out with Advantage 2 polymerase mix (Clontech) under conditions of $95\text{ }^{\circ}\text{C}$ for 7 sec, $66\text{ }^{\circ}\text{C}$ for 30 min and $72\text{ }^{\circ}\text{C}$ for 6 min. The normalization of double-strand cDNA was accomplished using the Trimmer-Direct cDNA normalization kit (Evorgen, Russia).

2.3. Rock bream genome sequence database and identification of rock bream PN-1

We have established a Rb cDNA shotgun sequence database based upon data from a next-generation DNA sequencing technology, the GS-FLX titanium system (DNA Link, Republic of Korea). A cDNA sequence that showed homology to known PN-1s was identified using the Basic Local Alignment Search Tool (BLAST) program available on NCBI.

2.4. Molecular characterization of RbPN-1

The full-length sequence of RbPN-1 was analyzed by BLAST and compared with other known PN-1 and serpin sequences. DNAssist (version 2.2) was used to determine the open reading frame (ORF) and main acid sequence. Identification of characteristic domains and motifs was performed using the PROSITE profile analysis (Bairoch et al., 1997) and SMART proteomics database (Letunic et al., 2009) and signal peptide was predicted using the SignalP program (Bendtsen et al., 2004). Identity and similarity percentages were calculated using the FASTA program (Pearson, 1990) and a matrix was generated by MatGAT program (Campanella et al., 2003). Pair-wise and multiple sequence alignments were performed using ClustalW2 (Thompson et al., 1994) and the phylogenetic relationship was determined using the neighbor-joining (NJ) method and the MEGA 4.1 program (Kumar et al., 2004). The resultant tree was tested for reliability using 1000 bootstrap replications. The structure of RbPN-1 was modeled based upon the crystallographic structures of plasminogen activator inhibitor-1 (PAI-1) chain A (PDB, 1dvmA) (Stout et al., 2000) that displayed high sequence similarity with PN-1 (Sommer et al., 1987). The three-dimensional (3D) model was generated utilizing Swiss-Model protein modeling server (Arnold et al., 2006) and manipulated using DeepView (Swiss-PdbViewer, 4.0.1).

2.5. Cloning of RbPN-1 open reading frame (ORF)

The pMALTM protein fusion and purification system (New England Biolabs, USA) was chosen for the cloning and expression of recombinant RbPN-1. A fragment encoding the ORF of RbPN-1 was amplified using gene-specific primers with corresponding restriction enzyme sites for *EcoRI* and *PstI* at the N- and C-terminus of RbPN-1, respectively (Table 4). The PCR was performed in a TaKaRa thermal cycler in a total volume of 50 μ L with 5U of Ex *Taq* polymerase (TaKaRa, Japan), 5 μ L of 10 \times Ex *Taq* buffer, 8 μ L of 2.5 mM dNTPs, 80 ng of template and 20 pmol of each primer. The reaction was carried out with an initial incubation at 94 $^{\circ}$ C for 3 min,

followed by 25 cycles of 94 °C for 30 s, 57 °C for 30 s and 72 °C for 60 s, and a final extension at 72 °C for 5 min. The PCR product (~1150 bp) was analyzed on a 1% agarose gel and purified using Accuprep™ gel purification kit (Bioneer Co., Korea). The digested pMAL-c2X vector (35 ng) and PCR product (70 ng) were ligated by incubation with Mighty Mix (7.5 μL; TaKaRa) for 2 h at 16 °C. The ligated pMAL-c2X/RbPN-1 product was transformed into DH5α cells and sequenced. Subsequently, the recombinant construct was transformed into competent *E. coli* BL21 (DE3) cells (Novagen, Germany).

Table 4. Description of primers used in cloning and transcriptional analysis of RbPN-1.

Name	Purpose	Sequence (5'→3')
RbPN-1 F1	ORF amplification (with signal peptide)	GAGAGAg ^a aattcATGAAGCACCTCTCATTATTTTGCCTGTATGC - <i>EcoRI</i>
RbPN-1 F2	ORF amplification (without signal peptide)	GAGAGAg ^a aattcCAGGGTCCCTCCTACGGC - <i>EcoRI</i>
RbPN-1 R	ORF amplification	GAGAGActg ^c cagTCAAGGCTGGTTGATCTGGCC - <i>PstI</i>
RbPN-1/qF	RT-PCR amplification	TGCATGTATCCAAGGCACTCCAGA
RbPN-1/qR	RT-PCR amplification	AAGGCTGGTTGATCTGGCCTATGA
RbHCII-2F	RT-PCR amplification	TTGGCTACACACTACGCTCTGTGA
RbHCII-2R	RT-PCR amplification	TCAGCCCTTTGGTCAGCTTTAGGA
Rb-β-actin-F	RT-PCR internal reference	TCATCACCATCGGCAATGAGAGGT
Rb-β-actin-R	RT-PCR internal reference	TGATGCTGTTGTAGGTGGTCTCGT

2.6. Overexpression and purification of recombinant RbPN-1 (rRbPN-1)

The rRbPN-1 was overexpressed in *E. coli* BL21 (DE3) cells by inducing with isopropyl- β -thiogalactopyranoside (IPTG). A starter culture volume of 10 mL *E. coli* BL21 (DE3) was diluted (1:10) up to 100 mL with fresh Luria broth (LB) medium supplemented with ampicillin (100 μ g/mL) and glucose (0.2% final concentration) and incubated at 37 °C with shaking at 200 rpm until optical density at 600 nm (OD_{600}) reached 0.6. IPTG was then added (0.25 mM final concentration) and incubated for 5 h at 20 °C. The induced cells were cooled on ice for 30 min and harvested by centrifugation at 3500 rpm for 30 min at 4 °C. Harvested cells were resuspended in 10 mL of column buffer (20 mM Tris-HCl, pH 7.4, 200 mM NaCl) and stored at -20°C. The rRbPN-1 was purified by the pMAL protein fusion and purification system. Briefly, the cells were thawed in an ice-water bath and subjected to eight 13 s sonication pulses on ice and centrifuged at 9000 \times g for 30 min at 4 °C. The resultant supernatant was defined as crude extract. Meanwhile, 1 mL of amylose resin was mixed with 1 mL of crude extract and placed on ice for 30 min to facilitate affinity binding. In the final purification step, the settled resin-extract mixture was loaded onto a 1 \times 5 cm column and washed with 12 \times volumes of the column buffer. Finally, the rRbPN-1 fused with maltose-binding protein (MBP) was eluted by applying a total of 3 mL elution buffer (column buffer with 10 mM maltose) in 0.5 mL aliquots. The concentration of the purified protein was determined by the Bradford method, using bovine serum albumin (BSA) as the standard (Bradford, 1976). The rRbPN-1 samples collected from different purification steps were analyzed on 12% SDS-PAGE with standard protein size marker (TaKaRa). The gel was stained with 0.05% Coomassie blue R-250, followed by a standard de-staining procedure.

2.7. Antiprotease activity assays

To characterize the inhibitory activity of rRbPN-1, trypsin and thrombin proteases were

employed and the hydrolysis of synthetic chromogenic substrates was monitored. The trypsin inhibitory assay was carried out by measuring residual activity of trypsin in a reaction mixture (400 μ L) that contained 50 mM Tris-HCl, pH 8.0 supplemented with trypsin (1 μ M final concentration) from porcine pancreas (Sigma) and either rRbPN-1 (125 nM – 4 μ M final concentrations) or buffer as a control. The reaction was initiated by addition of 100 μ L 0.2% w/v azocasein (Sigma) in the same buffer, and incubated overnight at 37 $^{\circ}$ C. The reaction was stopped by adding 200 μ L of 15% trichloroacetic acid and chilling on ice for 15 min. The precipitate was separated by centrifugation and OD₄₄₀ was measured spectrophotometrically. The inhibition assay of thrombin (bovine plasma; Sigma) was carried out in a 100 mM Tris-HCl, pH 8.0 buffer with a total volume of 200 μ L. A total of 0.25 μ M thrombin was separately pre-incubated with increasing concentrations of inhibitor (0.2- to 1.2-fold of enzyme) in the buffer for 5 min at 30 $^{\circ}$ C. Then, the remaining activity was detected by adding the chromogenic substrate solution of Phe-Val-Arg-p-nitroanilide hydrochloride (Sigma). The reaction mixture was incubated at 30 $^{\circ}$ C for 15 more min and the absorbance of formed p-nitroaniline was determined at OD₄₀₅. The blanks for all the assays were prepared similar to the samples, but without addition of enzyme. To determine the effect of heparin, it was added to a final concentration of 10 U/mL and separately assayed against trypsin and thrombin. In addition, all assays were conducted with the MBP to determine the effect of the fusion protein on the activity of rRbPN-1. The percent of inhibition (%I) was calculated using the formula: $\%I = [(A_o - A_i) / A_o] \times 100$, where A_i and A_o represents the absorbance with and without rRbPN-1, respectively.

2.8. Anticoagulation assay

Anticoagulant activity was determined using the activated partial thromboplastin time (APTT) assay. Human blood was mixed at a 9:1 (v/v) ratio with 3.8% sodium citrate. Plasma was obtained by centrifugation at 2400 \times g for 20 min. Citrated plasma (90 μ L) was mixed with various final

concentrations of rRbPN-1 and incubated for 1 min at 37 °C. Then, 100 µL of the APTT assay reagent (Pacific Hemostasis/Thermo Scientific, USA) was added to the mixture and incubated for 5 min at 37 °C. Thereafter, 0.025 mM CaCl₂ (100 µL) was added and clotting time (s) was immediately recorded by a coagulometer, Dualchannel clot-2 (SEAC, Italy). Water and MBP were used as controls.

2.9. Immune and injury challenge experiments

To determine the distribution pattern of RbPN-1 in different tissues, three healthy individuals (~50±2 g) were used. To investigate the immune response of RbPN-1, we devised three immune challenge experiments using LPS, *E. tarda* bacterium and RBIV. In addition, the expression of RbPN-1 (and heparin cofactor II, RbHCII) in response to injury was confirmed. Tissues were collected as described in Part II, Section 2.1.

The immune challenge experiments were performed as described earlier (Umasuthan et al., 2011b) or in Part I, section 2.5.2. For the injury experiment, a modified procedure from Wu et al (2004) was followed (Wu et al., 2004). Briefly, a group of fish was injured with two incisions (one on each side) on the dorsal surface, 2 cm in length and 0.5 cm in depth, using sterile surgical blades and transferred into individual experimental tanks just after injury. Another group was left as uninjured control. Rb hematic cells and gills were collected at 3, 6, 12, 24, and 48 h post-injection from each of the immune-challenged groups and their respective controls; hematic cells were collected from injured fish and their respective uninjured control. At least three fish were dissected for the tissue collection from each group at each time point.

2.10. RNA extraction and cDNA synthesis

Total RNA was extracted from tissues pooled from 3 fish (50 mg/fish) from each group, quantified and diluted as described in Part II, Sections 2.1 and 2.2. An aliquot of 2.5 µg RNA was

used to synthesize cDNA from each tissue using the PrimeScript™ first-strand cDNA synthesis kit (TaKaRa). Briefly, RNA was incubated with 1 µL of 50 µM oligo(dT)₂₀ and 1 µL of 10 mM dNTP for 5 min at 65 °C and immediately cooled on ice. Then, 4 µL of 5× PrimeScript™ buffer, 0.5 µL of RNase inhibitor (20 U) and 1 µL of PrimeScript™ RTase (200 U) were added and the mixture was incubated for 1 h at 42 °C. The reaction was terminated by raising the temperature to 70 °C for 15 min. The synthesized cDNA was diluted 40-fold prior to storage at -20 °C for further experiments.

2.11. RbPN-1 transcriptional analysis by qRT-PCR

The transcriptional analysis by qRT-PCR was performed as described earlier (Umasuthan et al., 2011b) or in Part I, section 2.5.4. The RbPN-1, RbHCII gene-specific primers and β-actin primers (designed based on a Rb β-actin sequence; Accession No. FJ975145) used in this study are presented in Table 4. The calculated relative expression level in each tissue was compared with respective expression levels in muscle for the tissue-specific expression analysis. For the analysis of fold-change in expression after immune and injury challenges, relative expression was compared with PBS-injected (from the corresponding time points) and uninjured controls, respectively. Statistical analysis was performed as described in Part I, Section 2.9.

3. RESULTS

3.1. Molecular characterization of RbPN-1

3.1.1. Sequence characterization of the full length RbPN-1

BlastX screening of the Rb cDNA library yielded a sequence with high similarity to the known PN-1 members, which was designated as rock bream protease nexin-1. The nucleotide and deduced amino acid sequences of the RbPN-1 are shown in Figure 12. The nucleotide sequence of RbPN-1 has been deposited in GenBank under the accession no. HQ385323. The cloned full-length RbPN-1 consisted of 1951 bp. The ORF was found to be composed of 1191 bp that would translate into a putative peptide of 397 amino acid residues. The predicted RbPN-1 protein had a molecular mass of 44 kDa and an isoelectric point of 9.62. Importantly, RbPN-1 was found to contain a domain profile spanning amino acid 37 to 397 (total of 361 residues), as predicted by SMART server; moreover, this domain comprised a characteristic signature sequence motif which consisted of 11 amino acid residues at positions ³⁷⁰VTVDRPFLFLI³⁸⁰, as determined by PROSITE program. Using the SignalP 3.0 program (<http://www.cbs.dtu.dk/services/SignalP/>), the N-terminus of the RbPN-1 was found to have a 23 amino acid putative signal peptide, representing a cleavage site at amino acids 23-24. In addition, a potential N-glycosylation site (¹⁶⁰NKTK¹⁶³) was observed in RbPN-1. Sequence analysis indicated a 172 bp 5'-untranslated region (5' UTR) and 588 bp 3'-UTR, which contained two RNA instability motifs (¹⁴⁷⁸ATTTA¹⁴⁸² and ¹⁷⁵⁶ATTTA¹⁷⁶⁰) and a polyadenylation signal (¹⁷⁴³AATAAA¹⁷⁴⁸).

			CCACAGT	GGTCTCAGTTTCAC	-172
TGGAATAAAGAGTTA	TTTTCTTTCACATT	GCGGACGAACCTTAT	TTTCTCCTTTGGACG	GAAGTGAAGAGCGGA	-150
CTGATACGGCCACAG	TTTACACCTGCGGGAT	AAGTCGAAGTAACGT	CACCTCGTGATAGGT	GCTGCAGGGTTTAAA	-75
ATG AAGCACCTCTCA	TTATTTTGCCTGTAT	GCAGTGGTGACCTTG	TATGGCCATACAGGT	GTGCTCTCGCAGGGT	75
--M--K--H--L--S	--L--F--C--L--Y	--A--L--V--T--L	--Y--G--H--T--G	--V--L--S--Q--G	25
CCCTCCTACGGCGAA	CGGGGCTCTGATCTT	GGCATAACAGGTGTTT	CAGCAAGTAGTCCGC	TCCAGGCCCTGGAA	150
--P--S--Y--G--E	--R--G--S--D--L	--G--I--Q--V--F	--Q--Q--V--V--R	--S--R--P--L--E	50
AATGTGGTGCTTTCA	CCCCATGGGGTAGCT	TCCATCCTTGGGATG	TTGCTACCAGGAGCC	CATGGAGTGACTCGG	225
--N--V--V--L--S	--P--H--G--V--A	--S--I--L--G--M	--L--L--P--G--A	--H--G--V--T--R	75
AAGCAGTCTCAAT	GCTCTCCGTTACAAG	AAAAAGGCCCGTAC	AATATGTTGAAGAGG	CTGCACAAAACCTTG	300
--K--Q--V--L--N	--A--L--R--Y--K	--K--K--G--P--Y	--N--M--L--K--R	--L--H--K--T--L	100
ACAGCCAAGTCCAAC	CAGGACCTCGTGCTG	ATTGCCAACGCCATG	TTCAGCCAGGAGGGC	TTCCCATGGAGGAG	375
--T--A--K--S--N	--Q--D--L--V--L	--I--A--N--A--M	--F--S--Q--E--G	--F--P--M--E--E	125
GCCTTCGTAGCCACC	AACAAAGCCAACCTC	CAGTGTGAGAGCAGG	AGCCTGGACTTCAGC	AACCCCAAGGGGCA	450
--A--F--V--A--T	--N--K--A--N--F	--Q--C--E--S--R	--S--L--D--F--S	--N--P--Q--G--A	150
GCAGATGAAATCAAT	GAATGGTCAACAAT	AAGACCAAAGGTAC	ATCCCAGCTTGATC	AAAGCAGACATGCTG	525
--A--D--E--I--N	--E--W--V--N--N	--K--T--K--G--H	--I--P--S--L--I	--K--A--D--M--L	175
GACTCAGCTCTGACC	CGTCTGGTCGCTGTC	AACTCAATCTACTTC	AAAGGCTTATGGAAG	TCCCGCTTCCAGCCT	600
--D--S--A--L--T	--R--L--V--A--V	--N--S--I--Y--F	--K--G--L--W--K	--S--R--F--Q--P	200
GAGAACACCAAGATG	AGGCCCTTCAACGGG	GCGGACGGAATGTA	TATAAAGTCCCAATG	ATGTCCCAACTCTCT	675
--E--N--T--K--M	--R--P--F--N--G	--G--D--G--N--V	--Y--K--V--P--M	--M--S--Q--L--S	225
GTCTTCAACATCAGC	ATGGCCACCACACT	CAGGGACTGAAATAT	AAGGTGATTGAGCTG	CCCTACCACGGCAAC	750
--V--F--N--I--S	--M--A--T--T--P	--Q--G--L--K--Y	--K--V--I--E--L	--P--Y--H--G--N	250
ACCATCAGCATGCTG	ATTGTTCTGCCCTCT	GACGAAGACAGCCC	CTGTCCCGGTTATC	CCACACATCAGCACA	825
--T--I--S--M--L	--I--V--L--P--S	--D--E--D--T--P	--L--S--R--V--I	--P--H--I--S--T	275
GCCACGGTGCAGAGC	TGGACCAAAGTATG	CACATGAGAAAAGTC	CGCCTGCTCATCCCC	AAGTTTACTGCTGAC	900
--A--T--V--Q--S	--W--T--K--L--M	--H--M--R--K--V	--R--L--L--I--P	--K--F--T--A--D	300
GCGGAGGTGGATTG	GAAGCCCCCTTTCA	GCGTGGGAATAACA	GACATGTTTCACTCAG	AACAAAGCTGACTTC	975
--A--E--V--D--L	--E--A--P--L--S	--A--L--G--I--T	--D--M--F--S--Q	--N--K--A--D--F	325
AGACACCTCAGTGCT	GAGCCTGTGCATGTA	TCCAAGGCACTCCAG	AAAGCCAAAGTTGTG	GTGAATGAAGATGGA	1050
--R--H--L--S--A	--E--P--V--H--V	--S--K--A--L--Q	--K--A--K--V--V	--V--N--E--D--G	350
ACAAAAGCAGCAGCT	GCCACTACTGCCATT	TTGCTGGCTCGGTCC	TCTCCGCTTGGGTT	ACAGTGGACAGACCT	1125
--T--K--A--A--A	--A--T--T--A--I	--L--L--A--R--S	--S--P--P--W--V	--T--V--D--R--E	375
TTCTCTTCTCATC	AGACATAACCCAACA	GGTACCATTCTCTTC	ATAGGCCAGATCAAC	CAGCCTTGAAGCCAT	1200
--F--L--F--L--I	--R--H--N--P--T	--G--T--I--L--F	--I--G--Q--I--N	--Q--P *	397
CCGTCACCTGGCCAGC	CCCTGGTAGCATCAC	AGGCCAGCACGGGAA	ATGCTTCTACACTGC	CACGCATGAACACAC	1275
ACATACATAAACACA	CACACACATAAACGC	ACACCCACATACACA	GACTTTTGCTGTAGA	CTTATGTACAGTGTG	1350
GACATATGTTATTTG	TTTTAAATATTGCTT	TTTATGTTACCCATT	TTCTGTAATGCATAA	CATTCTTTATAAAAG	1425
GTTTTGAGACTAAA	ATTTCCAGCCGTTT	TAATTTTGTATACT	TTTTTGA ATTTA TTA	CATTTTTAAAGACT	1500
TTGAATGTCAATTGT	GTATTTTCTCAACTC	TGGAGTAGGATAATC	AGTTTGTGTTGCATG	TCAGTGTTCAGTTT	1575
AAAAGTTCTCCATCT	CAAGTCATGCTACTC	CAGTCTGTTCTAAGT	TTCACCTCTAAGTTA	TGGCAATGTACATCA	1650
CATCTTGAACGCCTT	GCATTCAGCTACTTT	ACAATCATTGTTTCT	CTCACTGAGGAAGTC	TTCTGTTATCATACT	1725
TGCTTCATATCTGAT	CA ATAAA TACACAT	ATTA TAACATAACA	AAAAAAAAA		1779

Fig. 12. The complete nucleotide and deduced amino acid sequences of rock bream PN-1 cDNA. This nucleotide sequence has been deposited in GenBank under accession number

HQ385323. The start (ATG) and stop (TGA) codons are in bold. Predicted N-terminal signal peptide is underlined. The putative serpin domain profile is shaded in light grey and the serpin signature motif is boxed bold and shaded in dark grey. Two RNA instability motifs (ATTTA) are in bold italics and underlined. The polyadenylation signal is in bold italics. The poly (A) tail is underlined at the end of the nucleotide sequence.

3.1.2. Pair-wise and multiple alignment analysis of RbPN-1 vs. PN-1 orthologues

FASTA program was used to analyze the pair-wise identity and similarity of RbPN-1 and reveal its distinguished nature. RbPN-1 shared an overall identity (54%-85%) and similarity (70%-91%) with various vertebrate lineages (Table 5) which was also confirmed by MatGAT program. The greatest (85.4%) and least (28.1%) degree of identity were observed with PN-1s of the three-spined stickleback fish, *Gasterosteus aculeatus* and mosquito GDN, respectively. Orthologues of PAI-1, E1, has been reported to share high homology (Sommer et al., 1987) with PN-1s. RbPN-1 shared a relatively greater degree of homology with the higher vertebrate PAI-1s than with the corresponding members from different lower vertebrates, including the fish (Table 5). Furthermore, matured HCII (Umasuthan et al., 2011b) and RbPN-1 shared 23% of identity and 40% of similarity among them.

Table 5. Percent identity and similarity of the rock bream protease nexin - 1 to other vertebrate serpin, clade E, member 2 (PN-1) homologues and serpin clade E, member 1 (PAI-1) homologues from corresponding vertebrate species. Each parameter pair of serpin E2 and E1 is shown, separated by a slash (/).

Gene		SERPIN peptidase inhibitor, clade E, member 2 / SERPIN peptidase inhibitor, clade E, member 1				
Common name	Species	Molecular name	Accession No	I (%)	S (%)	AA
Stickleback	<i>Gasterosteus aculeatus</i>	Serpin E2 / Serpin E1	ENSGACP00000000289* / ENSGACP00000000928*	85.4 / 36.4	90.9 / 57.5	395 / 395
Puffer fish	<i>Tetraodon nigroviridis</i>	Serpin E2 / Serpin E1	ENSTNIP00000017318* / ENSTNIP00000005261*	83.9 / 31.8	90.2 / 53.5	397 / 363
Fugu	<i>Takifugu rubripes</i>	Serpin E2 / Serpin E1	ENSTRUP00000011515* / ENSTRUP00000011512*	83.4 / 34.7	91.2 / 57.9	397 / 400
Medaka	<i>Oryzias latipes</i>	PN-1 / Serpin E1	ENSORLP00000011683* / ENSORLP00000013125*	66.8 / 35.8	76.6 / 55.5	402 / 394
Zebrafish	<i>Danio rerio</i>	GDN / PAI-1	NP_956478 / NP_001108031	65.6 / 37.1	79.1 / 60.2	395 / 384
Frog	<i>Xenopus laevis</i>	Serpin E2 / Serpin E1	NP_001087103 / NP_001090520	54.3 / 39.1	71.1 / 58.5	395 / 403
Anole lizard	<i>Anolis carolinensis</i>	Serpin E2 / Serpin E1	ENSACAP00000004313* / ENSACAP00000001243*	55.4 / 31.8	71.1 / 43.9	396 / 279
Zebra finch	<i>Taeniopygia guttata</i>	GDN / -	ENSTGUP00000008214* / -	55.9 / -	72.8 / -	395 / -
Pig	<i>Sus scrofa</i>	Nexin-1 / PAI-1	NP_999452 / P79335	57.0 / 41.3	72.2 / 60.6	397 / 402
Dolphin	<i>Tursiops truncatus</i>	Serpin E2 / Serpin E1	ENSTTRP00000012718* / ENSTTRP00000000717*	56.9 / 40.6	71.8 / 59.7	398 / 402
Opossum	<i>Monodelphis domestica</i>	Nexin-1 like / PAI-1 like	XP_001365493 / XP_001371327	56.6 / 33.5	72.3 / 50.7	397 / 474
Horse	<i>Equus caballus</i>	PN-1 isoform 1 / PAI-1	XP_001495988 / XP_001492567	56.2 / 32.4	72.2 / 46.4	397 / 518
Dog	<i>Canis familiaris</i>	PN-1 IF 1 / PAI-1IF 1	XP_851657 / XP_849345	56.1 / 40.3	72.3 / 60.2	397 / 402
House mouse	<i>Mus musculus</i>	GDN precursor / PAI-1	NP_033281 / P22777	55.6 / 40.0	72.2 / 59.1	397 / 402
Bovine	<i>Bos taurus</i>	Serpin E2 / Serpin E1	AAI23835 / AAI03452	55.2 / 42.0	71.2 / 60.0	397 / 402
Guinea pig	<i>Cavia porcellus</i>	Serpin E2 / Serpin E1	ENSCPOP0000001823* / ENSCPOP00000000151*	55.2 / 39.0	71.8 / 57.1	397 / 402
Elephant	<i>Loxodonta africana</i>	Serpin E2 / Serpin E1	ENSLAFP00000000141* / ENSLAFP000000009550*	54.6 / 38.7	70.7 / 60.1	399 / 400
Rhesus monkey	<i>Macaca mulatta</i>	GDN / PAI-1 IF 2	XP_002799107 / XP_001107647	54.5 / 41.9	71.1 / 59.3	398 / 402
Human	<i>Homo sapiens</i>	Serpin E2 / Serpin E1	NP_006207 / AAH10860	54.6 / 41.4	71.0 / 59.8	398 / 402
Mega bat	<i>Pteropus vampyrus</i>	Serpin E2 / Serpin E1	ENSPVAP00000013659* / ENSPVAP000000009035*	53.6 / 40.3	71.8 / 60.1	398 / 401
Mosquito	<i>Culex quinquefasciatus</i>	GDN / PAI-1	XP_001866682 / XP_001866680	28.1 / 28.1	47.0 / 47.0	414 / 414

Pair-wise identity percentage was calculated using EMBOSS alignment (<http://www.ebi.ac.uk>) maintaining open gap penalty and gap extension penalty levels at 10.0 and 0.5, respectively. I, identity; S, similarity; AA, amino acids; IF, isoform. *ENSEMBL accession number.

ClustalW multiple alignment was employed to align complete amino acid sequences of RbPN-1 with PN-1 orthologues of various vertebrates including from mammalian, avian, amphibian, reptilian and fish (Fig. 13). The full-length of PN-1 polypeptides was found to vary only within the span of amino acid 395-402. In agreement with the fact that PN-1 is a secretory protein, some vertebrate PN-1s contained obvious N-terminal signal peptides. Signal peptide of RbPN-1 was identical in length with other fish members. Among two Cys residues observed in RbPN-1, one was located within the signal peptide and found to be conserved in fish members while the other was semi-conserved among the species (Fig. 14B). The matrix generated by the MatGAT program indicated that RbPN-1 shares high overall identity (82%) and similarity (90%) with other fish orthologues (Table 6). Our alignment study demonstrated that homology increased towards the C-terminal of the analyzed PN-1 sequences (Fig. 13). To analyze homology and identity of functional domains of PN-1s among the class pisces, we aligned targeted active regions that corresponded to well-characterized domains of mammalian PN-1s (McGrogan et al., 1988; Stone et al., 1994). Table 7 summarizes the findings: (1) Heparin binding site (HBS) that binds to heparin was found to be conserved among fish PN-1s and displayed significant variation from mammalian PN-1s. The corresponding HBS of RbPN-1 was located in the region of amino acid 91-106 in the premature peptide. (2) The relative number of positively charged residues in the HBS region of fish PN-1, especially RbPN-1, was low compared to mammalian PN-1s. (3) The hinge region in the RCL, located 11/12 residues upstream of P₁ was completely conserved. (4) In addition, a general conservation was apparent in the RCL region; notably, the scissile bond that determines protease specificity was Arg-Ser in all PN-1s. Also, a putative LRP-binding site (⁴⁸PLENVVLSPHGV⁵⁹) was detected, similar to that in human PN-1.



LRP binding site

OfPN-1 MKHLSLFLYALVTLYGHTGVLSQG---PSYGERGSDLGIQVFQVVRSHPLENVVLSPH 57
 TnPN-1 MNHLVFLCLLGLATFHSHDGAHSLA---SSYGERGSDLGIQVFQREVHSPRLDNIVLSPH 57
 TrPN-1 MKTSLFLCLFGLVVLRGHGALSQA---PSYGERGSDLGIQVFQVVRSHPLEDNIVLSPH 57
 SsPN-1 MGLPSELLCMLVTLGGHGVFSQAPSTPSYGERGSDLGIQVFQVVARSPQQNVVLSPH 60
 XlPN-1 MRRLLVFPFLV-AFLASVQPELDPL----SLEELGSDIGIQVENQVARTPHENIVMSPH 55
 AcPN-1 MDWQFALLFVA-LTSTCMCFPPNPM----SLEELGSDIGIQVENQLVKSHPKDNVVVSPH 55
 GgPN-1 MNWHFSLFL-L-GTLASVCSQFNFY----PLEELSSDVGIQVENQIVKARQDNVVVSPH 55
 HsPN-1 MNWHLPLFLASVTLPSICSHFNPL----SLEELGSDIGIQVENQIVKSHPHDNIVLSPH 56

* : : *

OfPN-1 GVASILGMLLPGAHGVTRKQVLNALRYKKKGPYNMLKRLHKTTLAKSNQDLVLIANAMFS 117
 TnPN-1 GVASILGMLLPGAHGETRQVLTALRYNCTGPKMLRKLHKTTLAKANQDSVLIANAMFT 117
 TrPN-1 GVASILGMLLPGAHGETRQVLTALRYKKNPYKMLKKLHKTTLAKANQDSLLIANAMFT 117
 SsPN-1 GVASILGMLLPGETRQLLTALRYKKNPYKMLRKLHKTTLAKSNQDLVLIANAMFS 120
 XlPN-1 GISSVLGMQLGADGRTKKQLTMVMRYKINEVAKSLKKTNRRAIVAKKNDIVTTANGVFA 115
 AcPN-1 GIASVLGMQLGADGRTKKQLTMVMRYSVNGVGVKVKKINKAIVAKKNDIVTTIANAVFA 115
 GgPN-1 GIASVLGMQLGADGRTKKQLTMVMRYSVNGVGVKALKKINRLIVSKKNDIVTTIANAVFA 115
 HsPN-1 GIASVLGMQLGADGRTKKQLAMVMRYGVNGVGVKILKINKAIVSKKNDIVTTIANAVFV 116

* : *

N-Gly

OfPN-1 QEGFPMEEAFAVATKANFQCESRSLDFSNPQGAADETNEVWNKTKGHIPLSIKADMLDS 177
 TnPN-1 KDGFPMEETERATKANFQCESRSLDFRHPTAADEINEVWSNKTGHIPLSIKADMLDS 177
 TrPN-1 KEGFPMEEAFAVATKANFQCESRSLDFRHPSKAADDINEVWSNKTGHIPLSVKADMLDS 177
 SsPN-1 QQGFPMEEAFMSSNRANFQCESRTLDFDTDEAAATINIWNQTKGHIPTLVKADMLDG 180
 XlPN-1 SSFAFKVEGSFVYKNDIHFSDVRSVDFQEKNTAASIIINQVWVKNQTKGMIEGLISPELLDS 175
 AcPN-1 KSGLKMVEPFSRNDVFCQSVKSIDFEDKDSACDVTNVHVVNKTGMDISLSPPDDIDS 175
 GgPN-1 KSGFKMEVPEVTRNKEVFCQSVKSIDFEDPNTACDSINQVWVKNETRGMIDQVVPDDIDS 175
 HsPN-1 KNASEIEVPEVTRNKEVFCQEVNRVNEFDPASACDSINAVVKNETRMDIDNLLSPDLIDG 176

... : *

OfPN-1 ALTRLVAVNSIYFKGLWKSRFQEPENTKMRFFNGGDGNVYKVPMSQLSVFNISMATTPQG 237
 TnPN-1 ALTRLVAVNSIYFKGLWKSRFQEPENTKLRHFTGGDGNVSKVPMSQLSVFNISMATTPQG 237
 TrPN-1 ALTRLVAVNSIYFKGLWKSRFQEDTKMRFFFTSGDGTVHKVPMMSQLSVFNIGMVTTPQG 237
 SsPN-1 ALTRLVAVNAIYFKGLWKSRFQEPENTKMRFFNAGDGNYSYKVSMSQLSVFNIGLASTPQG 240
 XlPN-1 SVTRLVLVNAIYFKGLWKSRFHPENTKRRTFHGPDGKDRQVPLAQLSLFRSGSASTNG 235
 AcPN-1 ALTRLILVNAIYFKGLWKSRFQEPENTKRRTFETAADGKTYQVPLAQLSVFCGGTSTPND 235
 GgPN-1 -LTRLVLVNAVYFKGLWKSRFEPENTKRRFFYGADGKTYQVPLMSQLSVFCGGTSTPNE 234
 HsPN-1 VLTRLVLVNAVYFKGLWKSRFQEPENTKRRTEVAADGKSYQVPLAQLSVFCGGTSAAND 236

: ** : ** : *

OfPN-1 LKYKVIELPYHGNTISMLIVLPSDEDTPLSRVIPHISTATVQSWTKLHMHRKVRLLIPKF 297
 TnPN-1 LKYKVIELPYHGNTVSMIALLPSEEDTPLSHIIPHISTATVQSWTQLMHRKIRLLIPKF 297
 TrPN-1 LKYKVIELPYHGNTVSMIALLPSEENTPLSHIIPHTISTASVQNTKLMHMKIRLLIPKF 297
 SsPN-1 LNKYKVIELPYHGNSISMLIALPSEEDTPLGDVIPHINTATVQSWTKLHHRKVRLLIPKF 300
 XlPN-1 LWYNIELPYHGGSISMLVALPTEKSTPLSAIIPHISTKTQLQSWMT-MSPRCVTLIPKF 294
 AcPN-1 LWYNIELPYHGETISMLIALPTESTTPLSAIIPHISTKTIQSWMTTMVQKRVQVILPKF 295
 GgPN-1 LWYNIELPYHGEMISMLIALPTEENTTPLSAIIPHISTKTIGSWMTTMVAKRVQVILPKF 294
 HsPN-1 LWYNIELPYHGESISMLIALPTESTTPLSAIIPHISTKTIDSWMTIMVPRKRVQVILPKF 296

* : *

OfPN-1 TADAEDLEAPLSALGITDMFSQNKADFRHLSA--EPVHVSKALQKAKVVVNEDEGTKAAA 355
 TnPN-1 TADAEDLKESSLALGITDMFSVERADFRHLSA--EPVYVSKALQKAKIEVNEDEGTKASA 355
 TrPN-1 TADAEDLKGSLALGLITDMFSSEERADFRHLSA--EPLYVSTALQKAKIEVNEDEGTKASA 355
 SsPN-1 SAEAEVDLQASLSALGITDIFDEKADFRHLST--EPVYISKALQKAKIEVNEDEGTKAAA 358
 XlPN-1 SVEAEADLKEPLRNLGITEMFDVSKANFAKISR-SESLHVSLLQKAKIEVNEDEGTKASG 353
 AcPN-1 TVEAETDLKEPLQELGIRDMEQSKANFLKTR-TASIHVSQILQKAKIEVSEDEGTKASA 354
 GgPN-1 TAVEAETDLKDELKALGITDMFDESKSNEFAKITR-TEGLHVSHLQKAKIEVSEDEGTKASA 353
 HsPN-1 TAVEAETDLKEPLKVLGITDMFDSSKANFAKITR-TEGLHVSLLQKAKIEVSEDEGTKASA 356

: : *

↓ ↓

	Accession no.
OfPN-1 ATTAILIAR-SSPPWVTVDPRPFLFLIRHNPTGTILFVGQINQP 397	HQ385323
TnPN-1 ATTAILIAR-SSPPWVTVDPRPFLFLIRHNPTGTILEFMGQINQP 397	ENSTNIP00000017318 ^a
TrPN-1 ATTAILIAR-SSPPWVAVDRPFLFLIRHNPTGTILEFMGQINQP 397	ENSTRUP00000011515 ^a
SsPN-1 VTTAILIAR-SSPPWVTVDPRPFLFLIRHNPTGTILFVGQINQP 400	NP_001133589
XlPN-1 ATTAVLIAR-SSPPWVTVDPRPFLFLIRHNPTGAVLFTGQINQP 395	NP_001087103
AcPN-1 ATTAILIAR-SSPPWFVVDRAEVEFTIRHNPTGAVLFMGQVKNP 396	ENSACAP00000004313 ^a
GgPN-1 ATTAILIAR-SSPPWFIVDRPFLFLIRHNPTGTILEFMGQINQP 395	ENSGALP00000008232 ^a
HsPN-1 ATTAILIAR-SSPPWFIVDRPFLFLIRHNPTGAVLFMGQINQP 398	NP_006207

***: * : *

"Signature"

Fig. 13. ClustalW multiple alignment of the deduced primary sequence of rock bream PN-1 with known vertebrate homologous PN-1 sequences. Residues in bold and shaded in dark grey are conserved; asterisks (*) indicate complete conservation (100%), while colons (:) indicate strong conservation and dots (.) weak conservation. The areas of light grey shading indicate identical residues among rock bream and other teleost PN-1 sequences. The dashes represent the gaps introduced to maximize the alignment. N-terminal signal peptides are underlined and the conserved serpin signature motifs are boxed. The P₁ – P₁' reactive site scissile bond is shown by downward arrows (↓) at Arg and Ser. Two N-glycosylation sites are boxed and noted. Species: Of, rock bream; Tn, green-spotted puffer fish; Tr: fugu; Ss, Atlantic salmon; Xl, African clawed frog; Ac, anole lizard; Gg, chicken; Hs, human. The accession numbers are shown at the N-terminus. ^a: ENSEMBL database accession number.

Table 6.

Sequence similarity - identity matrix showing the percent identity/similarity between PN-1 orthologues.

Species	OfPN-1	TnPN-1	TrPN-1	SsPN-1	XIPN-1	AcPN-1	GgPN-1	HsPN-1
OfPN-1		83.9	83.4	79	54.3	55.9	56.1	54.8
TnPN-1	90.2		86.9	74.5	54.8	55.8	57	55.4
TrPN-1	91.2	91.2		75	53	56.1	55.8	54.6
SsPN-1	89	85.3	87.5		53.3	54.1	54.1	53.7
XIPN-1	71.3	70.8	70	71.3		67.9	68.4	70.4
AcPN-1	71.5	72	71.3	72.8	82.6		79	76.9
GgPN-1	73.6	72.8	71.5	72.3	82.8	90.4		78.6
HsPN-1	71.9	71.4	70.9	71.3	82.2	88.4	88.2	

Identity percent, shaded region; similarity percent, non-shaded region. Matrix was generated by MatGAT program using BLOSUM62 scoring matrix and maintaining first gap penalty and extending gap penalty levels at 12 and 2, respectively.

Table 7. Conservation and characteristics of functional regions of RbPN-1 and its orthologues.

Species	Heparin binding site	Charge	Hinge, reactive centre loop and serpin signature [§]			
			Hinge	P ₁₀	P ₅	P ₁ ▼ P ₁ '
OfPN-1	⁹¹ NMLKRLHKTLLTAKSNQ ¹⁰⁶	+4	³⁴⁸ EDGTKAAAATTAILLAR-SSPPW	VTVD	PPFLFLIRHNP	TGTILFIGQINQP ³⁹⁷
TnPN-1	⁹¹ KMLRKLHKTLLTAKANQ ¹⁰⁶	+5	³⁴⁸ EDGTKASAATTAILLAR-SSPPW	VTVD	PPFLFLIRHNP	TGTILFMGQINQP ³⁹⁷
TrPN-1	⁹¹ KMLKKLHKTLLTAKANQ ¹⁰⁶	+5	³⁴⁸ EDGTKASAATTAILIAR-SSPPW	VAVD	PPFLFLIRHNP	TGTILFMGQINQP ³⁹⁷
SsPN-1	⁹⁴ KMLRKLHKTLLTAKSNQ ¹⁰⁹	+5	³⁵¹ EDGTKAAAVTTAILMAR-SSPPW	VIVD	PPFLFLIRHNP	TGTILFIGQVNQP ⁴⁰⁰
GaPN-1	⁸⁹ RMLKKLHKTLLTAKSNQ ¹⁰⁴	+5	³⁴⁶ EDGTKAAAATTAILLAR-SSPPW	VSD	PPFLFLIRHKPT	GAVLFMGQINQP ³⁹⁵
DrPN-1	⁸⁹ KMLRKLHKSLLTTSNA ¹⁰⁴ .*.*.:**.*:**.*.*	+5	³⁴⁶ EDGTKASATTSVILHAR-SSPPW	VTVD	PPFLFLIRHNS	SGTILFAGQINKP ³⁹⁵ *****:*.*.*:**.*.* ***** :.*.*:**.*.*
RnPN-1	⁹⁰ KVLKKINKAIVSKKNK ¹⁰⁵	+7	³⁴⁸ EDGTKAAVTTAILIAR-SSPPW	FIVDR	PFLFCIRHNP	TGAILFLGQVNKP ³⁹⁷
HsPN-1	⁹⁰ KILKKINKAIVSKKNK ¹⁰⁵	+7	³⁴⁸ EDGTKASAATTAILIAR-SSPPW	FIVDR	PFLFFIRHNP	TGAVLFMGQINKP ³⁹⁷

[§] predicted by SMART server; * identical; : conserved; . semi-conserved. ▼ denotes the scissile bond; P_x annotates the conventional notation of RCL residues. The hinge region and signature motif are indicated by light grey and dark grey shading, respectively. Species: Of, rock bream; Tn, green-spotted puffer fish; Tr, fugu; Ss, Atlantic salmon; Ga, stickleback, Dr, zebrafish; Rn, rat (P07092); Hs, human. For accession numbers, refer to Table 1 and Fig. 2. Superscripted numbers indicate the location of residues in the premature peptide.

3.1.3. Molecular modeling

Based on the deduced primary sequence, and using the human PAI-1, chain A (PDB, 1dvmA) as a template, we established the tertiary (3D) structure of RbPN-1. RbPN-1 shared 42% and 60% of identity and similarity, respectively, with the template (Fig. 14A). A Ramachandran plot statistic revealed that 95% and 85% of the residues of RbPN-1 were located in the allowed and most favored regions, respectively. The resulting model (Fig. 14B) resembled the typical serpin structure comprising 9 α -helices, 3 β -sheet sandwiches and coils. The RCL and Arg-Ser bond were clearly expelled from the surface towards the cognate protease. In our model, ⁷¹Lys, ⁷⁵Lys and ⁷²Arg were found on the exposed surface of helix D. Another ⁸⁰Lys located in the following loop region together with helix D, formed a positively-charged, basic cluster which could be anticipated as the putative HBS (Arcone et al., 2009; Stone et al., 1994) of the RbPN-1.

(A)

```
HsPAI-1      VHHPPSYVAHLASDFGVRVFQQAASKDRNVVFSFYGVASVLAQLTTGGTQQQIQ 60
RnPN-1      --QGSPSYGER--GSDLGIQVFQVVRSRPLENVVLSPHGVASILGMLPGAHVTRKQVLN 57
           : *** : .**:*:*****.: : .***:*:*****:*:** : * **:::

HsPAI-1      AMGFKIDDKGMAPALRHLYKELMGFWNKDEISTTDAIFVQRDLKLVQGFMPHFFLERF 120
RnPN-1      ALRYKK--KGPYNMLKRLHKTTLAKSNQDLVLIANAMFSQEGFPMEAEAFVATKANFQCE 115
           *: :* ** *:*:* * . *:* : ::* * .. : :*:.

HsPAI-1      VKQVDFSEVERARFIINDWVKHTKGMISHLLGTGAVQ-QLTRLVLVNALYFNGQWKTF 179
RnPN-1      SRSLDFSNPQGAADENWVNNKTKGHIPLIKADMDSALTRLVAVNSIYFKGLWKSFR 175
           :.***: : * **:*:.*** * . * : . : : ***** **:*:* * ** : *

HsPAI-1      PDSSTHRRLFHKSDBGSTVSPVMAQTNKFNYTEFTTPDGHYDILELPYHGDTLSMFIA 239
RnPN-1      QPENTKMRPFNGGDGNVYKVPMSQLSVFNISMATTPQGLKYKVIELPYHGNTISMLIVL 235
           ..* : * * : .**.. ***** * . ** : **:* * ..:*****:*:*:*:

HsPAI-1      PYEKEVPLSALTNILSAQLISHWKNMTRLRLLVLPKFSLETEVDLRKPLENLGMTDM 299
RnPN-1      PSDEDTPLSRVIPHISTATVQSWTKLMHRKVRLLIPKFTADAQVLEAPLSALGITDM 295
           * :.:*** : :* : . * . * ***** ::*:* . ** .**:*

HsPAI-1      RQFQADFTSLSDQELHVALALQVKIEVNESGTVASSSTAVIVSARMAPEEIIIDRPFL 359
RnPN-1      SQNKADFRHLS-AEPVHVSKALQKAKVVNEDGTKAAAAATTAILLARSSPPVWTVDRPFL 354
           * :*** ** **:*: ***. * : **.* * :.:. : * : * : :****

HsPAI-1      FVVRHNPTGTVLFMGQVMEP 379
RnPN-1      FLIRHNPTGITLFIGQINQP 374
           *:*****:*:*:* :*
```

(B)

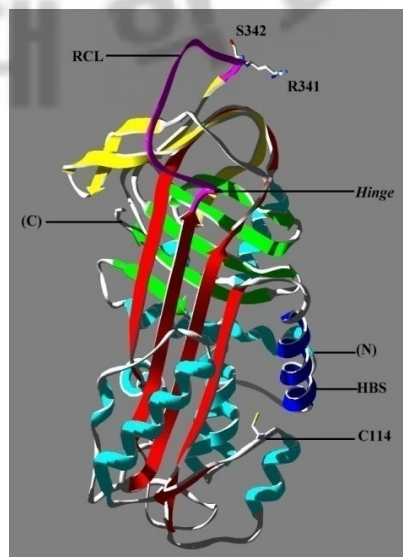


Fig. 14. Structural model of mature RbPN-1. (A) ClustalW alignment of the rock bream PN-1 (HQ385323) and human PAI-1 (PDB, 1dvmA). (B) Predicted tertiary structure of RbPN-1. Numbers correspond to positions of residues in the mature peptide. C, C-terminus; N, N-terminus; RCL, reactive centre loop; HBS, putative heparin binding site.

3.1.4. Phylogenetic study

Phylogenetic analysis to determine the relative evolutionary position of RbPN-1 using the deduced amino acid sequences of different PN-1s and PAI-1s with an invertebrate PN-1 from *Culex quinquefasciatus* as an out-group (Fig. 15) showed that there were two main clusters of vertebrate PAI-1s and vertebrate PN-1s. RbPN1 was positioned in the fish cluster where it was sub-grouped with PN-1s of Japanese pufferfish and green spotted pufferfish. This indicates that RbPN-1 has evolved from the common ancestral origin of PN-1s.

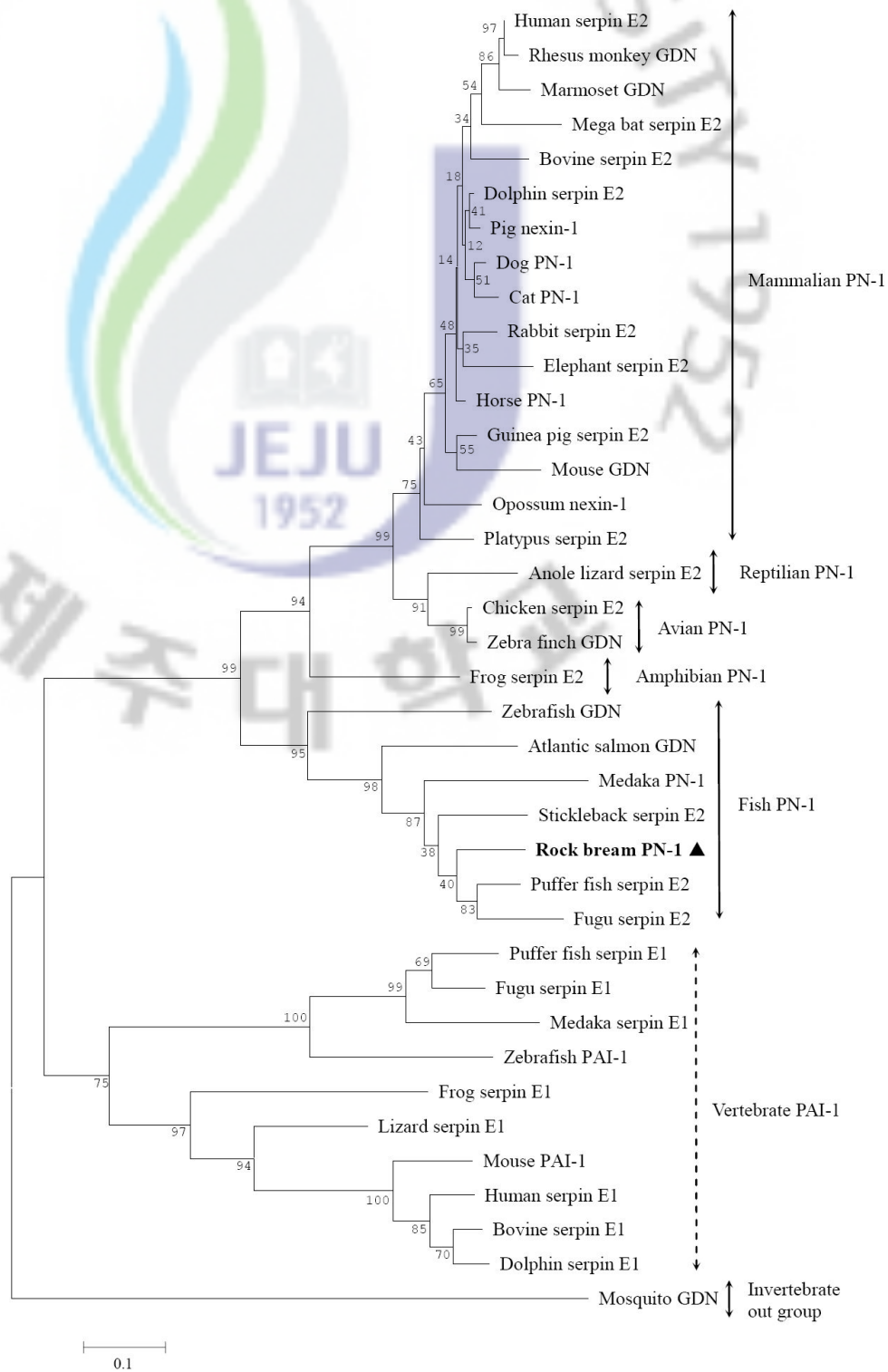


Fig. 15. Phylogenetic analysis of protease nexin-1 orthologues and PAI-1 members. The sequence of glia-derived nexin from mosquito (*Culex quinquefasciatus*) was used as the out-group. The number at each node indicates the percentage of bootstrapping after 1000 replications. The accession numbers are given in Table 5 and Fig. 13, with the exception of marmoset *Callithrix jacchus* (XP_002749886); cat *Felis catus* (MER102210^b); rabbit *Oryctolagus cuniculus* (ENSOCUP00000003766^a); platypus *Ornithorhynchus anatinus* (ENSOANP00000005635^a). ^a ENSEMBL database accession number; ^b MEROPS database identifier.

3.2. Overexpression and purification of recombinant RbPN-1 (rRbPN-1)

To study the function of RbPN-1, the coding sequence (excluding its signal peptide) was ligated into a pMAL-c2X expression system, resulting in the expression of rRbPN-1 that fused to the MBP. The rRbPN-1 was overexpressed in *E. coli* BL21 (DE3) cells by IPTG induction, and a 83.5 kDa MBP (42.5 kDa) fused mature rRbPN-1 (41 kDa) was purified. The 12% SDS-PAGE analysis at different steps in the purification procedure of rRbPN-1 are shown in Figure 16 which shows that rRbPN-1 was sufficiently induced (lane I) compared to un-induced cells (lane U); a relatively high soluble fraction was present in the crude extract (lane C). Lane P shows the homogeneity of purified rRbPN-1 fusion protein.

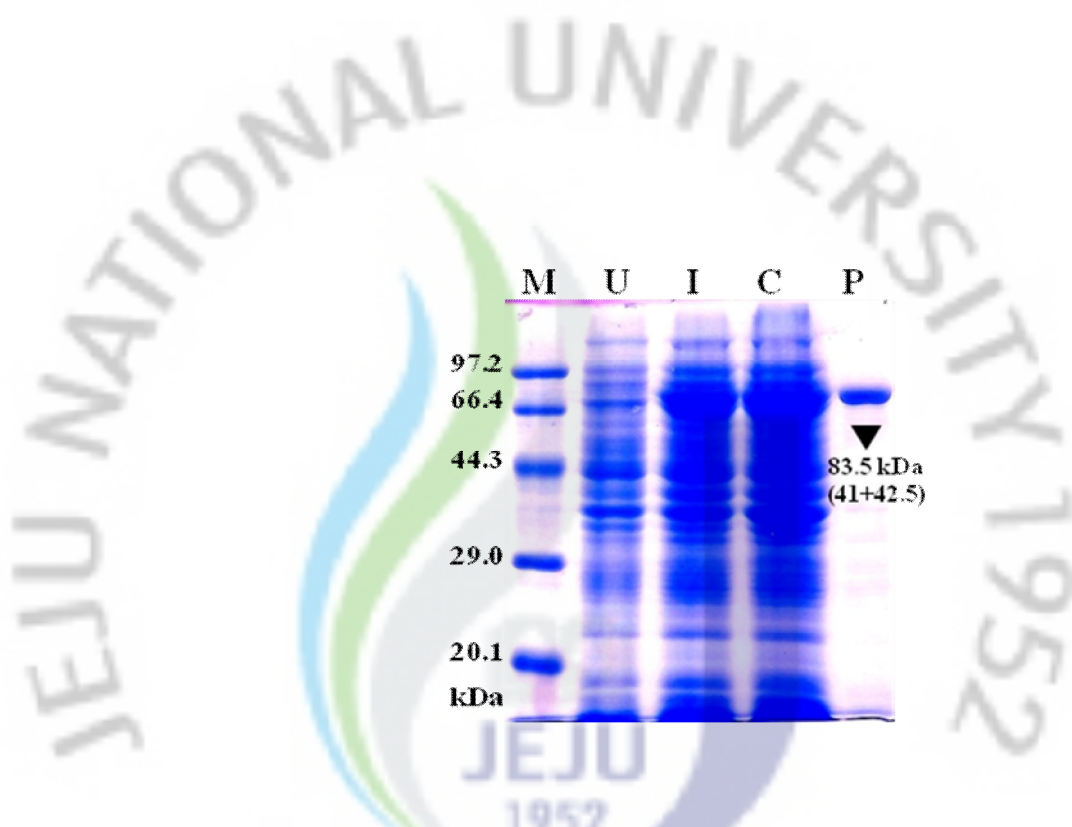


Fig. 16. SDS-PAGE analysis of overexpressed and purified mature recombinant RbPN-1 fusion protein. Lanes: M, protein marker (TaKaRa); U, total cellular extract from *E. coli* BL21 (DE3) before IPTG- induction; I, after IPTG induction (0.25 mM) at 20 °C for 5 h; C, crude extract of rRbPN-1; P, purified recombinant fusion protein (rRbPN-1/MBP).

3.3. *In vitro* antiprotease activity assays

The inhibitory effect of rRbPN-1 on the hydrolysis of synthetic chromogenic substrates by proteases (trypsin and thrombin) was investigated. Results showed that rRbPN-1 was able to inhibit the amidolytic activity of both proteases in a concentration-dependent manner under the assay conditions (Fig. 17). RbPN-1 was able to inhibit the trypsin and thrombin activity by an average of 48% and 89% at 8 μ M and 250 nM, respectively. Linear (Fig. 17A) and sigmoidal (Fig. 17B) plots confirm the concentration-dependent nature of trypsin and thrombin inhibition, respectively. Heparin was found to potentiate thrombin inhibition even at lower dose levels (100 nM) by RbPN-1, but not the trypsin inhibition. At higher doses, heparin failed to display its potentiating role of RbPN-1 against thrombin (Fig. 17B).

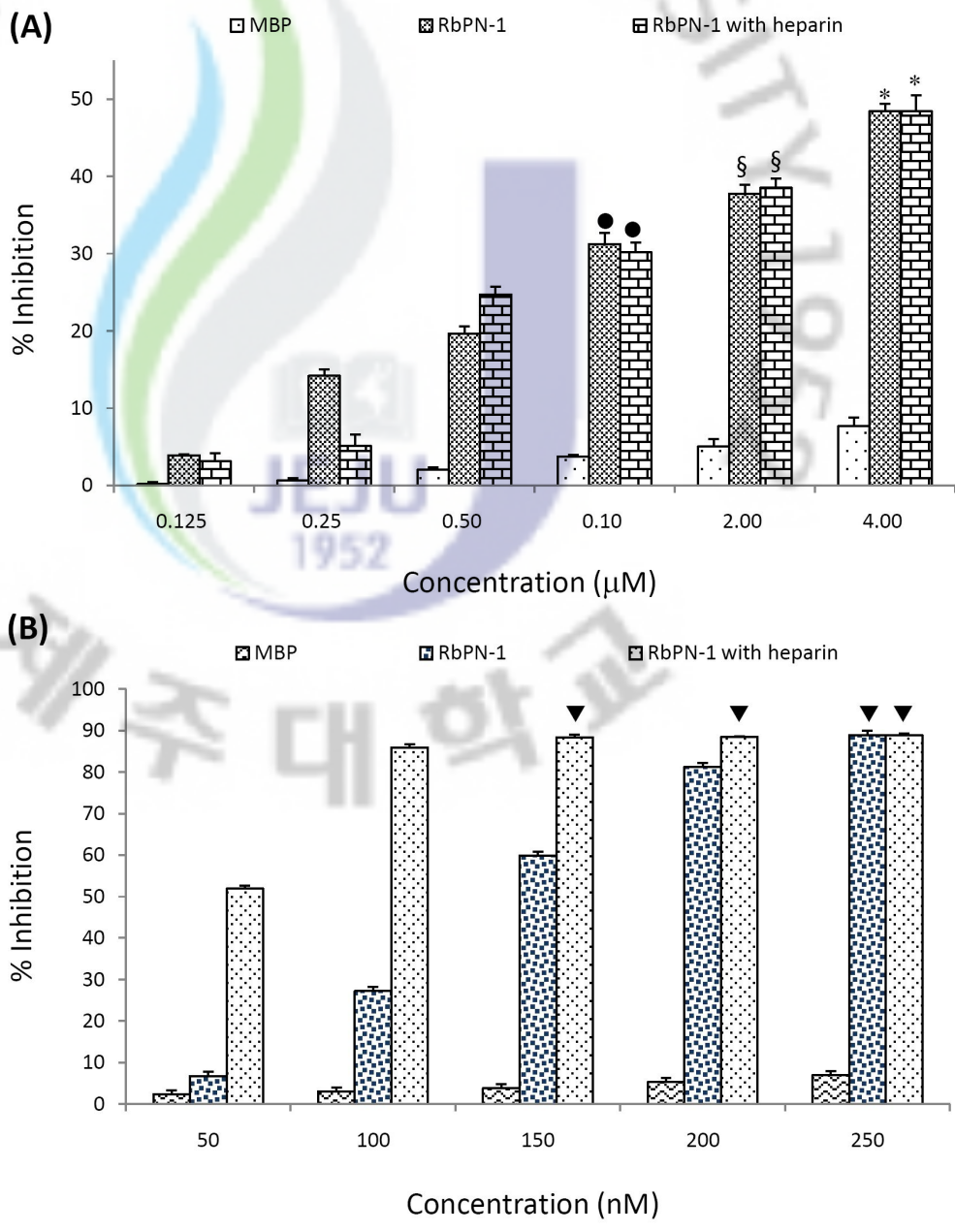


Fig. 17. *In vitro* antiprotease activity assays against (A) trypsin, (B) thrombin and the potentiating effect of heparin. Columns represent the percent inhibition of MBP, RbPN-1 and RbPN-1, respectively, in the presence of heparin at different concentrations. Error bars represent the SD (n=3). Data with different symbols are significantly different (p<0.05) among different assays.

3.4. In vitro anticoagulation assay

To characterize the anticoagulant property of rRbPN-1, we performed the classical APTT assay. rRbPN-1 prolonged APTT in a dose-dependent manner (Fig. 18). No significant inhibition occurred in control experiments, in which MBP was incubated with plasma. rRbPN-1 (14 μ g) was able to prolong the control clotting time from 38.1 s to 141 s within the dose range used in our experiment.

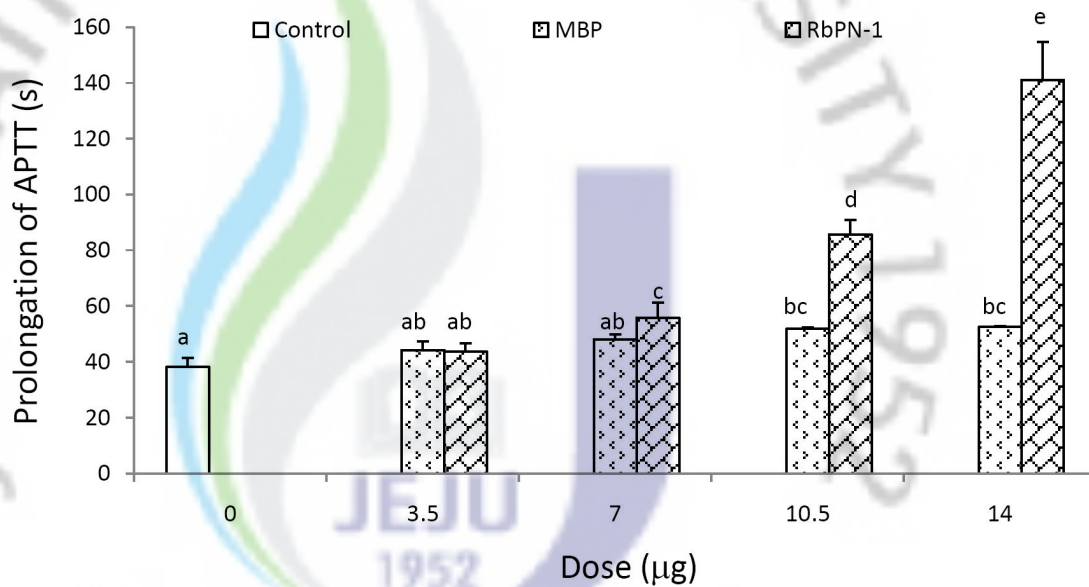


Fig. 18. *In vitro* anticoagulant activity assays for recombinant RbPN-1. Columns represent the activated partial thromboplastin time of control (water), MBP and RbPN-1, respectively, at different doses. Error bars represent the SD (n=3). Data with different letters are significantly different ($p<0.05$) among different groups.

3.5. Analysis of tissue specific expression profile of RbPN-1

To determine the tissue-specific RbPN-1 mRNA profile, qRT-PCR was performed on various Rb tissues using gene-specific primers designed based on RbPN-1 coding sequence. The relative expression fold of each tissue was calculated using Rb β -actin as the reference gene and further compared with expression level in muscle to determine the relative levels of tissue-specific expression (Fig. 19). RbPN-1 mRNA was found to be constitutively expressed in all tissues investigated. Detailed analysis revealed that RbPN-1 transcription was significantly higher ($p < 0.05$) in heart, gills and brain, moderately high in blood and liver, and poorly expressed in other tissues analyzed. Thus, the transcript levels of RbPN-1 showed a clear tissue-specific differential expression.

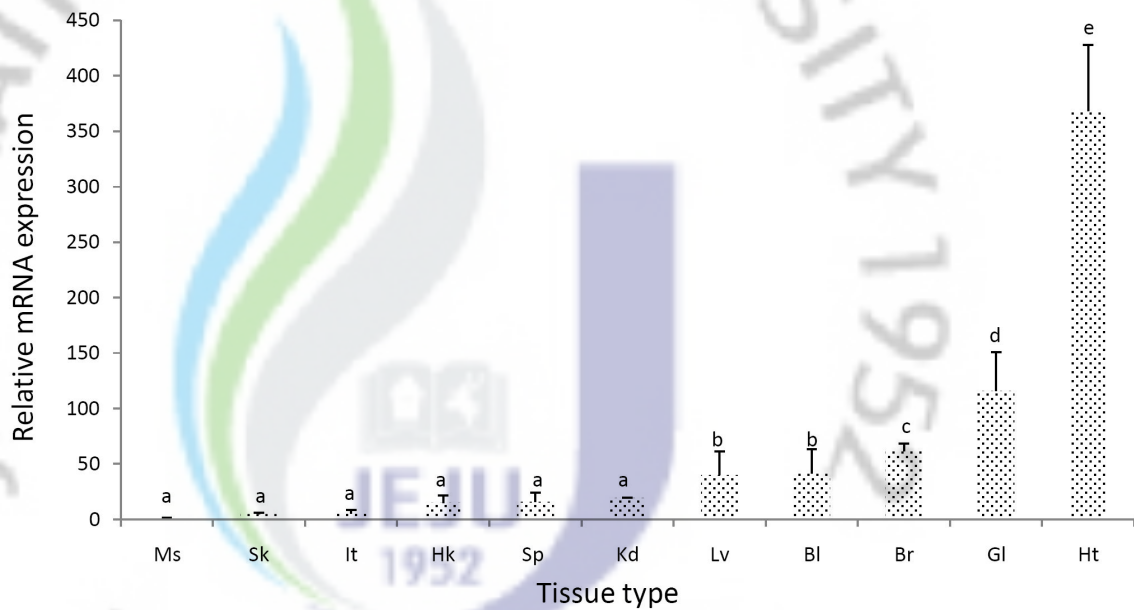


Fig. 19. Tissue-expression analysis of RbPN-1 mRNA determined by quantitative real-time PCR. The relative RbPN-1 mRNA expression of each tissue was calculated by the $2^{-\Delta\Delta CT}$ method using rock bream β -actin as the reference gene. Then, the relative mRNA level was compared with muscle expression to determine the relative fold change. Ms, muscle; Sk, skin; It, intestine; Hk, head kidney; Sp, spleen; Kd, kidney; Lv, liver; Bl, blood; Br, brain; Gl, gill; Ht, heart. Error bars represent the SD (n=3). Statistical analysis was performed by one-way ANOVA followed by Duncan's Multiple Range test. Data with different letters are significantly different ($p < 0.05$) among different tissues.

3.6. Transcriptional responses of RbPN-1

3.6.1. Against LPS, bacterium and RBIV stimulation

To evaluate the variations in RbPN-1 expression in response to exposure to LPS, *E. tarda* and RBIV, blood and gill tissue from challenged fish were used. The relative mRNA levels of RbPN-1 were calculated using the constitutively expressing Rb β -actin for normalization and compared with the respective PBS-injected controls at each time point. Further, the relative expression fold-change in hematic cells and gill at 12 h and 48 h post-infection, respectively, were compared to the PBS-injected controls (Fig. 20).

In hematic cells of fish challenged with LPS, RbPN-1 transcript level was significantly ($p < 0.05$) up-regulated at all the time points examined. RbPN-1 mRNA level increased up to 2.2-fold at 3 h p.i., followed by a slight decline and eventually reaching higher level at 12 h p.i. (3.34-fold) with a late-phase up-regulation response (2-fold) at 48 h p.i. (Fig. 20A). In contrast, evaluation of the hematic cells of *E. tarda* challenged animals indicated that bacterium significantly ($p < 0.05$) stimulated the RbPN-1 transcript level only at 12 h p.i., whereas the transcript level was either lower or insignificant at all the other time points (data not shown). Generally, the relative transcription level was increased following infection with RBIV at all the time points examined, with the exception of 6 h p.i. Following the vacillating up- and down- regulation that was observed at earlier time points, the RbPN-1 transcript level reached its highest point (3.4-fold) at 12 h p.i., then declined to basal level and again raised to 2.39-fold at 48 h p.i. (Fig. 20B). Thus, in all challenges, the relative transcription in hematic cells reached its elevated level at 12 h p.i.

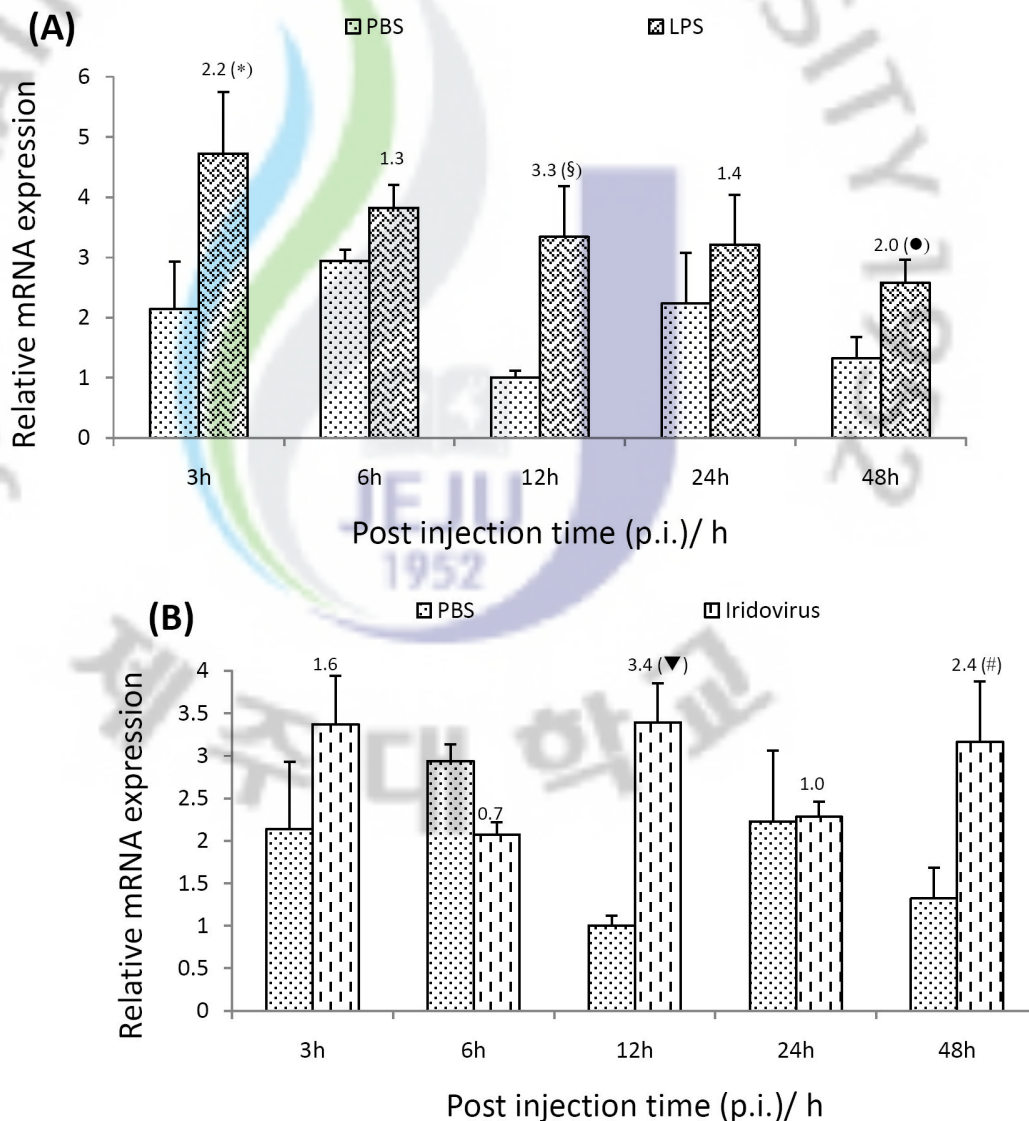


Fig. 20. RbPN-1 mRNA expression in hematic cells in response to challenge by (A) LPS and (B) iridovirus. The relative expression was calculated by the $2^{-\Delta\Delta CT}$ method using rock bream β -actin as the reference gene. Then, the relative mRNA level was compared with expression of 12 h - PBS control to determine the relative fold change. Relative fold (RF) values of each 'challenge: individual PBS control' pair are indicated above the error bars which represent the SD (n=3). Data with different symbols are significantly different ($p < 0.05$) among different time points and indicated only when RF is > 2 .

Figure 21 shows the relative transcription levels detected in gill tissues of challenged fish. During LPS exposure, the expression slightly fluctuated up to 24 h p.i. The late phase response, however, was characterized by significantly increased RbPN-1 transcription ($p < 0.05$) which reached its highest level (2.7-fold) at this time point (Fig. 21A). Interestingly, RbPN-1 transcription in gills of *E. tarda* infected animals was significantly elevated ($p < 0.05$) at all the time points examined. The fold-change of induced expression was within the range of 1.2–1.6 during the period of 3 h to 24 h p.i., and the relative induction reached its maximum (3.83-fold) at 48 h p.i. (Fig. 21B). RbPN-1 expression in gill tissues of RBIV infected fish presented a similar profile to the other challenges and the significantly ($p < 0.05$) highest transcription level was achieved at 48 h p.i. (1.75-fold). However, at the other time points the fold-change of RBIV induced expression was statistically insignificant (data not shown). It is important to note that even though each immune challenge generated a grossly similar response pattern, the tissue response profiles were distinct.

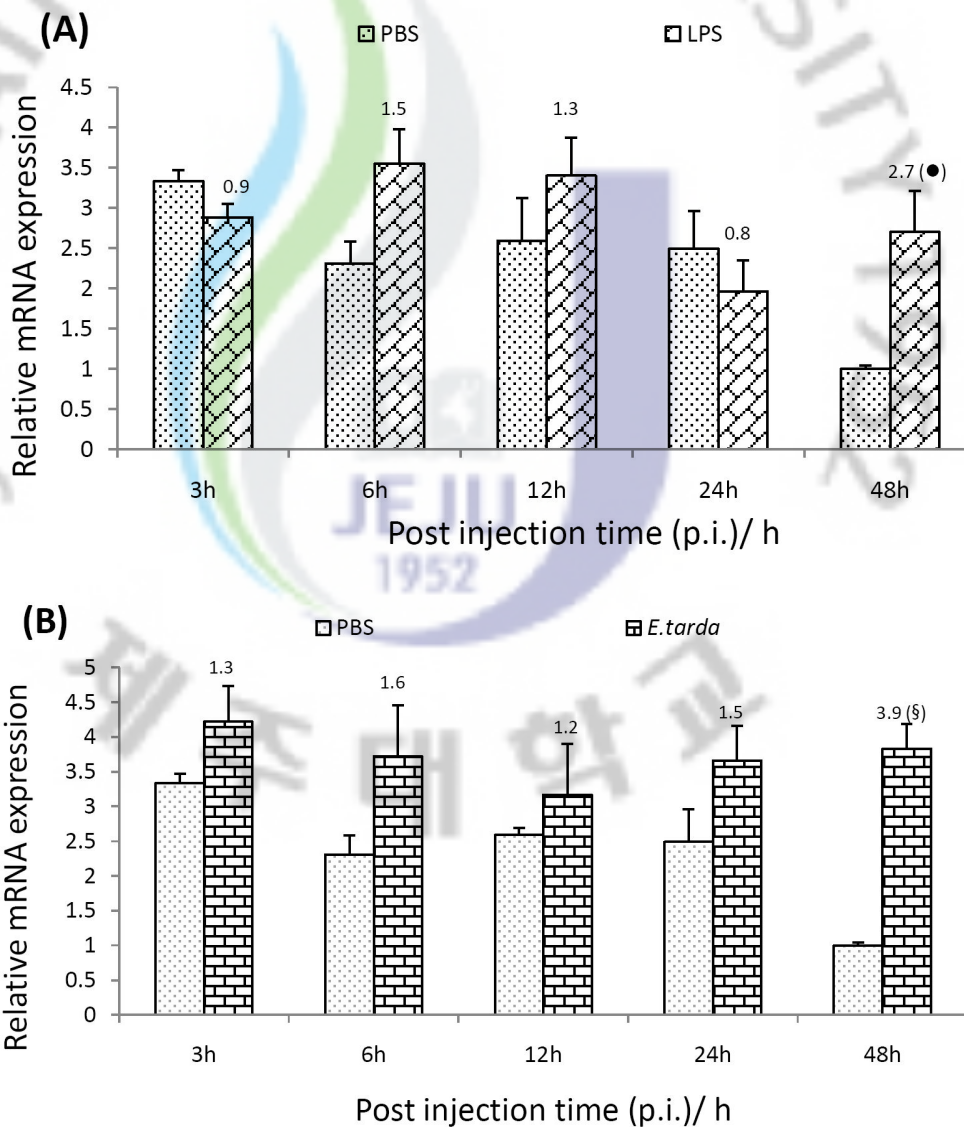


Fig. 21. RbPN-1 mRNA expression in gills in response to challenge by (A) LPS and (B) *E. tarda*. The relative expression was calculated by the $2^{-\Delta\Delta CT}$ method using rock bream β -actin as the reference gene. Then, the relative mRNA level was compared with expression of 48 h - PBS control to determine the relative fold change. RF values of each 'challenge: individual PBS control' pair are indicated above the error bars which represent the SD (n=3). Data with different symbols are significantly different ($p < 0.05$) among different time points and indicated only when RF is > 2 .

3.6.2. Against muscle injury

We also investigated the impact of injury on the expression of RbPN-1 (and heparin cofactor II, RbHCII) in hematic cells by performing a time course injury experiment. In addition to the β -actin reference, results were further compared with uninjured controls (Fig. 22). Interestingly, expression of both RbPN-1 and RbHCII was significantly ($p < 0.05$) suppressed below the level of uninjured control at all the time points examined. In injured fish, RbPN-1 displayed an immediate response, in which the expression declined to its lowest level (40%) and then transiently increased until the 12 h when another late phase down-regulatory response was observed until 48 h p.i. (Fig. 22A). The RbHCII mRNA level in hematic cells of injured animals also displayed an identical expression profile; however, the suppression of RbHCII expression was significantly robust ($p < 0.05$) and it reached the lowest level (27%) at 3 h p.i. With the exception of the 12 h time point, all time points examined revealed that RbHCII expression showed no significant level of variation among them (Fig. 22B).

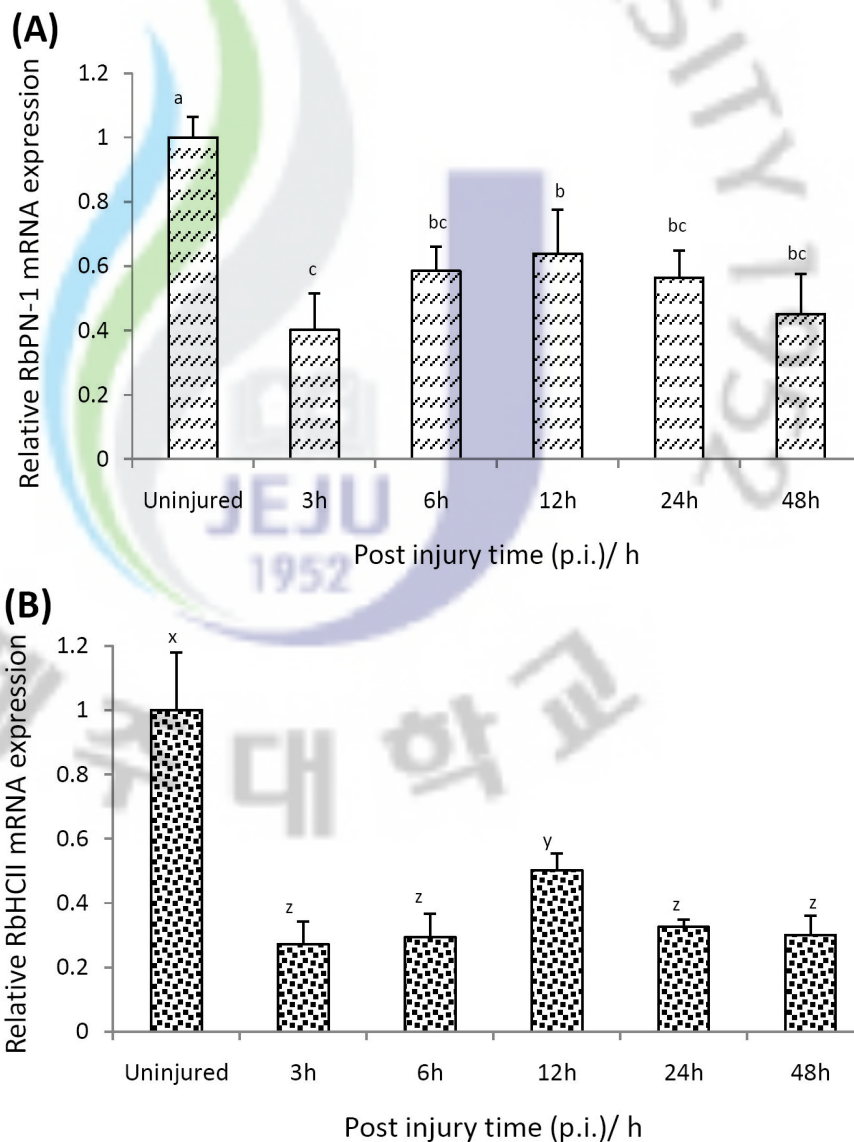


Fig. 22. Impact of muscle injury on mRNA expression of (A) protease nexin-1 and (B) heparin cofactor II in rock bream hematic cells. The relative expression was calculated by the $2^{-\Delta\Delta CT}$ method using rock bream β -actin as the reference gene. Then, the relative mRNA level was compared with expression of uninjured control to determine the relative fold change. Error bars represent the SD (n=3). Data with different letters are significantly different ($p < 0.05$) among different time points compared.

4. DISCUSSION

In the present study, a gene encoding the super family protein, clade E, member 2, known as the protease nexin-1, was isolated, sequenced and characterized from rock bream, *O. fasciatus*. Its antiprotease and anticoagulant activities were evaluated by use of a recombinant protein. Finally, the mRNA distribution in various tissues and its transcriptional response to immune and injury challenges were defined.

4.1. Molecular structural characterization

The superfamily members share numerous structural characteristics of having a moderate molecular mass (40–50 kDa), a signature domain located in the C-terminal region, a RCL and a scissile bond (P₁-P₁') (Law et al., 2006). They inhibit proteases by irreversibly binding and changing the conformation of proteases and (Huntington et al., 2000) to form SDS-stable complexes which are then degraded. A novel gene from Rb was identified by BLAST analysis as being the protease nexin-1 (Fig. 12, 14B). RbPN-1 has a molecular mass of 44 kDa and its primary structure possesses a broad domain and a putative scissile bond of ³⁶⁴Arg - ³⁶⁵Ser which precedes the signature proximal to the C-terminus. The length of the signal peptide in RbPN-1 was quite larger than that of mammals but identical (23 amino acids) to that of other fish (Fig. 2). The length of the premature peptide of PN-1s in different species is almost the same (395-400 amino acids), indicating it has not undergone appreciable changes during molecular evolution. RbPN-1 has one N-glycosylation site of ¹⁶⁰NKTK¹⁶³, similar to that in human and rat where ¹⁶⁰Asn residue is conserved in some of the different species analyzed. The N-glycosylation sites have been suggested in facilitating the post-translational modifications and formation of different PN-1 molecular forms (Mansuy et al., 1993). Thus, we could expect different isoforms of PN-1 to exist in Rb. While mature rat and human PN-1s contain three Cys residues (McGrogan et al., 1988; Sommer et al.,

1987) with no disulfide bridge, mature RbPN-1 has only one Cys (¹³⁷Cys) which was conserved among all the species considered except frog (Fig. 13).

Our findings support the fact that several functional domains of PN-1 are highly conserved among pisces (Table 7). Though serpins are regulators of proteases, they are under the control of allosteric regulatory molecules. GAGs and/or ECM co-factors that regulate the activity and localization of PN-1 include collagen type IV (Crisp et al., 2002), thrombomodulin (Bouton et al., 2007) and proteo-glycans such as heparan sulfate with heparin being the major and potent co-factor of PN-1 (Scott et al., 1985). The HBS of rat PN-1 is proposed to encompass seven lysyl residues (Stone et al., 1994). However, in some species, residues have been replaced by Arg/others. Substitution of ⁹¹Lys/Arg → ⁹¹Asn in RbPN-1 leads to a relatively low charge (+4) compared to other fish. Thus, RbPN-1 may have comparatively low heparin association kinetics. Apart from that, fish HBSs show unique patterns of conservation. Hence we propose that fish PN-1s may establish charge-independent, hydrophobic interactions with heparin in the physiological environment. However, detailed investigations are necessary to prove this. HBS of PN-1, HCII and ATIII were found to be similar (Rovelli et al., 1992; Stone et al., 1994). The analysis of HBSs of RbPN-1 and RbHCII showed that the positions of all charged residues (Lys, His and Arg) were conserved, though a few were substituted by one another. It is also noteworthy that both RbPN-1 and RbHCII share 40% of sequence similarity. These findings indicate evolutionary conservation of intra-species structural features of members. The clearance of PN-1–protease complex occurs via LRP, facilitated by heparin at the cell surface (Crisp et al., 2000; Knauer et al., 1997b). The LRP-binding site in RbPN-1 (⁴⁸PLENVVLSPHGV⁵⁹) is partially conserved compared to that of human, ⁴⁷PHDNIVISPHGI⁵⁸ (Knauer et al., 1997a) where in spite of the substitutions, the charge, polarity and hydrophobicity remain intact. Thus, we suggest a similar LRP mediated mechanism is at work in fish. Though the hinge region (Glu-X-Gly-X-Glu) is not conserved between PN-1 and

other serpins (McGrogan et al., 1988), all the PN-1 peptides including RbPN-1 harbor a conserved stretch of “Glu-X-Gly-X-Lys” (Table 3). The examination of the serpin signature in the PN-1s revealed a substitution from Val in fish to Phe in other lineages and of the eleven residues in this motif, only the second residue varies extensively among the different fish examined.

Pair-wise alignments showed a transient decrease in identity and similarity from fish to mammals (Table 5). The multiple alignment study showed that PN-1 homologues from fish are closer than to those of other lineages and share distinct features. PN-1 homologues from various lineages indicate that the homology increases towards the C-terminus, along the serpin domain and reaches its maximum at the RCL region, similar to RbHCII. The mammalian PAI-1 members display closer homology to RbPN-1 than fish PAI-1 members which is in agreement with our previous findings of RbHCII (Umasuthan et al., 2011b).

Phylogenetic analysis of PN-1s and PAI-1s from 38 different species generated a tree composed of two major clusters of serpin E1 (PAI-1) and serpin E2 (PN-1). Fish PN-1 members clustered closely and independently, where RbPN-1 was placed with green spotted pufferfish and Japanese pufferfish, with a bootstrap value of 83. Despite the high identity values of RbPN-1 with mammalian PAI-1s, RbPN-1 is closer to fish PAI-1s in phylogeny. In addition, the tree reflects the currently accepted relationships (Fig. 15).

An attempt to visualize the tertiary structure of RbPN-1 revealed a conventional serpin structure portraying the expelled RCL with a scissile bond and a hinge region and a putative HBS that is rich in positively charged residues on/near the helix D region (Fig. 14B), similar to rat PN-1 model (Arcone et al., 2009). Taken together with the characteristics discussed, the tertiary structure further indicates that RbPN-1 is a novel member of serpin superfamily.

4.2. Functional characterization of recombinant RbPN-1

To characterize the RbPN-1 at its physiological and functional level using *in vitro* assays against proteases, we re-cloned the RbPN-1, without its signal peptide. PN-1 is known to inhibit a broad spectrum of serine proteases (SPs). The Arg at P₁' facilitates the inhibition of the trypsin-like enzymes. In particular, PN-1 can act as an antiprotease with rapid second-order kinetics against certain SPs (Scott et al., 1985). Using purified rRbPN-1, its dose-dependent antiprotease activity against trypsin and thrombin was characterized. The rRbPN-1 inhibited trypsin and thrombin by 48% (8 μM) and 89% (250 nM) on average, respectively. Both trypsin and PN-1 are significantly expressed in the brain, and brain trypsin has been shown to be inhibited by PN-1 (Koistinen et al., 2009). Heparin significantly enhances the antithrombotic activity of RbPN-1, particularly at lower concentrations of serpin. In the presence of heparin, PN-1 becomes a potent and rapid inhibitor of thrombin and factor X_{ia} (FXIa), even more than the heparin-mediated ATIII and C1 inhibitor, the most important thrombin and FXIa inhibitors, respectively (Boulaftali et al., 2010; Knauer et al., 2000; Scott et al., 1985). We speculate that serpin-action mediated by GAGs is an evolutionary remnant originating from the lower vertebrate lineages. Our study provides the first evidence to the physiological inhibitory activity of a PN-1 member from a lower order vertebrate family. However the underlying antithrombotic mechanism of PN-1 in fish remains to be investigated. The rRbPN-1 was found to prolong the APTT in a dose-dependent manner. The anticoagulant effect modulated by a recombinant PN-1 (Bouton et al., 2007) and a platelet PN-1 (Boulaftali et al., 2010) have been reported. Indeed, the reason behind the anticoagulant activity of RbPN-1 might be its antithrombotic property.

4.3. Expression analysis

PN-1 expression during various developmental stages of tissues in vertebrates like frog (Onuma et al., 2006), chicken (Rodriguez-Niedenfuhr et al., 2003), mouse (Mansuy et al., 1993), rat (olfactory bulb) (Gloor et al., 1986; Simpson et al., 1994), monkey (Zhang et al., 2007) and human (cerebral cortex) (Choi et al., 1990) have been investigated. Using qRT-PCR, we analyzed the transcript levels of RbPN-1 in various Rb tissues and found that it is constitutively expressed in all tissues where the expression in heart, gill and brain is being the highest and blood and liver being the second highest. Though mammalian PN-1 is found localized to the brain, RbPN-1 is expressed predominantly in heart. Similarly, PN-1 mRNA has been detected in cardiac tissues of embryos and adults of rodents (Gloor et al., 1986; Mansuy et al., 1993). The presence of PN-1 in mouse lung and Rb gill may indicate another novel physiological role for PN-1 in respiratory organs. A substantial level of RbPN-1 transcripts was found in Rb liver, though not in adult mouse liver (Zhang et al., 2007). While terapod PN-1 orthologues shared some expression patterns and functions, the distinct spatial distribution of PN-1 in adult Rb tissues suggest possible divergent physiological functions of PN-1 in fish.

Thrombin, a principal component of the blood coagulation cascade is a multifunctional SP. It induces apoptosis in astrocytes (Donovan and Cunningham, 1998), acts as a chemotactic agent for monocytes (Bar-Shavit et al., 1983b) and a potent mitogen of various cells (Low et al., 1982). It also modulates neurite outgrowth of neuroblastomas (Gurwitz and Cunningham, 1988) and stellation of astrocytes (Cavanaugh et al., 1990). Thrombin found implicated in common pathophysiological conditions like atherosclerosis (Mansilla et al., 2008), Alzheimer's disease (Mentz et al., 1999; Vaughan et al., 1994) and carcinoma (Gao et al., 2008) shows that its uncontrolled activity may disrupt the hemeostasis and physiological integrity. Therefore, thrombin exists in "equilibrium" with endogenous protease inhibitors, in particular with PN-1. Thrombin down-

regulates PN-1 expression in rat muscle (Richard et al., 2004), which is the potent inhibitor of thrombin in the peri-cellular environment. Whereas, thrombin-stimulated cell division (Low et al., 1982), its reversal effect on neurite outgrowth (Gurwitz and Cunningham, 1988) and astrocyte stellation (Cavanaugh et al., 1990) are reciprocally regulated by the PN-1. Since studies also show that thrombin can mediate immune-related phenomena like inflammation, revascularization and wound healing, we hypothesized that PN-1 may contribute to host immune mechanisms. Hence, we investigated the relative mRNA levels of RbPN-1 upon different immune challenges.

LPS, a well-characterized endotoxin used in experimental designs aiming to induce inflammatory responses up-regulated RbPN-1 expression in hematic cells and the elevated level was maintained up to 2 days p.i. In contrast to other serpins that are synthesized by the liver and secreted into plasma, PN-1 is synthesized by various cells including platelets/thrombocytes (Gronke et al., 1989) and monocytes/macrophages. It has been reported that LPS consistently increased PN-1 expression in monocytes at both mRNA and protein levels (Mansilla et al., 2008) and PN-1 is also identified as a LPS-induced candidate gene in rat (Cook et al., 2004). The importance of fish thrombocytes, one of the main cell type of fish hematic cell population, in linking the innate and adaptive branches of immunity has been previously described (Passantino et al., 2005). These findings support that PN-1 might contribute to the immune potential of blood cells, particularly thrombocytes. *E. tarda* is a bacterium that has a significant impact on the Rb aquaculture industry, only induced a significant up-regulation at 12 h p.i in hematic cells. In accordance with a study in Japanese flounder using hirame rhabdovirus (HRV) (Aoki et al., 2000), RBIV up-regulated PN-1 expression in hematic cells throughout the experimental period, except at 6 h p.i., suggesting a protective role of RbPN-1 against viral pathogens. Interestingly, all three challenges we examined induced maximal PN-1 transcription in hematic cells at 12 h p.i.

The expression profile that was observed in gills of the pathogen-challenged fish was

different from that of hematic cells. LPS was found to stimulate only a late-phase response, at 48 h p.i. Whereas, *E.tarda* up-regulated PN-1 transcription at all time points examined, with a maximum level at 2 days p.i. RBIV induced PN-1 mRNA to a greater level at 48 h p.i. Thus, RbPN-1 has unique temporal transcriptional responses against challenges in hematic cells and gill. The relatively high level of PN-1 mRNA and its response in hematic and gill tissues suggests the existence of a regulatory mechanism for PN-1, particularly against proteases whose levels might be elevated by bacterial/viral infections.

An enhanced expression of PN-1 observed in lesions of the central and peripheral nervous systems (Lino et al., 2007; Meier et al., 1989), during intra-cerebral hemorrhage (ICH) (Wu et al., 2008) and in kidney during glomerulopathy (Moll et al., 1996) suggests that PN-1 modulates proteases in these disease conditions. This idea gained credence when it was observed that injury/inflammatory-related growth factors and cytokines can dynamically modulate PN-1 expression in muscle (Mbebi et al., 1999) and astrocytes (Hultman et al., 2010). Hence, the impact of injury in PN-1 and HCII of Rb was investigated (Umasuthan et al., 2011a). The expression of both serpins was suppressed throughout the experimental period with a drastic decline immediately and at the late phase of injury. Thrombin plays a crucial role in inflammatory and post-injury events and requires the counterbalance of serpins to have a balanced activity. Thus, it is apparent that relative levels of thrombin and serpins will be determined according to the severity of injury conditions. The mechanism underlying our observations in the Rb injury experiment could involve a higher amount of active thrombin to facilitate blood coagulation and this requirement could possibly explain why the serpins' level appeared to be negatively regulated immediately after injury. Following a transient increase, which was below the control level, both serpins demonstrated a late phase suppression, which could be accounted if thrombin was mediating the post-injury, wound healing and repair processes. In addition, evidence in Richard et al. (2004) has

indicated that thrombin could down-regulate the PN-1 expression. Thus, our findings along with the past observations reinforce the fact of counter-balance between serpins like PN-1 and HCII and proteases like thrombin is crucial in post-injury and healing events and it modulates the overall impact on the healing kinetics.

In summary, this is the first report of cloning and characterization of a novel PN-1 orthologue from a teleost fish, rock bream, *O. fasciatus*. RbPN-1 is similar to other fish PN-1s, and harbors both unique and shared characteristics with tetrapod PN-1s. Recombinant RbPN-1 has antiprotease and anticoagulant properties. RbPN-1 is constitutively expressed and induced by the immune-modulators LPS, intact bacterium and virus. The injury response of RbPN-1 suggests that it exists in balance with proteases, in particular with thrombin, a mechanism by which it may mediate the wound healing process. Collectively, our findings indicate that RbPN-1 can play various roles related to controlling proteases, coagulation and post-injury events. Further studies are required for the complete understanding of the molecular and physiological mechanism of PN-1.

REFERENCES

- Andersen, O., Flensburg, R., Norberg, K., Salte, R., 2000. Salmon antithrombin has only three carbohydrate side chains, and shows functional similarities to human beta-antithrombin. *Eur J Biochem* 267, 1651-1657
- Aoki, T., Hirono, I., Kim, M.G., Katagiri, T., Tokuda, Y., Toyohara, H., et al., 2000. Identification of viral induced genes in Ig⁺ leucocytes of Japanese flounder *Paralichthys olivaceus*, by differential hybridisation with subtracted and un-subtracted cDNA probes. *Fish Shellfish Immunol* 10, 623-630
- Arcone, R., Chinali, A., Pozzi, N., Parafati, M., Maset, F., Pietropaolo, C., et al., 2009. Conformational and biochemical characterization of a biologically active rat recombinant Protease Nexin-1 expressed in *E. coli*. *Biochim Biophys Acta* 1794, 602-614
- Arnold, K., Bordoli, L., Kopp, J., Schwede, T., 2006. The SWISS-MODEL workspace: a web-based environment for protein structure homology modelling. *Bioinformatics* 22, 195-201
- Baglin, T.P., Carrell, R.W., Church, F.C., Esmon, C.T., Huntington, J.A., 2002. Crystal structures of native and thrombin-complexed heparin cofactor II reveal a multistep allosteric mechanism. *Proc Natl Acad Sci U S A* 99, 11079-11084
- Bairoch, A., Bucher, P., Hofmann, K., 1997. The PROSITE database, its status in 1997. *Nucleic Acids Res* 25, 217-221
- Baker, J.B., Low, D.A., Simmer, R.L., Cunningham, D.D., 1980. Protease-nexin: A cellular component that links thrombin and plasminogen activator and mediates their binding to cells. *Cell* 21, 37-45
- Bar-Shavit, R., Kahn, A., Fenton, J.W., 2nd, Wilner, G.D., 1983a. Chemotactic response of monocytes to thrombin. *J Cell Biol* 96, 282-285
- Bar-Shavit, R., Kahn, A., Wilner, G.D., Fenton, J.W., 2nd, 1983b. Monocyte chemotaxis: stimulation by specific exosite region in thrombin. *Science* 220, 728-731
- Bendtsen, J.D., Nielsen, H., von Heijne, G., Brunak, S., 2004. Improved prediction of signal peptides: SignalP 3.0. *J Mol Biol* 340, 783-795
- Bergman, B.L., Scott, R.W., Bajpai, A., Watts, S., Baker, J.B., 1986. Inhibition of tumor-cell-mediated extracellular matrix destruction by a fibroblast proteinase inhibitor, protease nexin I. *Proc Natl Acad Sci U S A* 83, 996-1000
- Blinder, M.A., Marasa, J.C., Reynolds, C.H., Deaven, L.L., Tollefsen, D.M., 1988. Heparin cofactor II: cDNA sequence, chromosome localization, restriction fragment length

- polymorphism, and expression in *Escherichia coli*. *Biochemistry* 27, 752-759
- Boulaftali, Y., Adam, F., Venisse, L., Ollivier, V., Richard, B., Taieb, S., et al., 2010. Anticoagulant and antithrombotic properties of platelet protease nexin-1. *Blood* 115, 97-106
- Bourin, M.C., Lindahl, U., 1993. Glycosaminoglycans and the regulation of blood coagulation. *Biochem J* 289 (Pt 2), 313-330
- Bouton, M.C., Venisse, L., Richard, B., Pouzet, C., Arocas, V., Jandrot-Perrus, M., 2007. Protease nexin-1 interacts with thrombomodulin and modulates its anticoagulant effect. *Circ Res* 100, 1174-1181
- Bradford, M.M., 1976. A rapid and sensitive method for the quantitation of microgram quantities of protein utilizing the principle of protein-dye binding. *Anal Biochem* 72, 248-254
- Campanella, J., Bitincka, L., Smalley, J., 2003. MatGAT: An application that generates similarity/identity matrices using protein or DNA sequences. *BMC Bioinformatics* 4, 29
- Cavanaugh, K.P., Gurwitz, D., Cunningham, D.D., Bradshaw, R.A., 1990. Reciprocal modulation of astrocyte stellation by thrombin and protease nexin-1. *J Neurochem* 54, 1735-1743
- Chang, W.C., Lee, T.Y., Shien, D.M., Hsu, J.B., Horng, J.T., Hsu, P.C., et al., 2009. Incorporating support vector machine for identifying protein tyrosine sulfation sites. *J Comput Chem* 30, 2526-2537
- Chasan, R., Anderson, K.V., 1989. The role of easter, an apparent serine protease, in organizing the dorsal-ventral pattern of the *Drosophila* embryo. *Cell* 56, 391-400
- Choi, B.H., Suzuki, M., Kim, T., Wagner, S.L., Cunningham, D.D., 1990. Protease nexin-1. Localization in the human brain suggests a protective role against extravasated serine proteases. *Am J Pathol* 137, 741-747
- Church, F.C., Meade, J.B., Pratt, C.W., 1987. Structure-function relationships in heparin cofactor II: spectral analysis of aromatic residues and absence of a role for sulfhydryl groups in thrombin inhibition. *Arch Biochem Biophys* 259, 331-340
- Church, F.C., Noyes, C.M., Griffith, M.J., 1985. Inhibition of chymotrypsin by heparin cofactor II. *Proc Natl Acad Sci U S A* 82, 6431-6434
- Church, F.C., Pratt, C.W., Hoffman, M., 1991. Leukocyte chemoattractant peptides from the serpin heparin cofactor II. *J Biol Chem* 266, 704-709
- Clynen, E., Schoofs, L., Salzet, M., 2005. A Review of the Most Important Classes of Serine Protease Inhibitors in Insects and Leeches. *Medicinal Chemistry Reviews - Online* 2, 197-206

- Cohen, W.M., Wu, H.F., Featherstone, G.L., Jenzano, J.W., Lundblad, R.L., 1991. Linkage between blood coagulation and inflammation: stimulation of neutrophil tissue kallikrein by thrombin. *Biochem Biophys Res Commun* 176, 315-320
- Colwell, N.S., Grupe, M.J., Tollefsen, D.M., 1999. Amino acid residues of heparin cofactor II required for stimulation of thrombin inhibition by sulphated polyanions. *Biochim Biophys Acta* 1431, 148-156
- Colwell, N.S., Tollefsen, D.M., 1998. Isolation of frog and chicken cDNAs encoding heparin cofactor II. *Thromb Haemost* 80, 784-790
- Cook, D.N., Wang, S., Wang, Y., Howles, G.P., Whitehead, G.S., Berman, K.G., et al., 2004. Genetic regulation of endotoxin-induced airway disease. *Genomics* 83, 961-969
- Copple, B.L., Moulin, F., Hanumegowda, U.M., Ganey, P.E., Roth, R.A., 2003. Thrombin and protease-activated receptor-1 agonists promote lipopolysaccharide-induced hepatocellular injury in perfused livers. *J Pharmacol Exp Ther* 305, 417-425
- Crisp, R.J., Knauer, D.J., Knauer, M.F., 2000. Roles of the heparin and low density lipid receptor-related protein-binding sites of protease nexin 1 (PN1) in urokinase-PN1 complex catabolism. The PN1 heparin-binding site mediates complex retention and degradation but not cell surface binding or internalization. *J Biol Chem* 275, 19628-19637
- Crisp, R.J., Knauer, M.F., Knauer, D.J., 2002. Protease nexin 1 is a potent urinary plasminogen activator inhibitor in the presence of collagen type IV. *J Biol Chem* 277, 47285-47291
- Dawes, K.E., Gray, A.J., Laurent, G.J., 1993. Thrombin stimulates fibroblast chemotaxis and replication. *Eur J Cell Biol* 61, 126-130
- Di Cera, E., Cantwell, A.M., 2001. Determinants of thrombin specificity. *Ann N Y Acad Sci* 936, 133-146
- Donovan, F.M., Cunningham, D.D., 1998. Signaling pathways involved in thrombin-induced cell protection. *J Biol Chem* 273, 12746-12752
- Droege, M., Hill, B., 2008. The Genome Sequencer FLX System--longer reads, more applications, straight forward bioinformatics and more complete data sets. *J Biotechnol* 136, 3-10
- Eaton, D.L., Baker, J.B., 1983. Evidence that a variety of cultured cells secrete protease nexin and produce a distinct cytoplasmic serine protease-binding factor. *J Cell Physiol* 117, 175-182
- Farrell, D.H., Wagner, S.L., Yuan, R.H., Cunningham, D.D., 1988. Localization of protease nexin-1 on the fibroblast extracellular matrix. *J Cell Physiol* 134, 179-188
- Gao, S., Krogdahl, A., Sorensen, J.A., Kousted, T.M., Dabelsteen, E., Andreasen, P.A., 2008.

- Overexpression of protease nexin-1 mRNA and protein in oral squamous cell carcinomas. *Oral Oncol* 44, 309-313
- Gettins, P.G., 2000. Keeping the serpin machine running smoothly. *Genome Res* 10, 1833-1835
- Gloor, S., Odink, K., Guenther, J., Nick, H., Monard, D., 1986. A glia-derived neurite promoting factor with protease inhibitory activity belongs to the protease nexins. *Cell* 47, 687-693
- Gronke, R., Knauer, D., Veeraraghavan, S., Baker, J., 1989. A form of protease nexin I is expressed on the platelet surface during platelet activation. *Blood* 73, 472-478
- Gurwitz, D., Cunningham, D.D., 1988. Thrombin modulates and reverses neuroblastoma neurite outgrowth. *Proc Natl Acad Sci U S A* 85, 3440-3444
- Hanumanthaiah, R., Day, K., Jagadeeswaran, P., 2002. Comprehensive analysis of blood coagulation pathways in teleostei: evolution of coagulation factor genes and identification of zebrafish factor VIIIi. *Blood Cells Mol Dis* 29, 57-68
- Hayakawa, Y., Hirashima, Y., Kurimoto, M., Hayashi, N., Hamada, H., Kuwayama, N., et al., 2002. Contribution of basic residues of the A helix of heparin cofactor II to heparin- or dermatan sulfate-mediated thrombin inhibition. *FEBS Lett* 522, 147-150
- He, L., Vicente, C.P., Westrick, R.J., Eitzman, D.T., Tollefsen, D.M., 2002. Heparin cofactor II inhibits arterial thrombosis after endothelial injury. *J Clin Invest* 109, 213-219
- Heutinck, K.M., ten Berge, I.J., Hack, C.E., Hamann, J., Rowshani, A.T., 2010. Serine proteases of the human immune system in health and disease. *Mol Immunol* 47, 1943-1955
- Hewett, J.A., Roth, R.A., 1995. The coagulation system, but not circulating fibrinogen, contributes to liver injury in rats exposed to lipopolysaccharide from gram-negative bacteria. *J Pharmacol Exp Ther* 272, 53-62
- Hoffman, M., Loh, K.L., Bond, V.K., Palmieri, D., Ryan, J.L., Church, F.C., 2003. Localization of heparin cofactor II in injured human skin: a potential role in wound healing. *Exp Mol Pathol* 75, 109-118
- Huang, C.J., Lee, M.S., Huang, F.L., Chang, G.D., 1995. A protease inhibitor of the serpin family is a major protein in carp perimeningeal fluid: II. cDNA cloning, sequence analysis, and *Escherichia coli* expression. *J Neurochem* 64, 1721-1727
- Hultman, K., Blomstrand, F., Nilsson, M., Wilhelmsson, U., Malmgren, K., Pekny, M., et al., 2010. Expression of plasminogen activator inhibitor-1 and protease nexin-1 in human astrocytes: Response to injury-related factors. *J Neurosci Res* 88, 2441-2449
- Huntington, J.A., Read, R.J., Carrell, R.W., 2000. Structure of a serpin-protease complex shows

- inhibition by deformation. *Nature* 407, 923-926
- Irving, J.A., Pike, R.N., Lesk, A.M., Whisstock, J.C., 2000. Phylogeny of the serpin superfamily: implications of patterns of amino acid conservation for structure and function. *Genome Res* 10, 1845-1864
- Jagadeeswaran, P., Sheehan, J.P., 1999. Analysis of blood coagulation in the zebrafish. *Blood Cells Mol Dis* 25, 239-249
- Kamp, P., Strathmann, A., Ragg, H., 2001. Heparin cofactor II, antithrombin-beta and their complexes with thrombin in human tissues. *Thromb Res* 101, 483-491
- Knauer, D.J., Majumdar, D., Fong, P.C., Knauer, M.F., 2000. SERPIN regulation of factor XIa. The novel observation that protease nexin 1 in the presence of heparin is a more potent inhibitor of factor XIa than C1 inhibitor. *J Biol Chem* 275, 37340-37346
- Knauer, M.F., Hawley, S.B., Knauer, D.J., 1997a. Identification of a binding site in protease nexin I (PN1) required for the receptor mediated internalization of PN1-thrombin complexes. *J Biol Chem* 272, 12261-12264
- Knauer, M.F., Kridel, S.J., Hawley, S.B., Knauer, D.J., 1997b. The efficient catabolism of thrombin-protease nexin 1 complexes is a synergistic mechanism that requires both the LDL receptor-related protein and cell surface heparins. *J Biol Chem* 272, 29039-29045
- Koistinen, H., Koistinen, R., Zhang, W.M., Valmu, L., Stenman, U.H., 2009. Nexin-1 inhibits the activity of human brain trypsin. *Neuroscience* 160, 97-102
- Kumar, S., Tamura, K., Nei, M., 2004. MEGA3: Integrated software for Molecular Evolutionary Genetics Analysis and sequence alignment. *Brief Bioinform* 5, 150-163
- Law, R.H., Zhang, Q., McGowan, S., Buckle, A.M., Silverman, G.A., Wong, W., et al., 2006. An overview of the serpin superfamily. *Genome Biol* 7, 216
- Letunic, I., Doerks, T., Bork, P., 2009. SMART 6: recent updates and new developments. *Nucleic Acids Res* 37, D229-232
- Lino, M.M., Atanasoski, S., Kvajo, M., Fayard, B., Moreno, E., Brenner, H.R., et al., 2007. Mice lacking protease nexin-1 show delayed structural and functional recovery after sciatic nerve crush. *J Neurosci* 27, 3677-3685
- Livak, K.J., Schmittgen, T.D., 2001. Analysis of relative gene expression data using real-time quantitative PCR and the $2^{-\Delta\Delta C(T)}$ Method. *Methods* 25, 402-408
- Low, D.A., Baker, J.B., Koonce, W.C., Cunningham, D.D., 1981. Released protease-nexin regulates cellular binding, internalization, and degradation of serine proteases. *Proc Natl*

- Acad Sci U S A 78, 2340-2344
- Low, D.A., Scott, R.W., Baker, J.B., Cunningham, D.D., 1982. Cells regulate their mitogenic response to thrombin through release of protease nexin. *Nature* 298, 476-478
- Mangan, M.S., Kaiserman, D., Bird, P.I., 2008. The role of serpins in vertebrate immunity. *Tissue Antigens* 72, 1-10
- Mansilla, S., Boulaftali, Y., Venisse, L., Arocas, V., Meilhac, O., Michel, J.B., et al., 2008. Macrophages and platelets are the major source of protease nexin-1 in human atherosclerotic plaque. *Arterioscler Thromb Vasc Biol* 28, 1844-1850
- Mansuy, I.M., van der Putten, H., Schmid, P., Meins, M., Botteri, F.M., Monard, D., 1993. Variable and multiple expression of Protease Nexin-1 during mouse organogenesis and nervous system development. *Development* 119, 1119-1134
- Mark, D.E., Lazzari, K.G., Simons, E.R., 1988. Are serine proteases involved in immune complex activation of neutrophils? *J Leukoc Biol* 44, 441-447
- Mast, A.E., Enghild, J.J., Pizzo, S.V., Salvesen, G., 1991. Analysis of the plasma elimination kinetics and conformational stabilities of native, proteinase-complexed, and reactive site cleaved serpins: comparison of alpha 1-proteinase inhibitor, alpha 1-antichymotrypsin, antithrombin III, alpha 2-antiplasmin, angiotensinogen, and ovalbumin. *Biochemistry* 30, 1723-1730
- Mbebi, C., Hantai, D., Jandrot-Perrus, M., Doyennette, M.A., Verdier-Sahuque, M., 1999. Protease nexin I expression is up-regulated in human skeletal muscle by injury-related factors. *J Cell Physiol* 179, 305-314
- McGrogan, M., Kennedy, J., Ping Li, M., Hsu, C., Scott, R.W., Simonsen, C.C., et al., 1988. Molecular Cloning and Expression of Two Forms of Human Protease Nexin I. *Nat Biotech* 6, 172-177
- Meier, R., Spreyer, P., Ortmann, R., Harel, A., Monard, D., 1989. Induction of glia-derived nexin after lesion of a peripheral nerve. *Nature* 342, 548-550
- Mentz, S., Lacalle, S.d., Baerga-Ortiz, A., Knauer, M.F., Knauer, D.J., Komives, E.A., 1999. Mechanism of Thrombin Clearance by Human Astrocytoma Cells. *Journal of Neurochemistry* 72, 980-987
- Michie, H.R., Manogue, K.R., Spriggs, D.R., Revhaug, A., O'Dwyer, S., Dinarello, C.A., et al., 1988. Detection of circulating tumor necrosis factor after endotoxin administration. *N Engl J Med* 318, 1481-1486

- Moll, S., Schaeren-Wiemers, N., Wohlwend, A., Pastore, Y., Fulpius, T., Monard, D., et al., 1996. Protease nexin 1 in the murine kidney: glomerular localization and up-regulation in glomerulopathies. *Kidney Int* 50, 1936-1945
- Nitsch, C., Scotti, A.L., Monard, D., Heim, C., Sontag, K.H., 1993. The glia-derived protease nexin 1 persists for over 1 year in rat brain areas selectively lesioned by transient global ischaemia. *Eur J Neurosci* 5, 292-297
- Onuma, Y., Asashima, M., Whitman, M., 2006. A Serpin family gene, protease nexin-1 has an activity distinct from protease inhibition in early *Xenopus* embryos. *Mech Dev* 123, 463-471
- Park, K.C., Osborne, J.A., Tsoi, S.C., Brown, L.L., Johnson, S.C., 2005. Expressed sequence tags analysis of Atlantic halibut (*Hippoglossus hippoglossus*) liver, kidney and spleen tissues following vaccination against *Vibrio anguillarum* and *Aeromonas salmonicida*. *Fish Shellfish Immunol* 18, 393-415
- Parker, K.A., Tollefsen, D.M., 1985. The protease specificity of heparin cofactor II. Inhibition of thrombin generated during coagulation. *J Biol Chem* 260, 3501-3505
- Passantino, L., Cianciotta, A., Patrino, R., Ribaud, M.R., Jirillo, E., Passantino, G.F., 2005. Do fish thrombocytes play an immunological role? Their cytoenzymatic profiles and function during an accidental piscine candidiasis in aquarium. *Immunopharmacol Immunotoxicol* 27, 345-356
- Pearson, W.R., 1990. Rapid and sensitive sequence comparison with FASTP and FASTA. *Methods Enzymol* 183, 63-98
- Pike, R.N., Buckle, A.M., le Bonniec, B.F., Church, F.C., 2005. Control of the coagulation system by serpins. Getting by with a little help from glycosaminoglycans. *FEBS J* 272, 4842-4851
- Pratt, C.W., Whinna, H.C., Meade, J.B., Treanor, R.E., Church, F.C., 1989. Physicochemical aspects of heparin cofactor II. *Ann N Y Acad Sci* 556, 104-115
- Ragg, H., Lokot, T., Kamp, P.B., Atchley, W.R., Dress, A., 2001. Vertebrate serpins: construction of a conflict-free phylogeny by combining exon-intron and diagnostic site analyses. *Mol Biol Evol* 18, 577-584
- Ragg, H., Ulshofer, T., Gerewitz, J., 1990. On the activation of human leuserpin-2, a thrombin inhibitor, by glycosaminoglycans. *J Biol Chem* 265, 5211-5218
- Rau, J.C., Beaulieu, L.M., Huntington, J.A., Church, F.C., 2007. Serpins in thrombosis, hemostasis and fibrinolysis. *J Thromb Haemost* 5 Suppl 1, 102-115
- Rawlings, N.D., Tolle, D.P., Barrett, A.J., 2004. Evolutionary families of peptidase inhibitors.

- Biochem J 378, 705-716
- Richard, B., Arocas, V., Guillin, M.C., Michel, J.B., Jandrot-Perrus, M., Bouton, M.C., 2004. Protease nexin-1: a cellular serpin down-regulated by thrombin in rat aortic smooth muscle cells. *J Cell Physiol* 201, 138-145
- Roberts, T.H., Hejgaard, J., 2008. Serpins in plants and green algae. *Funct Integr Genomics* 8, 1-27
- Rodriguez-Niedenfuhr, M., Prols, F., Christ, B., 2003. Temporal and spatial protease nexin 1 expression during chick development. *Gene Expr Patterns* 3, 611-614
- Rovelli, G., Stone, S.R., Guidolin, A., Sommer, J., Monard, D., 1992. Characterization of the heparin-binding site of glia-derived nexin/protease nexin-1. *Biochemistry* 31, 3542-3549
- Scott, R.W., Bergman, B.L., Bajpai, A., Hersh, R.T., Rodriguez, H., Jones, B.N., et al., 1985. Protease nexin. Properties and a modified purification procedure. *J Biol Chem* 260, 7029-7034
- Sheehan, J., Templer, M., Gregory, M., Hanumanthaiah, R., Troyer, D., Phan, T., et al., 2001. Demonstration of the extrinsic coagulation pathway in teleostei: identification of zebrafish coagulation factor VII. *Proc Natl Acad Sci U S A* 98, 8768-8773
- Sheffield, W.P., Schuyler, P.D., Blajchman, M.A., 1994. Molecular cloning and expression of rabbit heparin cofactor II: a plasma thrombin inhibitor highly conserved between species. *Thromb Haemost* 71, 778-782
- Shrivastava, S., McVey, J.H., Dorling, A., 2007. The interface between coagulation and immunity. *Am J Transplant* 7, 499-506
- Silverman, G.A., Bird, P.I., Carrell, R.W., Church, F.C., Coughlin, P.B., Gettins, P.G., et al., 2001. The serpins are an expanding superfamily of structurally similar but functionally diverse proteins. Evolution, mechanism of inhibition, novel functions, and a revised nomenclature. *J Biol Chem* 276, 33293-33296
- Sim, R.B., Laich, A., 2000. Serine proteases of the complement system. *Biochem Soc Trans* 28, 545-550
- Simpson, C.S., Johnston, H.M., Morris, B.J., 1994. Neuronal expression of protease-nexin 1 mRNA in rat brain. *Neurosci Lett* 170, 286-290
- Sommer, J., Gloor, S.M., Rovelli, G.F., Hofsteenge, J., Nick, H., Meier, R., et al., 1987. cDNA sequence coding for a rat glia-derived nexin and its homology to members of the serpin superfamily. *Biochemistry* 26, 6407-6410
- Stone, S.R., Brown-Luedi, M.L., Rovelli, G., Guidolin, A., McGlynn, E., Monard, D., 1994.

- Localization of the heparin-binding site of glia-derived nexin/protease nexin-1 by site-directed mutagenesis. *Biochemistry* 33, 7731-7735
- Stone, S.R., Nick, H., Hofsteenge, J., Monard, D., 1987. Glial-derived neurite-promoting factor is a slow-binding inhibitor of trypsin, thrombin, and urokinase. *Arch Biochem Biophys* 252, 237-244
- Stout, T.J., Graham, H., Buckley, D.I., Matthews, D.J., 2000. Structures of active and latent PAI-1: a possible stabilizing role for chloride ions. *Biochemistry* 39, 8460-8469
- Thompson, J.D., Higgins, D.G., Gibson, T.J., 1994. CLUSTAL W: improving the sensitivity of progressive multiple sequence alignment through sequence weighting, position-specific gap penalties and weight matrix choice. *Nucleic acids research* 22, 4673-4680
- Tollefsen, D.M., 1994. The interaction of glycosaminoglycans with heparin cofactor II. *Ann N Y Acad Sci* 714, 21-31
- Tollefsen, D.M., 2007. Heparin cofactor II modulates the response to vascular injury. *Arterioscler Thromb Vasc Biol* 27, 454-460
- Tollefsen, D.M., Pestka, C.A., Monafó, W.J., 1983. Activation of heparin cofactor II by dermatan sulfate. *J Biol Chem* 258, 6713-6716
- Umasuthan, N., Whang, I., Kim, J.O., Oh, M.J., Jung, S.J., Choi, C.Y., et al., 2011a. Rock bream (*Oplegnathus fasciatus*) serpin, protease nexin-1: Transcriptional analysis and characterization of its antiprotease and anticoagulant activities. *Dev Comp Immunol*
- Umasuthan, N., Whang, I., Lee, Y., Lee, S., Kim, Y., Kim, H., et al., 2011b. Heparin cofactor II (RbHCII) from rock bream (*Oplegnathus fasciatus*): molecular characterization, cloning and expression analysis. *Fish Shellfish Immunol* 30, 194-208
- Vasseur, S., Hoffmeister, A., Garcia-Montero, A., Barthet, M., Saint-Michel, L., Berthezene, P., et al., 2003. Mice with targeted disruption of p8 gene show increased sensitivity to lipopolysaccharide and DNA microarray analysis of livers reveals an aberrant gene expression response. *BMC Gastroenterol* 3, 25
- Vaughan, P.J., Su, J., Cotman, C.W., Cunningham, D.D., 1994. Protease nexin-1, a potent thrombin inhibitor, is reduced around cerebral blood vessels in Alzheimer's disease. *Brain Research* 668, 160-170
- Wallace, A., Rovelli, G., Hofsteenge, J., Stone, S.R., 1989. Effect of heparin on the glia-derived-nexin-thrombin interaction. *Biochem J* 257, 191-196
- Wu, H., Zhao, R., Qi, J., Cong, Y., Wang, D., Liu, T., et al., 2008. The expression and the role of

- protease nexin-1 on brain edema after intracerebral hemorrhage. *J Neurol Sci* 270, 172-183
- Wu, Y., Wang, S., Peng, X., 2004. Serum acute phase response (APR)-related proteome of loach to trauma. *Fish Shellfish Immunol* 16, 381-389
- Yee, S.B., Harkema, J.R., Ganey, P.E., Roth, R.A., 2003. The coagulation system contributes to synergistic liver injury from exposure to monocrotaline and bacterial lipopolysaccharide. *Toxicol Sci* 74, 457-469
- Zhang, H., Lin, H.Y., Yang, Q., Wang, H.X., Chai, K.X., Chen, L.M., et al., 2007. Expression of prostatic serine protease and protease nexin-1 (PN-1) in rhesus monkey ovary during menstrual cycle and early pregnancy. *J Histochem Cytochem* 55, 1237-1244

ACKNOWLEDGEMENT

Prof. Jehee Lee!, I would like to sincerely acknowledge the precious opportunity you granted to commence my post-graduate studies at your Molecular Genetics Lab in Jeju National University. You were the innovative guider who enlightened my endeavours with your ideas and advices. I believe that the foundation you have laid on me is much strong enough to build my future career.

Faculty members attached to department of Marine Life Sciences in JNU, Prof. Choon-Bok Song, Prof. Moon-Soo Heo, Prof. Gi-Young Kim, Prof. Kwang-Sik Choi, Prof. You-Jin Jeon, Prof. In-Kyu Yeo, Prof. Kyeong-Jun Lee, Prof. Joon-Bom Lee and Prof. Young-Dong Lee!, your teaching, discussions and laboratory facilities provided were the key factors of my graduate research career and they are greatly appreciated. I owe Prof. Gi-Young Kim and Prof. In-Kyo Yeo for being the members of supervising committee in my thesis defense.

Dr. Ilson Whang!, a special word of thanks for your inspirative guidance and intellectual ideas in my laboratory experiments and writings.

My previous and present lab members, Dr. Mahanama De Zoysa, Dr. Chamilani Nikapitiya, Dr. Wan Qiang, Saranya Revathy Kasthuri, Youngdeuk Lee, Yucheol Kim, Sukkyoung Lee, Hyowan Kim and Oh Minyoung! If not you, I wonder how it would be possible for me to complete my studies in MGL. I also acknowledge the new MGL members from Sri Lanka, Sanjaya, Anushka, Niroshana and Ajith as well as Janaka, Prasad and Kalpa for all supports and companionship.

Finally, my dearest wife, Hamsa!, I appreciate as you stand with me in the form of moral support, forever.